Accepted Manuscript

Synthesis of heteroaryl/aryl kojic acid conjugates as stimulators of glucose uptake by GLUT4 translocation

Deepak K. Sharma, Jyotsana Pandey, Akhilesh K. Tamrakar, Debaraj Mukherjee

PII: S0223-5234(14)00776-4

DOI: 10.1016/j.ejmech.2014.08.041

Reference: EJMECH 7274

To appear in: *European Journal of Medicinal Chemistry*

Received Date: 7 June 2014

Revised Date: 9 August 2014

Accepted Date: 11 August 2014

Please cite this article as: D.K. Sharma, J. Pandey, A.K. Tamrakar, D. Mukherjee, Synthesis of heteroaryl/aryl kojic acid conjugates as stimulators of glucose uptake by GLUT4 translocation, *European Journal of Medicinal Chemistry* (2014), doi: 10.1016/j.ejmech.2014.08.041.

Graphical abstract

Insulin mimics (**2a-3f**) based on indolylkojic acid scaffold(**B**) were synthesized. In mechanistic studies, biologically active compounds were found to enhance GLUT4 translocation to cell surface via PI3K pathway.

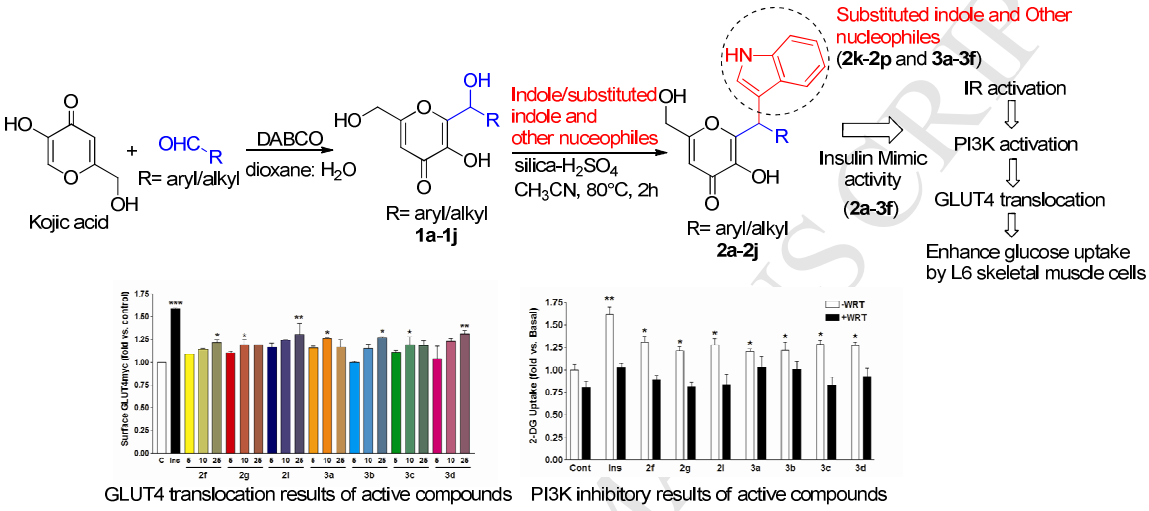

GLUT4 translocation results of active compounds

PI3K inhibitory results of active compounds

Synthesis of heteroaryl/aryl kojic acid conjugates as stimulators of glucose uptake by GLUT4 translocation

Deepak K. Sharma,[a,b] *Jyotsana Pandey,*[c] *Akhilesh K. Tamrakar,* [a,c] *Debaraj Mukherjee*[a,b]*

[a]Academy of Scientific and Innovative Research (AcSIR), India

[b]CSIR-Indian Institute of Integrative MedicineJammu, J & K, 180001, India

[c]CSIR-Central Drug Research Institute, Lucknow-226031, India

Keywords. Heteroaryl/aryl kojic acid conjugates, Insulin receptor, GLUT4 translocation, PI3K

***Corresponding Author:** Debaraj Mukherjee. Tel.:+91-191-2569000; fax: +91-191-2569111; e-mail: dmukherjee@iiim.ac.in, IIIM/1690/2014

ABSTRACT. Insulin exerts its metabolic actions through the insulin receptor (IR) and plays an essential role in treatment of diabetes. The inconvenience of daily injections and the undesirable side-effects associated with insulin injections demand novel drugs for the disease. To search for bioactive insulin mimetic, we synthesized a chemical library of small molecules (**2a**-**3f**) based on the indolylkojic acid scaffold (**B**). An *In vitro* screening assay was performed to stimulate glucose transport in rat L6 skeletal muscle cells, post treatment of the compounds (**2a**-**3f**) for the time period incubation of 16h. Compounds **2f**, **2g**, **2l**, **3a**, **3b**, **3c** and **3d** have shown significant glucose uptake stimulation as compared to the controls at micromolar concentrations. In mechanistic studies, we observed that these compounds exert their biological action by enhancing GLUT4 translocation to cell surface via PI3K-dependent signaling pathway in agreement to the insulin mode of action. Hence, these promising conjugates should be useful for further drug development in diabetes treatment.

1.0. Introduction

Type 2 diabetes mellitus (T2DM) is a metabolic syndrome characterized by high blood glucose levels due to either insulin resistance or relative insulin deficiency [1]. The prevalence of diabetes is increasing worldwide and it has been predicted that the number of patient's worldwide suffering from T2DM will rise to over 360 million by 2030 [2,3]. Insulin resistance is the major pathophysiological defect in T2DM which is characterized by the inability of insulin sensitive cells to respond adequately to normal levels of insulin. Insulin resistance occurs primarily within the skeletal muscles, liver and fat tissue leading to alteration of whole body glucose homeostasis [4]. Skeletal muscle has major contribution in postprandial glucose disposal which accounts for more than 80% of insulin-dependent glucose disposal in human [5]. Glucose uptake is the rate-limiting step in glucose utilization in diabetic and non diabetic skeletal muscle [6]. In skeletal muscle cells glucose uptake is the result of the enhanced translocation and redistribution of glucose transporter 4 (GLUT4) from intracellular vesicles to plasma membrane, where it facilitates the entry of the glucose inside the cells [7].

The discovery of the small molecule insulin mimetic demethylasterriquinone B1 from microbial sources such as *Aspergillus terreus*, *Pseudomassaria* fungi represented a major breakthrough in medicinal chemistry. This discovery demonstrated that a small, nonpeptidyl natural molecule is capable of mimicking the biological function of a protein hormone by interacting with the insulin receptor and causing activation of insulin receptor tyrosin kinase (IRTK) [8]. Despite these promising early results [9,10], molecules of this family have not yet entered in clinical trials. A possible major concern is the safety of candidate pharmaceuticals that contain the potentially problematic quinone substructure. Recent developments on the replacement of the quinone in demethylasterriquinone B1 (**A**) with kojic acid (Fig. 1) showed that it is possible to design products which do not present this safety issue but are equally active biologically [11,12].

Fig. 1.

In continuation of our ongoing research program in the area of medicinal chemistry, we decided to design small molecules based on the indolylkojic acid scaffold and thereafter its role in GLUT4 translocation. In this current approach, we have introduced a one carbon spacer in between indole/substituted indole/aryl/heteroaryl moiety and the naturally occurring kojic acid as the modification site in indolylkojic acid scaffold (**B**). Thereafter, we have studied their glucose uptake stimulatory effect in skeletal muscle cells as shown in figure 2. In skeletal muscle cells

glucose uptake stimulation by insulin is the result of increased translocation of GLUT4 to cell surface via activation of Phosphoinositide 3-kinase (PI3K) signaling pathway [13,14]. Hence to confirm that the compounds under study have the insulin mimetic activity we have also performed an inhibitor study of PI3K signaling pathway. Wortmannin (WRT) is a specific inhibitor for PI3K. In the presence of WRT the PI3K pathway is inhibited and translocation of GLUT4 by insulin or insulin mimetic compounds are restricted to the basal level only.

Fig. 2.

2.0. Results and Discussion

2.1. Chemistry.

The earlier reported synthetic routes for indolylkojic acid (**B**) are based on a Claisen rearrangement [12] and Stille coupling [11] as shown in figure 3. However, these routes require multistep sequences making the processes less attractive for quick access of a library of molecules for SAR studies particularly with variations in the indole portion.

Fig. 3.

We have isolated kojic acid from its natural source *Aspergillus flavus* using literature method [15] and utilized it as a raw material for the generation of target structure **1**. Reddy *et al.* [16] developed one pot multi-component method for the synthesis of this class of compounds using $InCl_3$ in solvent free condition at 120°C. However, we observed that method suffers from serious drawbacks such as formation of diindolylmethane [17] as a side product, use of harsh condition (120°C) which limit this methodology for gram scale synthesis and subsequent bio-evaluation. Further, the earlier reported method [16] has very narrow substrate scope e.g. they have not taken nucleophiles other than indole for this particular reaction. To overcome these above mentioned drawbacks we developed a synthetic strategy which is scalable, simple and flexible enough to create diversity. We performed initial screening of the catalyst for the synthesis of compound **1a** as shown in table 1. For this purpose we treated kojic acid (1 mmol) with benzaldehyde (1.2 mmol) in the presence of various catalysts in dioxane: water (1:1, 4 mL) at room temperature for 24h (Table 1). Compound **1a** was obtained in excellent yield using DABCO (entry 3, Table 1). A slight excess of aldehyde was found to be necessary for achieving the complete consumption of the α,β-unsaturated cyclohexenone.

Table 1.

To check the substrate scope of the reaction, various aldehydes including aromatic (**1a-1h**) and aliphatic (**1i**, **1j**) were allowed to react under the optimized condition as shown in table 2.

Table 2.

In all cases products (**1a-1j,** Table 2) were obtained in good to excellent yields. In general aromatic aldehydes with electron-withdrawing substituents gave slightly better yield than those having electron donating groups (**1b** vs **1e**). With aliphatic aldehydes, reactions with small chain aldehydes like valeraldehyde (**1i**) went to completion but long chain aldehydes like nonaldehyde (**1j**) needed prolonged time period (2 days).

Our next target was to remove the secondary hydroxyl group of the adduct (**1a-1j**) with incoming nucleophiles to obtain product **2a-2j** (Table 3). Here we have investigated the role of modified silica-H_2SO_4 for *C*-alkylation of indole due its low cost and recyclability [18-20]. Thus, compounds **1a-1j** (1 equiv.) in CH_3CN were stirred with indole (1.5 equiv) at 80^oC for 2h using silica-H_2SO_4 (10 mol%) as catalyst to obtain kojic acid-indole conjugates **2a-2j** in excellent yields as shown in table 3.

Table 3.

To expand the scope of the substitution reaction various types of substituted indoles and other nucleophiles such as thiophenol, phenol, pyrrole, thiophene and benzthiophene were allowed to react with **1a** under the optimized conditions as shown in table 4. Products **2k-3f** were obtained in excellent yields (Table 4). As anticipated, regioselectivity was observed in the case of phenol giving only the *para* substituted product (**3c**); *C*-alkylation with 2-methylthiophene occurred at *C*-5 position (**3d**) and with pyrrole at *C*-2 position (**3f**).

Table 4.

2.2. Biological evaluation

2.2.1. Glucose uptake stimulatory effect of compounds in L6 skeletal muscle cells. All the synthesized compounds were evaluated for glucose uptake stimulatory effect in L6 skeletal muscle cells stably expressing rat GLUT4 with a *myc* epitope inserted in the first exofacial loop (L6-GLUT4*myc*) and results are depicted in figure 4. From the tested compounds (**2a-2j**),

compounds synthesized using electron donating benzaldehyde i.e. **2f** and **2g** [21] shows significant stimulation of glucose uptake with respective 1.21- and 1.25- fold stimulation ($p<0.05$) over control. In case substituted indoles (**2k-2p**), compound **2l** having 5-methoxyindole was showing better activity than other substituted indoles and showed 1.25 fold ($p<0.05$) increase in glucose uptake. Compound **1a** substituted with various nucleophiles (**3a-3f**) other than indole (**2a**) gives better activity. Among compounds **3a-3f,** Compounds **3a, 3b**, **3c** and **3d** showed significant stimulation of glucose uptake with respective 1.33 ($p<0.01$), 1.38 ($p<0.01$), 1.34 ($p<0.01$) and 1.21($p<0.05$) fold increase at 10µM concentration. Compound **3b** was found to be most potent in the series of synthesized insulin mimics. Insulin was taken as positive control, which showed 1.65-fold ($p<0.001$) stimulation of glucose uptake at 100 nM concentration. All other tested compounds showed very less or no effect on glucose uptake in L6 myotubes. The apparent inhibitory effect of some compounds (**2a-2e**, **2h-2k**, **2o** and **2p**) on glucose uptake might be possible due to many reasons like adverse effect on cell viability or antagonist effect on cellular components of biological pathways. Analysis of statistical significance of differences in measurements between samples was done by one-way ANOVA with Dunnets post hoc test (Graph Pad Prism version 3). $p<0.05$ was considered statistically significant.

Fig. 4.

Furthermore the dose dependent effect of the active compounds **2f**, **2g**, **2l** and **3a**-**3b** on glucose uptake at doses of 5 µM, 10 µM and 25 µM is shown in figure 5, taking insulin as a positive control for the experiment. Insulin at a concentration of 100 nM showed 1.6-fold ($p<0.001$) stimulation of glucose uptake compared to basal. All the compounds caused a dose-dependent increase in glucose uptake in L6-GLUT4*myc* cells. Compounds **2l** and **3b** was found to be equipotent to insulin among active compounds and showed comparable activity to insulin at the concentration of 25 µm**.**

Fig. 5.

2.2.2. Effect of compounds on GLUT4 translocation in L6-GLUT4*myc* myotubes. In skeletal muscle, translocation and redistribution of the GLUT4 to the plasma membrane is a characteristic feature for increased glucose uptake [22]. Hence the effect of compounds on surface GLUT4 level in non-permeabilized L6-GLUT4*myc* myotubes was measured by an

antibody-coupled colorimetric assay as previously described [23]. As shown in figure 6, similar to glucose uptake data, compounds **2f**, **2g**, **2l**, **3a**, **3b**, **3c** and **3d** caused increase in surface level of GLUT4*myc* with respect to the control in a dose dependent manner in a concentration range of 5µM, 10µM and 25µM.

Fig. 6.

2.2.3. Inhibitor based study for insulin mimetic pathway detection. To investigate the signaling pathway responsible for the observed biological activity of **2f**, **2g**, **2l**, **3a**, **3b**, **3c** and **3d** and their effect on the PI3K-signaling pathway was observed. The PI3K-pathway is the major signaling pathway in the insulin action leading to increased translocation and distribution of GLUT4 at the cell surface [24]. To confirm whether **2f**, **2g**, **2l**, **3a**, **3b**, **3c** and **3d** compounds stimulated glucose uptake in skeletal muscle cells following a pathway similar to insulin, the involvement of PI3K was investigated using inhibitor studies. Wortmannin (WRT) is a specific inhibitor for PI3K that blocks the insulin-signaling pathway [25]. Similar to the effect of insulin, treatment of cells with **2f**, **2g**, **2l**, **3a**, **3b**, **3c** and **3d** compounds at 10 µM for 16 hours with a final one hour in the presence of wortmannin completely abolished the glucose uptake stimulatory effect of these compounds (Figure 7). These results indicate the involvement of wortmannin-sensitive PI3-kinase mediated signaling pathway underlying the biological effect of these compounds to stimulate glucose uptake in skeletal muscle cells.

Fig. 7.

3.0. Conclusion

In conclusion, we have designed and synthesized of orally active insulin mimics based on indolylkojic acid scaffold. The synthetic strategy used is concise, simple, high yielding and flexible enough to create diversity. Our study describes the glucose uptake stimulatory effect of the compounds **2f**, **2g**, **2l**, **3a**, **3b**, **3c** and **3d**. These compounds exert their biological activity by enhancing GLUT4 translocation to the cell surface via PI-3-Kinase-dependent signaling pathway similar to the insulin's mode of action. Results obtained during the study are indicative of future application of these molecules as effective therapeutic agents in the management of insulin resistance and type 2 diabetes. Further *in vivo* study is required to establish the observed *in vitro* results and to explore the effect on other insulin sensitive tissues involved in glucose metabolism.

4.0. Experimental section

4.1. Chemistry. General information. ^{1}H and ^{13}C NMR spectra were recorded on 400 and 500 MHz spectrometers with TMS as the internal standard. Chemical shifts are expressed in parts per million (δ ppm). Silica gel coated aluminium plates were used for TLC. Final products were purified by column chromatography on silica gel (60-120/100-200 mesh) using petroleum ether–ethyl acetate as the eluent to obtain the pure products. Exact Mass of all products were analysed by using HRMS with QTOF analyser. Reagents used were purchased from Sigma Aldrich.

4.2. General procedure for preparation of compounds (1a-1j): A mixture of kojic acid (1 mmol) and aldehyde (1.2 mmol) was stirred in the presence of DABCO (1.2 mmol) in dioxane:H_2O (1:1, 4mL) at room temperature for 24 h. After completion of the reaction, the product was extracted with ethyl acetate (3×15 ml). The combined organic layer was dried with anhydrous sodium sulphate, concentrated in vacuo, and purified by column chromatography (methanol: dichloromethane =0.5:9.5) to afford the pure product.

Kojic Acid: $C_6H_6O_4$ obtained as a colourless solid. M.pt: 195-205°C ^{1}HNMR (400MHz, CD_3OD): δ 4.30 (s, 2H), 6.40 (s, 1H), 7.86 (s, 1H); ^{13}CNMR (125MHz, CD_3OD): 177.56, 171.13, 148.05, 141.72, 111.41, 61.84. HRMS (-ESI): calcd 142.0266 and found 142.0264.

3-hydroxy-2-(hydroxy(phenyl)methyl)-6-(hydroxymethyl)-4H-pyran-4-one (1a): $C_{13}H_{12}O_5$ obtained in 94% yield as a colourless solid. M.pt: 140-150°C. ^{1}HNMR (400 MHz, CD_3OD): δ 4.38 (dd, *J* = 15.7 Hz, 32.8 Hz, 2H), 6.19 (s, 1H), 6.46 (s, 1H), 7.29 (t, *J* = 7.3 Hz, 1H), 7.36 (t, *J* = 7.4 Hz, 2H) 7.49 (d, *J* = 7.4 Hz, 2H); ^{13}CNMR (125 MHz, DMSO-d_6): 173.85, 167.54, 150.34, 141.22, 140.84, 128.24, 127.40, 125.99, 108.76, 65.88, 59.39. HRMS (-ESI): calcd 247.0606; found 247.0610.

2-((4-fluorophenyl)(hydroxy)methyl)-3-hydroxy-6-(hydroxymethyl)-4H-pyran-4-one (1b): $C_{13}H_{11}FO_5$ obtained in 98% yield as an orange solid. M.pt: 195-205°C. ^{1}HNMR (400 MHz, CD3OD): δ 4.27 (dd, *J* = 15.7 Hz, 30.0Hz, 2H), 6.05 (s, 1H), 6.34 (s, 1H), 6.98 (t, *J* = 8.7 Hz, 2H), 7.39 (dd, *J* = 8.4, 5.5 Hz, 2H); ^{13}CNMR (125 MHz, CD_3OD): 176.9, 169.6, 165.0, 162.6, 142.9, 137.7, 129.3, 116.3, 110.9, 68.0, 61.2. HRMS (-ESI): calcd 265.0512; found 265.0514.

2-((4-chlorophenyl)(hydroxy)methyl)-3-hydroxy-6-(hydroxymethyl)-4H-pyran-4-one (1c): $C_{13}H_{11}ClO_5$ obtained in 97% yield as a red solid. M.pt: 130-140°. ^{1}HNMR (400 MHz, CD_3OD): δ 4.27 (dd, *J* = 15.7 Hz, 30.0 Hz, 2H), 6.05 (s, 1H), 6.34 (s, 1H), 7.25 (d, *J* = 8.4 Hz, 2H), 7.35

(d, *J* = 8.4 Hz, 2H); ^{13}CNMR (125 MHz, CD_3OD+DMSO-d_6): 176.61, 169.81, 151.77, 142.81, 140.95, 134.55, 129.76, 129.16, 110.09, 67.78, 61.17. HRMS (-ESI): calcd 281.0217; found 281.0219

2-((4-bromophenyl)(hydroxy)methyl)-3-hydroxy-6-(hydroxymethyl)-4H-pyran-4-one (1d): $C_{13}H_{11}BrO_5$ obtained in 94% yield as a red solid. M.pt: 95-105°C. ^{1}HNMR (400 MHz, CD_3OD): δ 4.33 – 4.16 (dd, *J* = 15.7 Hz, 27.2 Hz, 2H), 6.04 (s, 1H), 6.34 (s, 1H), 7.29 (d, *J* = 7.5 Hz, 2H), 7.40 (d, *J* = 7.0 Hz, 2H); ^{13}CNMR (125 MHz, CD_3OD): 176.73, 169.82, 151.61, 142.84, 141.13, 132.61, 129.20, 122.68, 109.84, 67.86, 61.10. HRMS (+ESI): calcd 328.9848; found 328.9840.

3-hydroxy-2-(hydroxy(4-methoxyphenyl)methyl)-6-(hydroxymethyl)-4H-pyran-4-one (1e): $C_{14}H_{14}O_6$ obtained in 91% yield as a red solid. M.pt: 210-220°C. ^{1}HNMR (400 MHz, DMSO-d_6+D_2O): δ 3.70 (s, 3H), 4.26 (dd, *J* = 15.7 Hz, 26.8 Hz 2H), 5.91 (s, 1H), 6.31 (s, 1H), 6.88 (d, *J* = 8.4 Hz, 2H), 7.30 (d, *J* = 8.4, 2H); ^{13}CNMR (125 MHz, DMSO-d_6): 173.89, 167.43, 158.57, 150.62, 140.52, 133.14, 127.7, 113.61, 108.72, 65.60, 59.41, 55.00. HRMS (-ESI): calcd 277.0712 ; found 277.0714.

2-((2,5-dimethoxyphenyl)(hydroxy)methyl)-3-hydroxy-6-(hydroxymethyl)-4H-pyran-4-one (1f): $C_{15}H_{16}O_7$ obtained in 89% yield as a red solid. M.pt: 240-250°C. ^{1}HNMR (400 MHz, CD_3OD): δ 3.61 (s, 3H), 3.73 (s, 3H), 4.24 (dd, *J* = 15.7 Hz, 32.6 Hz, 2H), 6.33 (s, 1H), 6.34 (s, 1H), 6.87 (d, *J* = 8 Hz, 1H), 7.00 (t, *J* = 8 Hz, 1H), 7.13 (d, *J* = 7.6 Hz, 1H); ^{13}CNMR (125 MHz CD_3OD): 176.97, 169.54, 155.23, 151.93, 142.99, 130.47, 114.85, 114.42, 112.95, 109.63, 64.02, 61.10, 56.72, 56.13. HRMS (-ESI): calcd 307.0818; found 307.0820.

2-((2,3-dimethoxyphenyl)(hydroxy)methyl)-3-hydroxy-6-(hydroxymethyl)-4H-pyran-4-one (1g): $C_{15}H_{16}O_7$ obtained in 89% yield as a red solid. M.pt: 240-250°C. ^{1}HNMR (400MHz, CD_3OD): δ 3.61 (s, 3H), 3.73 (s, 3H), 4.24 (q, *J* = 15.7 Hz, 2H), 6.33 (s, 1H), 6.34 (s, 1H), 6.87 (d, *J* = 8 Hz, 1H), 7.00 (t, *J* = 8 Hz, 1H), 7.13 (d, *J* = 7.6 Hz, 1H); ^{13}CNMR (125MHz, DMSO-d_6): 173.95, 167.32, 151.90, 150.05, 145.36, 134.38, 123.60, 119.55, 111.92, 108.62, 61.02, 59.89, 59.29, 55.54. HRMS (-ESI): calcd 307.0818 and found 307.0820.

3-hydroxy-2-(hydroxy(naphthalen-2-yl)methyl)-6-(hydroxymethyl)-4H-pyran-4-one (1h): $C_{17}H_{14}O_5$ obtained in 89% yield as a dark red solid. M.pt: 250-260°C. ^{1}HNMR (400MHz, CD_3OD): δ 4.25 (dd, *J* = 15.7 Hz, 35.7 Hz, 2H), 6.24 (s, 1H), 6.35 (s, 1H), 7.37 (s, 2H), 7.47 (d, *J* = 7.9 Hz, 1H), 7.74 (s, 3H), 7.86 (s, 1H); ^{13}CNMR (125MHz, CD_3OD): 176.76, 169.83,

152.09, 142.87, 139.18, 134.74, 134.56, 129.27, 129.07, 128.68, 127.31, 127.15, 126.00, 125.20, 109.82, 68.64, 61.13. HRMS (+ESI): calcd 299.0919 and found 299.0916.

3-hydroxy-6-(hydroxymethyl)-2-(1-hydroxypentyl)-4H-pyran-4-one (1i): $C_{11}H_{16}O_5$ obtained in 78% yield as a brown semisolid. ^{1}HNMR (400MHz, DMSO-d_6): δ 0.83 (t, J = 6.8 Hz, 3H), 1.21-1.28 (m, 4H), 1.58-1.71 (m, 2H), 4.30 (d, J = 5.6 Hz, 2H), 5.77 (t, J = 5.6 Hz, 1H), 6.32 (s, 1H); ^{13}CNMR (125MHz, DMSO-d_6): 173.88, 167.36, 151.12, 140.78, 108.61, 64.23, 59.46, 33.54, 27.14, 21.80, 13.83. HRMS (-ESI): calcd 227.0919 and found 227.0921.

3-hydroxy-6-(hydroxymethyl)-2-(1-hydroxynonyl)-4H-pyran-4-one (1j): $C_{15}H_{24}O_5$ obtained in 72% yield as a brown semisolid. ^{1}HNMR (400MHz, CD_3OD): δ 0.77-0.79 (m, 3H), 1.18-1.19 (m, 12H), 1.67-1.73 (m, 2H), 4.33 (s, 2H), 5.39 (s, 1H), 6.36 (s, 1H); ^{13}CNMR (125MHz, CD_3OD): 176.67, 169.59, 152.84, 142.83, 109.75, 66.89, 61.25, 35.25, 33.41, 30.60, 30.42, 30.36, 26.47, 23.74, 14.46. HRMS (+ESI): calcd 285.1702 and found 285.1698.

4.3. General procedure for preparation of compounds 2a-2j: compound **1a-1j** (1 equiv.), silica-H_2SO_4 (10 mol%) and indole (1.5 equiv) taken in CH_3CN as solvent was stirred at 80 ^oC for 2 hr. After completion of the reaction, the product was extracted with ethyl acetate (3×15 ml). The combined organic layer was dried with anhydrous sodium sulphate, concentrated in vacuo, and purified by column chromatography (methanol: dichloromethane =0.25:9.75) to afford the pure product.

2-((1H-indol-3-yl)(phenyl)methyl)-3-hydroxy-6-(hydroxymethyl)-4H-pyran-4-one (2a): $C_{21}H_{17}NO_4$ obtained in 96% yield as a colourless solid. M.pt: 210-220°C. ^{1}HNMR (400MHz, CD_3OD): δ 4.20 (s, 2H), 5.96 (s, 1H), 6.35 (s, 1H), 6.82 (t, J = 7.5 Hz, 1H), 6.95 (s, 1H), 6.98 (t, J = 7.6 Hz, 1H), 7.14 (t, J = 7.1 Hz, 1H), 7.20 (t, J = 7.5 Hz, 3H), 7.26 (t, J = 8.2 Hz, 3H); ^{13}CNMR (125MHz, DMSO-d_6): 173.63, 167.22, 151.05, 140.78, 140.34, 136.07, 128.43, 128.13, 126.85, 126.26, 123.86, 121.29, 118.77, 118.37, 112.75, 111.61, 108.94, 59.55. 41.07. HRMS (+ESI): calcd 348.1236 and found 348.1235.

2-((4-fluorophenyl)(1H-indol-3-yl)methyl)-3-hydroxy-6-(hydroxymethyl)-4H-pyran-4-one (2b): $C_{21}H_{16}FNO_4$ obtained in 98% yield as a brown solid. M.pt: 230-240°C. ^{1}HNMR (400MHz, CD_3OD): δ 4.30 (s, 2H), 6.11 (s, 1H), 6.49 (s, 1H), 6.93-7.00 (m, 3H), 7.06-7.07 (m, 2H), 7.30-7.37(m, 4H); ^{13}CNMR (125MHz, CD_3OD): 176.62, 169.44, 164.24, 162.30, 153.94, 142.73, 138.22, 137.43, 131.42, 127.91, 125.00, 122.84, 120.12, 116.22, 114.41, 112.59, 109.98, 61.25, 41.40. HRMS (+ESI): calcd 366.1142 and found 366.1144.

2-((4-chlorophenyl)(1H-indol-3-yl)methyl)-3-hydroxy-6-(hydroxymethyl)-4H-pyran-4-one (2c): $C_{21}H_{16}ClNO_4$ obtained in 96% yield as a brown solid. M.pt: 180-190°C. ^{1}HNMR (400MHz, CD_3OD): δ 4.20 (s, 2H), 5.98 (s, 1H), 6.34 (s, 1H), 6.84 (t, *J* = 7.5 Hz, 1H), 6.95-7.00 (m, 2H), 7.17-7.27 (m, 6H); ^{13}CNMR (125MHz, CD_3OD): 173.04, 169.49, 153.51, 142.83, 140.37, 138.22, 133.80, 131.23, 129.57, 127.87, 125.02, 122.80, 120.08, 119.82, 114.01, 112.51, 109.91, 61.21, 41.46. HRMS (+ESI): calcd 382.0846 and found 382.0848.

2-((4-bromophenyl)(1H-indol-3-yl)methyl)-3-hydroxy-6-(hydroxymethyl)-4H-pyran-4-one (2d): $C_{21}H_{16}BrNO_4$ obtained in 94% yield as a brown solid. M.pt: 170-180°C. ^{1}HNMR (400MHz, CD_3OD): δ 4.33 (s, 2H), 6.09 (s, 1H), 6.48 (s, 1H), 6.96 (t, *J* = 7.4 Hz, 1H), 7.00-7.15 (m, 2H), 7.30 (d, *J* = 8.0 Hz, 3H), 7.38 (d, *J* = 8.1 Hz, 1H), 7.47 (d, *J* = 8.2 Hz, 2H); ^{13}CNMR (125MHz, CD_3OD): 173.04, 169.49, 153.51, 142.83, 140.84, 138.22, 132.58, 131.56, 127.85, 125.02, 122.80, 121.78, 120.09, 119.78, 113.90, 112.50, 109.95, 61.23, 41.54. HRMS (+ESI): calcd 426.0341 and found 426.0333.

2-((1H-indol-3-yl)(4-methoxyphenyl)methyl)-3-hydroxy-6-(hydroxymethyl)-4H-pyran-4-one (2e): $C_{22}H_{19}NO_5$ obtained in 91% yield as a brown solid. M.pt: 230-240°C. ^{1}HNMR (400MHz, CD_3OD): δ 3.78 (s, 3H), 4.31 (s, 2H), 6.05 (s, 1H), 6.48 (s, 1H), 6.87 (d, *J* = 8.3 Hz, 2H), 6.94 (t, *J* = 7.4 Hz, 1H), 7.05 (s, 1H), 7.09 (t, *J* = 7.5 Hz, 1H), 7.33 (dd, *J* = 25.2, 8.2 Hz, 4H); ^{13}CNMR (125MHz, CD_3OD): 176.75,169.32, 160.02, 154.80, 142.51, 138.32, 138.17, 133.43, 130.70, 127.96, 125.03, 122.80, 119.97, 114.95,114.82, 112.57, 109.98, 61.24, 55.99, 41.33. HRMS (+ESI): calcd 378.1341 and found 378.1343.

2-((2,5-dimethoxyphenyl)(1H-indol-3-yl)methyl)-3-hydroxy-6-(hydroxymethyl)-4H-pyran-4-one (2f): $C_{23}H_{21}NO_6$ obtained in 89% yield as a brown solid. M.pt: 230-240°C. ^{1}HNMR (400MHz, CD_3OD): δ 3.64 (s, 3H), 3.74 (s, 3H), 4.22 (d, *J* = 8.0 Hz, 2H), 6.24 (s, 1H), 6.34 (s, 1H), 6.82-6.88 (m, 3H), 6.98 (t, *J* = 7.5 Hz, 1H), 7.06 (s, 1H), 7.10 – 7.19(m, 1H), 7.24 (d, *J* = 8.1 Hz, 1H), 7.35 (d, *J* = 7.9 Hz, 1H); ^{13}CNMR (125MHz, CD_3OD): 176.63, 169.56, 153.06, 144.37, 142.17, 138.08,127.72, 127.62, 126.99, 125.62, 124.49, 122.77, 120.08, 119.74, 114.68, 112.45, 109.79, 61.18, 56.42, 56.11, 37.43. HRMS (+ESI): calcd 408.1447 and found 408.1449.

2-((2,3-dimethoxyphenyl)(1H-indol-3-yl)methyl)-3-hydroxy-6-(hydroxymethyl)-4H-pyran-4-one (2g): $C_{23}H_{21}NO_6$ obtained in 89% yield as a brown solid. M.pt: 230-240°C. ^{1}HNMR (400MHz, CD_3OD): δ 3.65 (s, 3H), 3.75 (s, 3H), 4.20 (s, 2H), 6.36 (s, 1H), 6.39 (s, 1H), 6.80-6.89 (m, 5H), 6.97 (t, *J* = 7.7 Hz, 1H), 7.22 (t, *J* = 7.7 Hz, 2H); ^{13}CNMR (125MHz,

CD_3OD): 176.57, 169.31, 154.23, 154.10, 148.09, 142.64, 138.16, 134.95, 128.02, 124.96, 122.86, 119.93, 119.62, 114.85, 112.65, 112.40, 109.87, 61.25,56.34, 56.24, 35.54. HRMS (+ESI): calcd408.1447 and found 408.1449.

2-((1H-indol-3-yl)(naphthalen-2-yl)methyl)-3-hydroxy-6-(hydroxymethyl)-4H-pyran-4-one (2h): $C_{25}H_{19}NO_4$ obtained in 91% yield as a brown solid. M.pt: 230-240°C. ^{1}HNMR (400MHz, CD_3OD): δ 4.21 (s, 2H), 6.18 (s, 1H), 6.37 (s, 1H), 6.82 (t, *J* = 7.5 Hz, 1H), 6.93 -7.06 (m, 2H), 7.22 (d, *J* = 8.0 Hz, 1H), 7.27 (d, *J* = 8.2 Hz, 1H), 7.33 (dd, *J* = 6.1, 3.2 Hz, 2H), 7.42 (d, *J* = 8.4 Hz, 1H), 7.63-7.72 (m, 4H); ^{13}CNMR (125MHz, CD_3OD+DMSO-d_6): 176.17, 169.49, 153.43, 142.85, 139.59, 138.13, 134.96, 134.03, 129.57, 129.31, 129.01, 128.39, 128.27, 128.23, 127.73, 127.40, 125.56, 123.12, 120.51, 120.17, 114.63, 113.11, 110.45, 61.37, 42.13. HRMS (+ESI): calcd 398.1392 and found 398.1389.

2-(1-(1H-indol-3-yl)pentyl)-3-hydroxy-6-(hydroxymethyl)-4H-pyran-4-one (2i): $C_{19}H_{21}NO_4$ obtained in 87% yield as a brown solid. M.pt: 130-140°C. ^{1}HNMR (400MHz, CD_3OD): δ 0.91 (t, *J* = 6.9 Hz, 3H), 1.21 – 1.53 (m, 4H), 2.03 – 2.33 (m, 2H), 3.37 (s, 1H), 4.36 (q, *J* = 15.5 Hz, 2H), 6.42 (s, 1H), 6.99 (t, *J* = 7.4 Hz, 1H), 7.08 (t, *J* = 7.4 Hz, 1H), 7.23 (s, 1H), 7.33 (d, *J* = 8.1 Hz, 1H), 7.66 (d, *J* = 7.9 Hz, 1H); ^{13}CNMR (125MHz, CD_3OD): 176.41, 169.21, 155.66, 142.53, 137.96, 128.09, 123.39, 122.51, 119.80, 119.72, 115.61, 112.29, 109.49, 61.25, 36.12, 33.14, 28.75, 23.74, 14.46. HRMS (+ESI): calcd 328.1549 and found 328.1551.

2-(1-(1H-indol-3-yl)nonyl)-3-hydroxy-6-(hydroxymethyl)-4H-pyran-4-one (2j): $C_{23}H_{29}NO_4$ obtained in 86% yield as a brown solid. M.pt: 110-120°C. ^{1}HNMR (400MHz, CD_3OD): δ 0.90 (t, *J* = 6.6 Hz, 3H), 1.46 – 1.19 (m, 12H), 2.29 – 2.04 (m, 2H), 3.33 (s, 1H), 4.36 (q, *J* = 15.5 Hz, 2H), 6.41 (s, 1H), 6.99 (t, *J* = 7.4 Hz, 1H), 7.09 (t, *J* = 7.5 Hz, 1H), 7.23 (s, 1H), 7.34 (d, *J* = 8.1 Hz, 1H), 7.65 (d, *J* = 7.9 Hz, 1H); ^{13}CNMR (125MHz, CD_3OD): 176.41, 169.21, 155.66, 142.53, 137.96, 128.09, 123.39, 122.51, 119.80, 119.72, 115.61, 112.29, 109.52, 61.25, 36.12, 33.14, 33.01, 30.58,30.42, 30.37, 28.75, 23.74, 14.46. HRMS (+ESI): calcd 384.2175 and found 384.2171.

4.4. General procedure for preparation of compounds 2k-2p and 3a-3f: Compound **1a** (1 equiv.), silica-H_2SO_4 (10 mol%), substituted indoles and other nucleophiles (1.5 equiv) was stirred in CH_3CN at 80 ^oC for 2 hr. After completion of the reaction, the product was extracted with ethyl acetate (3x15 ml). The combined organic layer was dried with anhydrous sodium

sulphate, concentrated in vacuo, and purified by column chromatography (methanol: dichloromethane =0.25:9.75) to afford the pure product.

3-hydroxy-6-(hydroxymethyl)-2-(phenyl(2-phenyl-1H-indol-3-yl)methyl)-4H-pyran-4-one (2k): $C_{27}H_{21}NO_4$ obtained in 89% yield as a grey solid. M.pt: 190-200°C ^{1}HNMR (400MHz, CD_3OD): δ 4.11 (dd, *J* = 56.8, 15.8 Hz, 2H), 6.15 (s, 1H), 6.36 (s, 1H), 6.77 (t, *J* = 7.6 Hz, 1H), 6.98 (dd, *J* = 15.5, 7.7 Hz, 3H), 7.20 – 7.03 (m, 4H), 7.27 (t, *J* = 7.2 Hz, 2H), 7.35 (t, *J* = 7.5 Hz, 2H), 7.48 (d, *J* = 7.5 Hz, 2H); ^{13}CNMR (125MHz, DMSO-d_6): 173.73, 167.51, 150.71, 141.49, 140.14, 136.88, 136.32, 132.17, 128.79, 128.68, 128.36, 127.96, 127.34, 126.41, 121.38, 121.17, 118.76, 11.32, 108.98, 59.35, 41.8. HRMS (+ESI): calcd 424.1549 and found 424.1552.

3-hydroxy-6-(hydroxymethyl)-2-((5-methoxy-1H-indol-3-yl)(phenyl)methyl)-4H-pyran-4-one (2l): $C_{22}H_{19}NO_5$ obtained in 92% yield as a brown solid. M.pt: 130-140°C ^{1}HNMR (400MHz, CD_3OD): δ 3.21 (s, 3H), 4.21 (s, 2H), 5.95 (s, 1H), 6.36 (s, 1H), 6.57 – 6.72 (m, 2H), 6.91 (s, 1H), 7.15 (dd, *J* = 8.1, 5.6 Hz, 2H), 7.21 (t, *J* = 7.4 Hz, 2H), 7.21 (t, *J* = 7.4 Hz, 2H), 7.29 (d, *J* = 7.3 Hz, 2H); ^{13}CNMR (125MHz, DMSO-d_6): 173.96, 167.17, 153.01, 151.51, 140.62, 139.95, 130.89, 128.49, 128.11, 126.92, 126.54, 124.37, 112.48, 112.34, 111.16, 108.94, 100.37, 59.34, 55.23, 41.8. HRMS (+ESI): calcd 378.1341 and found 378.1345.

3-((3-hydroxy-6-(hydroxymethyl)-4-oxo-4H-pyran-2-yl)(phenyl)methyl)-1H-indole-5-carbonitrile (2m): $C_{22}H_{16}N_2O_4$ obtained in 94% yield as a colourless solid. M.pt: 240-250°C ^{1}HNMR (400MHz, CD_3OD): δ 4.21 (d, *J* = 3.1 Hz, 2H), 6.02 (s, 1H), 6.36 (s, 1H), 7.16-7.25 (m, 7H), 7.40 (d, *J* = 8.5 Hz, 1H), 7.58 (s, 1H); ^{13}CNMR (125MHz, CD_3OD): 176.56, 169.42, 153.24, 142.88, 140.80, 140.05, 129.74, 129.5, 128.36, 127.88, 127.83, 125.75, 125.50, 121.75, 115.81, 113.81, 110.10, 102.65, 61.26, 41.81. HRMS (+ESI): calcd 373.1188 and found 373.1191.

5-hydroxy-2-(hydroxymethyl)-3-((1-methyl-1H-indol-3-yl)(phenyl)methyl)-4H-pyran-4-one (2n): $C_{22}H_{19}NO_4$ obtained in 91% yield as a dark red solid. M.pt: 180-190°C. ^{1}HNMR (400MHz, CD_3OD): δ 3.64 (s, 3H, NMe), 4.20 (s, 2H), 5.98 (s, 1H), 6.34 (s, 1H), 6.82 – 6.88 (m, 2H), 7.04 (t, *J*= 7.2Hz, 1H), 7.12-7.27(m, 7H); ^{13}CNMR (125MHz, DMSO-d_6 +CD_3OD): 173.68, 166.76, 151.02, 139.97, 138.86, 135.95, 126.82, 125.86, 125.47, 120.22, 117.48, 111.20, 107.94, 58.53, 39.2, 30.30. HRMS (+ESI): calcd 362.1392 and found 362.1389.

5-hydroxy-2-(hydroxymethyl)-3-((1-pentyl-1H-indol-3-yl)(phenyl)methyl)-4H-pyran-4-one (2o): $C_{26}H_{27}NO_4$ obtained in 89% yield as a dark brown solid. M.pt: 150-160°C. ^{1}HNMR

(400MHz, CD_3OD): δ 0.90 (t, *J* = 7.1 Hz, 3H), 1.23 – 1.40 (m, 8H), 1.73 – 1.91 (m, 2H), 4.32 (s, 2H), 6.11 (s, 1H), 6.48 (s, 1H), 6.97 (t, *J* = 7.4 Hz, 1H), 7.06 (s, 1H), 7.15 (t, *J* = 7.6 Hz, 1H), 7.23-7.39 (m, 7H); ^{13}CNMR (125MHz, CD_3OD): 137.91, 129.55, 128.52, 128.05, 122.69, 122.04, 120.21, 119.98, 110.68, 61.23, 47.06, 31.04, 30.73, 30.16, 23.36, 14.39. HRMS (+ESI): calcd 418.2018 and found 418.2015.

3-((1-benzyl-1H-indol-3-yl)(phenyl)methyl)-5-hydroxy-2-(hydroxymethyl)-4H-pyran-4-one (2p): $C_{28}H_{23}NO_4$ obtained in 89% yield as a colourless solid. M.pt: 160-170°C. ^{1}H NMR (400 MHz,CD_3OD) δ 4.19 (s, 2H), 5.25 (s, 2H), 6.03 (s, 1H), 6.39 (s, 1H), 6.85 (t, *J*=6.8 Hz 1H), 6.97-7.02 (m, 4H), 7.12-7.28 (m, 10H), ^{13}CNMR (125MHz, DMSO-d_6): 173.73, 167.51, 150.71, 141.49, 140.14, 136.88, 136.32, 132.17, 128.79, 128.68, 128.36, 127.96, 127.34, 126.41, 121.38, 121.17, 118.76, 111.32, 108.98, 59.35, 54.89, 50.12. HRMS (+ESI): calcd 437.1627 and found 437.1625.

3-hydroxy-6-(hydroxymethyl)-2-(phenyl(phenylthio)methyl)-4H-pyran-4-one (3a): $C_{19}H_{16}O_4S$ obtained in 94% yield as a red solid. M.pt: 80-90°C. ^{1}H NMR (400 MHz,CD_3OD) δ 4.32 (q, *J* = 15.7 Hz, 2H), 5.86 (s, 1H), 6.26 (s, 1H), 7.14 (d, *J* = 3.9 Hz, 3H), 7.21 (d, *J* = 7.0 Hz, 1H), 7.25 (t, *J* = 7.3 Hz, 2H), 7.28 – 7.34 (m, 2H), 7.46 (d, *J* = 7.3 Hz, 2H), ^{13}CNMR (125MHz, DMSO-d_6):173.32, 167.50, 146.85, 141.68, 136.91, 133.50, 131.30, 129.08, 128.78, 128.24, 128.09, 127.66, 108.85, 59.42, 48.56. HRMS (+ESI): calcd 341.0848 and found 341.0846.

3-hydroxy-6-(hydroxymethyl)-2-(((4-methoxyphenyl)thio)(phenyl)methyl)-4H-pyran-4-one (3b): $C_{20}H_{18}O_5S$ obtained in 89% yield as a light brown solid. M.pt: 110-120°C. ^{1}HNMR (400MHz, CD_3OD): δ δ 3.64 (s, 3H), 4.34 (q, *J* = 15.6 Hz, 2H), 5.70 (s, 1H), 6.27 (s, 1H), 6.70 (d, *J* = 8.7 Hz, 2H), 6.77 (d, *J* = 8.8 Hz, 1H), 7.14 – 7.30 (m, 5H), 7.43 (d, *J* = 7.1 Hz, 2H); ^{13}CNMR (125MHz, CD_3OD): 176.08, 169.60, 161.83, 150.15, 143.16, 138.43, 137.26, 129.77, 129.75, 129.17, 124.90, 115.56, 109.69, 61.23, 55.65, 51.43. HRMS (+ESI): calcd 371.0953 and found 371.0943.

3-hydroxy-6-(hydroxymethyl)-2-((4-hydroxyphenyl)(phenyl)methyl)-4H-pyran-4-one (3c): $C_{19}H_{16}O_5$ obtained in 92% yield as a orange solid. M.pt: 170-180°C; ^{1}HNMR (400MHz, CD_3OD): δ 4.19-4.22 (m, 2H), 5.69 (s, 1H), 6.36 (s, 1H), 6.63 (d, *J* = 8.4 Hz, 2H), 6.95 (d, *J* =8.4 Hz, 2H), 7.10 – 7.19 (m, 5H); ^{13}CNMR (125MHz, DMSO-d_6): 173.55, 170.37, 167.25, 156.20,

150.41, 141.55, 140.63, 130.10, 129.73, 128.46, 126.71, 115.23, 108.91, 59.77, 46.96. HRMS (+ESI): calcd 325.1076 and found 325.1077.

3-hydroxy-6-(hydroxymethyl)-2-((5-methylthiophen-2-yl)(phenyl)methyl)-4H-pyran-4-one (3d): $C_{18}H_{16}O_4S$ obtained in 87% yield as a light brown solid. M.pt: 80-90°C. ^{1}HNMR (400MHz, CD_3OD): δ 2.31 (s, 3H), 4.26 (s, 2H), 5.89 (s, 1H), 6.36 (s, 1H), 6.52 (d, *J* = 3.24 Hz, 1H), 6.58 (d, *J* = 3.24 Hz, 1H) 7.14 – 7.23 (m, 5H); ^{13}CNMR (125MHz, DMSO-d_6): 173.59, 167.37, 149.09, 141.24, 139.97, 139.57, 138.94, 128.58, 128.01, 127.20, 126.40, 124.90, 109.01, 59.45, 43.32, 14.86. HRMS (+ESI): calcd 329.0848 and found 329.0850.

2-(benzo[b]thiophen-3-yl(phenyl)methyl)-3-hydroxy-6-(hydroxymethyl)-4H-pyran-4-one (3e): $C_{21}H_{17}O_4S$ obtained in 87% yield as a colourless solid. M.pt: 140-150°C. ^{1}HNMR (400MHz, CD_3OD): δ 4.23-4.25 (m, 2H), 6.11 (s, 1H), 6.33 (s, 1H), 6.26-7.50 (m, 7H), 7.50 (s, 1H) 7.65 (d, *J* = 8Hz 2H) 8.00 (d, J=7.2 Hz, 1H); ^{13}CNMR (125MHz, DMSO-d_6): 173.64, 167.44, 149.25, 141.42, 139.55, 138.69, 137.83, 133.87, 128.68, 128.44, 127.24, 125.12, 124.55, 124.31, 123.04, 121.64, 109.05, 59.44, 42.21. HRMS (+ESI): calcd 365.0848 and found 365.0843.

3-hydroxy-6-(hydroxymethyl)-2-(phenyl(1H-pyrrol-2-yl)methyl)-4H-pyran-4-one (3f): $C_{17}H_{15}NO_4$ obtained in 85% yield as a black solid. M.pt: 120-130°C. ^{1}HNMR (400MHz, CD_3OD): δ 4.26 (q, *J* = 15.6 Hz, 2H), 5.77 (s, 1H), 5.89 -5.95 (m, 2H), 6.35 (s, 1H), 6.59 (s, 1H), 7.12-7.20 (m, 5H); ^{13}CNMR (125MHz, DMSO-d_6): 173.64, 167.28, 149.93, 140.91, 140.38, 128.37, 127.89, 116.79, 117.41, 108.90, 107.43, 106.97, 59.47, 48.57, 41.37. HRMS (-ESI): calcd 296.0923 and found 296.0924.

4.5. Glucose Uptake Assay All the synthesized compounds were evaluated for glucose uptake stimulatory effect in L6 skeletal muscle cells stably expressing rat GLUT4 with a myc epitope inserted in the first exofacial loop (L6-GLUT4*myc*), a kind gift of Dr Amira Klip, Program in Cell Biology, The Hospital for Sick Children, Toronto, Canada. Cells were maintained in DMEM supplemented with 10% FBS and 1% antibiotic/antimycotic solution (10,000 U/ml penicillin G, 10 mg/ml streptomycin, 25 µg/ml amphotericin B) in a humidified atmosphere of air and 5% CO_2 at 37°C [26,27]. Differentiation was induced by switching confluent cells to medium supplemented with 2% FBS. Experiments were performed in differentiated myotubes 6–7 days after seeding. At differentiated myotubes stage the cells were treated with test compounds 16 hours and glucose uptake was measured by incubating cells for 5

min in HEPES-buffered saline containing 10 µM 2-DG (0.5 µCi/ml 2-[^{3}H] DG) at room temperature, followed by cell lysis and measurement of radioactivity incorporated by scintillation counting, as described previously [25]. Nonspecific uptake was determined in the presence of cytochalasin B (25 µM) during the assay and these values were subtracted from all other values. Glucose uptake measured in duplicates and normalized to total protein, was expressed as percent stimulation activity with respect to control cells.

4.6. GLUT4 translocation assay. GLUT4 translocation to cell surface was determined in L6-GLUT4*myc* myotubes by measuring the cell surface level of GLUT4*myc* by an antibody-coupled colorimetric assay as previously described [23]. Essentially, cells grown in 24-well plates and treated as indicated were fixed in 3% paraformaldehyde for 30 min and quenched in 100 mM glycine for 10 min. Following blocking with 5% skimmed milk for 10 min, cells were incubated with anti-*myc* antibody solution (1.0 µg/ml in PBS with 3% skimmed milk) for 1 h. After labeling, excess antibodies were removed by extensive washing in ice-cold PBS. Cell surface GLUT4-bound antibodies were probed by HRP-conjugated secondary antibodies followed by detection of bound HRP by O-phenylenediamine dihydrochloride reagent. The reaction was stopped by addition of 3N HCl and the supernatant was collected to read optical density at 492 nm. The fraction of GLUT4*myc* at the cell surface, measured in triplicate, was expressed as fold induction with respect to unstimulated cells.

4.7. Inhibitor study for PI3K. Experiments were performed in differentiated myotubes 6–7 days after seeding. At differentiated myotubes stage the cells were treated with test compounds 16 hours with final one hour in presence of wortmannin (1µm) and glucose uptake was measured by incubating cells for 5 min in HEPES-buffered saline containing 10 µM 2-DG (0.5 µCi/ml 2-[^{3}H] DG) at room temperature, followed by cell lysis and measurement of radioactivity incorporated by scintillation counting, as described previously [25]. Nonspecific uptake was determined in the presence of cytochalasin B (25 µM) during the assay and these values were subtracted from all other values. Glucose uptake measured in duplicates and normalized to total protein, was expressed as percent stimulation activity with respect to control cells.

Acknowledgments

Authors are thankful to Director IIIM Jammu for encouragement and DST (GAP-1145) for funding.

Supplementary data

^{1}H, ^{13}C NMR and experimental details are provides in SI.

References

[1] V. Kumar, N. Fausto, A. K. Abbas, R. S. Cotran, S. L. Robbins, Robbins and Cotran Pathologic Basis of Disease (7th ed.). Philadelphia, Pa., Saunders. (2005) 1194–1195. ISBN 0-7216-0187-1.

[2] P. Hossain, B. Kawar, M. El Nahas, Obesity and diabetes in the developing world-a growing challenge, N. Eng. J. Med. 356 (2007) 213-215.

[3] T. J. Hsieh, Y. H. Tsai, M. C. Liao, Y. C. Du, P. J. Lien, C. C. Sun, F. R. Chang, Y. C. Wu, Anti-diabetic properties of non-polar Toona sinensis Roem extract prepared by supercritical-CO_2 fluid. Food Chem. Toxicol. 50 (2011) 779-789.

[4] K. L. Hoehn, C. Hohnen Behrens, A. Cederberg, L. E. Wu, N. Turner, T. Yuasa, Y. Ebina, D. E. James, IRS1-independent defects define major nodes of insulin resistance. Cell Metab. 7 (2008) 421-433.

[5]R. A. DeFronzo, E. Jacot, E. Maeder, J. Wahren, J. P. Felber, The effect of insulin on the disposal of intravenous glucose. Results from indirect calorimetry and hepatic and femoral venous catheterization, Diabetes. 30 (1981) 1000-1007.

[6] F. H. Ziel, N. Venkatesan, M. B. Davidson, Glucose transport is rate limiting for skeletal muscle glucose metabolism in normal and STZ-induced diabetic rats. Diabetes. 37 (1988) 885-890.

[7] N. J. Bryant, R. Govers, D. E. James Regulated transport of the glucose transporter GLUT4. Nature Rev. Mol. Cell Biol. 3 (2002) 267–277.

[8] B. Zhang, G. Salituro, D. Szalkowski, Z. Li, Y. Zhang, I. Royo, D. Vilella, M. T. Díez, F. Pelaez, C. Ruby, R. L. Kendall, X. Mao, P. Griffin, J. Calaycay, J. R. Zierath, J. V. Heck, R. G. Smith, D. E. Moller, Discovery of a small molecule insulin mimetic with antidiabetic activity in mice, Science. 284 (1999) 974-977.

[9] R. P. Nankar, M. Doble, Non-peptidyl insulin mimetics as a potential antidiabetic agent. Drug Discovery Today, 18 (2013) 748–755.

[10] K. He, C. B. Chan, X. Liu, Y. Jia, H. R. Luo, S. A. France, Y. Liu, W. D. Wilson. K. Ye, Identification of a molecular activator for insulin receptor with potent anti-diabetic effects, J Biol Chem. 286 (2011) 37379-88.

[11] M. C. Pirrung, L. Deng, B. Lin, N. J. Webster, Quinone replacements for small molecule insulin mimics, Chembiochem. 9 (2008) 360-362.

[12] X. Xiong, M. C. Pirrung, Modular synthesis of candidate indole-based insulin mimics by Claisen rearrangement, Org Lett. 10 (2008) 1151-1154.

[13] J. E. Henriksen, F. Alford, A. Handberg, A. Vaag, G. M. Ward, A. Kalfas, H. B. Nielsen, Increased glucose effectiveness in normoglycemic but insulin-resistant relatives of patients with non-insulin-dependent diabetes mellitus. A novel compensatory mechanism, J. Clin. Invest. 94 (1994) 1196-1204.

[14] S. E. Leney, J. M. Tavare, The molecular basis of insulin-stimulated glucose uptake: signalling, trafficking and potential drug targets, J. Endocrinol. 203 (2009) 1-8.

[15] M. Rosfarizan, S. Madihah, A. B. Ariff, Isolation of a kojic acid-producing funguscapable of using starch as a carbon source. Lett. Appl. Microbiol. 26 (1998) 27-30.

[16] B. V. S. Reddy, M. R. Reddy, C. Madan, K. P. Kumar, M. S. Rao, Indium(III) chloride catalyzed three-component coupling reaction: A novel synthesis of 2-substituted aryl(indolyl)kojic acid derivatives as potent antifungal and antibacterial agents, Bioorg. Med. Chem. Lett. 20 (2010) 7507–7511.

[17] G. Babu, N. Sreedhar, P. T. Perumal, A convenient method of synthesis of bis(indolyl)-methane indiumtrichloride catalyzed reactions of indole with aldehydes and schiff bases. Synth. Commun. 30 (2000) 1609–1614.

[18] C. Ramesh, P. M. Lei, D. Janreddy, V. Kavala, C.W. Kuo, C. F. Yao, Synthesis of indolylquinolines, indolylacridines, and indolylcyclopenta[b]quinolines from the Baylis-Hillman adducts: an in situ [1,3]-sigmatropic rearrangement of an indole nucleus to access indolylacridines and indolylcyclopenta[b]quinolines, J. Org. Chem. 77 (2012) 8451-8464.

[19] Z. Shafiq, L. Liu, Z. Liu, D. Wang, Y. J. Chen, A highly alpha-regioselective AgOTf-catalyzed nucleophilic substitution of the Baylis-Hillman acetates with indoles, Org. Lett. 9 (2007) 2525-2528.

[20] C. Piemontesi, Q. Wang, J. Zhu, Synthesis of 3,3-disubstituted oxindoles by one-pot integrated Brønsted base-catalyzed trichloroacetimidation of 3-hydroxyoxindoles and

Brønsted acid-catalyzed nucleophilic substitution reaction, Org. Biomol. Chem., 11 (2013) 1533-1536.

[21] The most biologically potent compounds observed in current studies are often the most electron-rich. To check their stability towards biological oxidising agents, we monitor the stability of compound **2g** towards mild oxidising agent {2-iodobenzoic acid (IBX)} at different reaction vessel temperatures (0°C and 40°C) from 0-16h. Even at 40°C (bath temperature) we did not observed formation of any oxidised product (fully conjugated). Since 40°C is the optimum temperature below which most of the biological invitro assays have been carried out, we may conclude that the synthesized product are stable toward biological oxidising agents.

[22] H. Zaid, C. N. Antonescu, V. K. Randhawa, A. Klip, Insulin action on glucose transporters through molecular switches, tracks and tethers, Biochem J. 413 (2008) 201-215.

[23]A. K. Tamrakar, N. Jaiswal, P. P. Yadav, R. Maurya, A. K. Srivastava, Pongamol from Pongamia pinnata stimulates glucose uptake by increasing surface GLUT4 level in skeletal muscle cells, Mol. Cell. Endocrinol. 339 (2011) 98-104.

[24] C. M. Taniguchi, B. Emanuelli, C. R. Kahn, Critical nodes in insulin signaling pathways: insight into insulin action, Nat. Rev. Mol. Cell. Biol. 7 (2006) 85-96.

[25] A. K. Tamrakar, J. D. Schertzer, T.T. Chiu, K. P. Foley, P. J. Bilan, D. J. Philpott, A. Klip, NOD2 activation induces muscle cell-autonomous innate immune responses and insulin resistance, Endocrinology. 151 (2010) 5624-5637.

[26] K. Kishi, V. Muromoto,V. Nakaya, I. Miyata, A. Hagi, H. Hayashi, Y. Ebina, Bradykinin directly triggers GLUT4 translocation via an insulin-independent pathway, Diabetes. 47 (1998) 550-558.

[27] A. Ueyama, K. L. Yaworsky, Q. Wang, Y. Ebina, A. Klip, GLUT-4myc ectopic expression in L6 myoblasts generates a GLUT-4-specific pool conferring insulin sensitivity, Am. J. Physiol. 277 (1999) 572-578.

Table 1. Reaction of kojic acid with benzaldehyde in the presence of various catalysts in dioxane/H_2O at room temperature

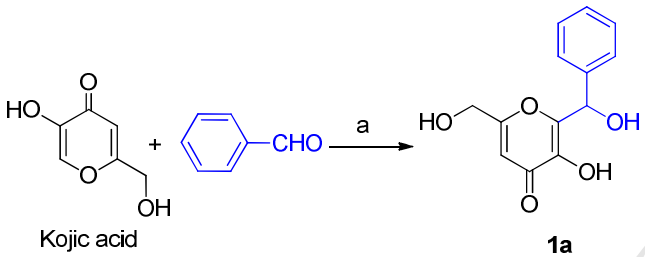

Kojic acid **1a**

Entry	Catalyst	Time (d)	yield [b] (%) of **1a**
1	Imidazole	1	72%
2	DMAP	1	60%
3	DABCO	1	94%
4	DBU	1	47%
5	Pyridine	1	54%
6	Et_3N	1	30%

[a]kojic acid (1 mmol) with benzaldehyde (1.2 mmol) in the presence of various catalysts (entry 1-6, 1.5 mmol) in dioxane:H_2O (1:1, 4 mL) at room temperature for 24 h. [b]Isolated yield after column chromatography.

Table 2. Products of reaction between kojic acid with aryl/alkyl aldehydes.

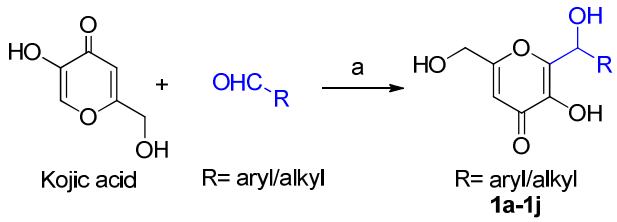

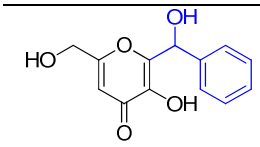

1a, 94%

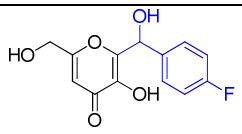

1b,98%

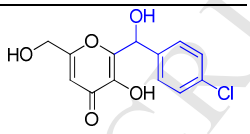

1c,97%

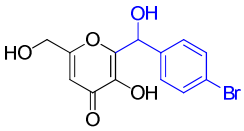

1d, 94%

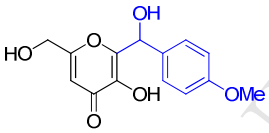

1e, 91%

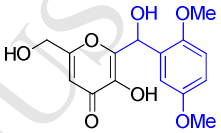

1f, 89%

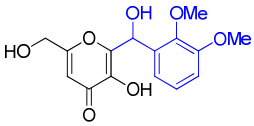

1g, 89%

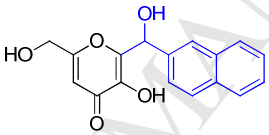

1h, 89%

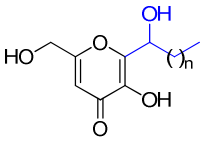

1i, n= 3, 85% and

1j, n=7, 83%[b]

[a] Reagents and conditions: (a) Kojic acid (1 mmol), RCHO (1.2 mmol), DABCO (1.2mmol), dioxane:H_2O (1:1), room temp., 24 h. [b]Reaction took 2 days for complete conversion.

Table 3. Nucleophilic substituion of indole on various aldol adducts.

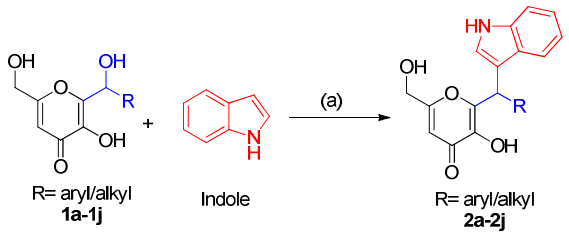

R= aryl/alkyl
1a-1j

Indole

R= aryl/alkyl
2a-2j

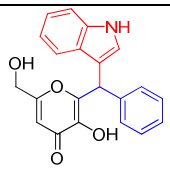

2a, 98%

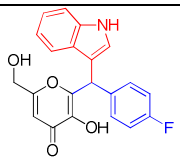

2b, 98%

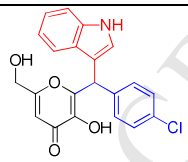

2c, 96%

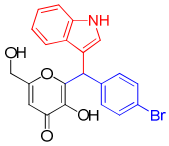

2d, 94%

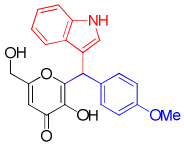

2e, 91%

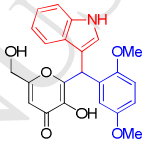

2f, 89%

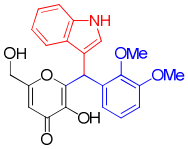

2g, 89%

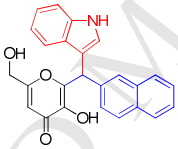

2h, 91%

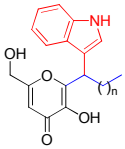

2i,n=3, 87% and

2j, n=7 86%

[a] Reagents and conditions: (a) **1a -1j** (1equiv.), indole (1.5 equiv), silica-H_2SO_4 (10 mol %), CH_3CN, 80°C, 2h.

Table 4. Nucleophilic substitution of **1a** by variously substituted indoles and different nucleophiles.

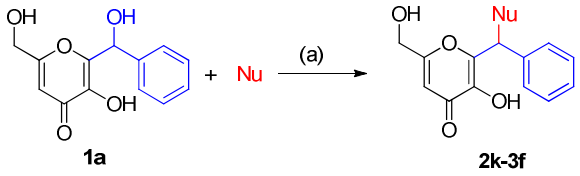

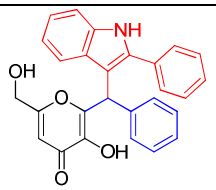

2k, 89%

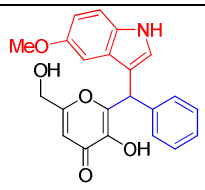

2l, 92%

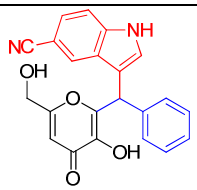

2m, 94%

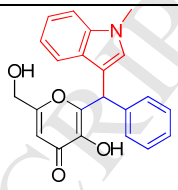

2n, 91%

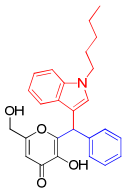

2o, 89%

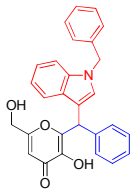

2p,89%

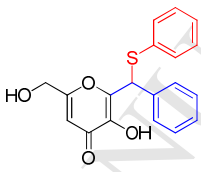

3a, 94%

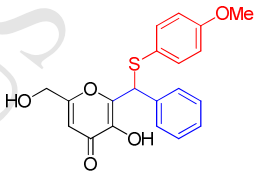

3b, 89%

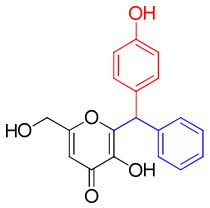

3c, 92%

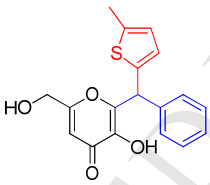

3d, 87%

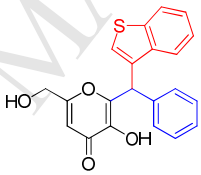

3e, 87%

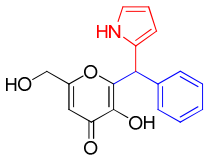

3f, 85%

[a] Reagents and conditions: (a) **1a** (1equiv.), Nu (substituted indoles and other nucleophiles 1.5 equiv), silica-H_2SO_4 (10 mol %), CH_3CN, 80°C, 2h.

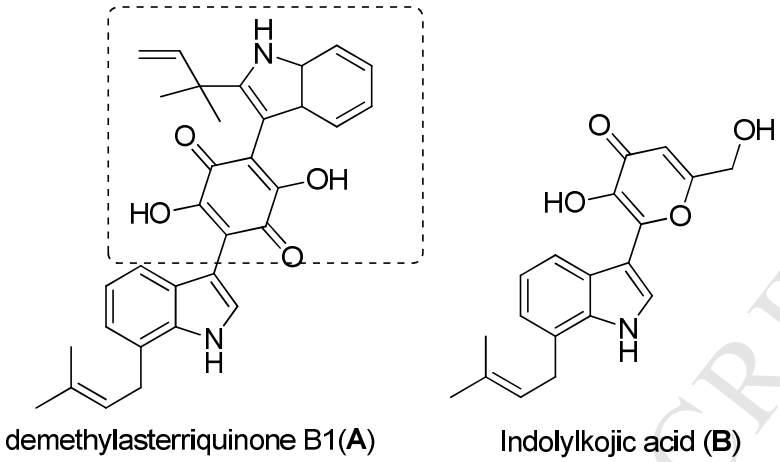

Fig. 1. Orally active insulin mimic natural product demethyasterriquinone B1(**A**) and its kojic acid derived analogue (**B**) which retains insulin mimic activity.

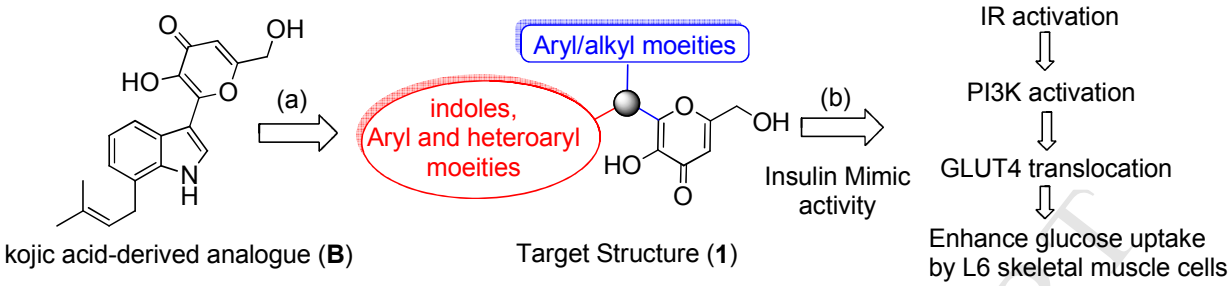

Fig. 2. Objective of current work (a) synthesis of target molecule based on indolylkojic acid scaffold with one carbon spacer (b) Glucose uptake stimulatory effect in L6 skeletal muscle cells via insulin like mode of action of target structure.

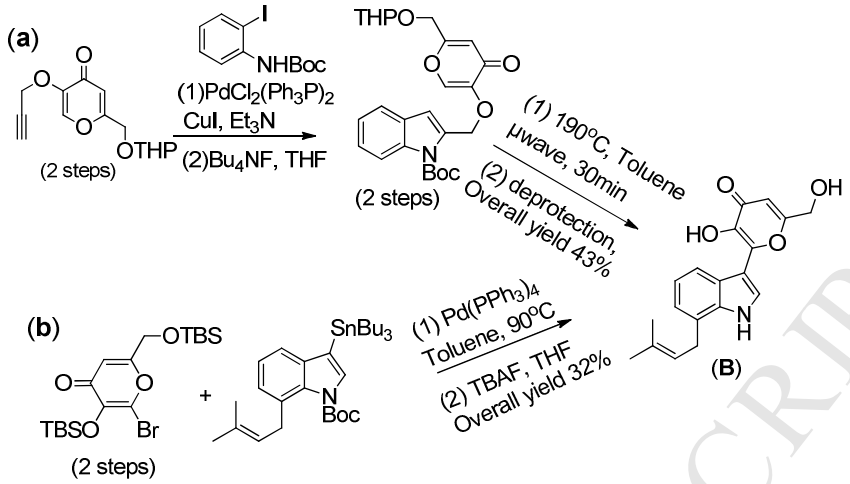

Fig. 3. Literature methods for synthesis of indolylkojic acid (**B**): (a) Sonogashira coupling and heteroaromatic Claisen rearrangement,of a protected iodoaniline with propargyl kojate (b) Stille coupling between stannyl derivative of indole and halide derivative of kojic acid.

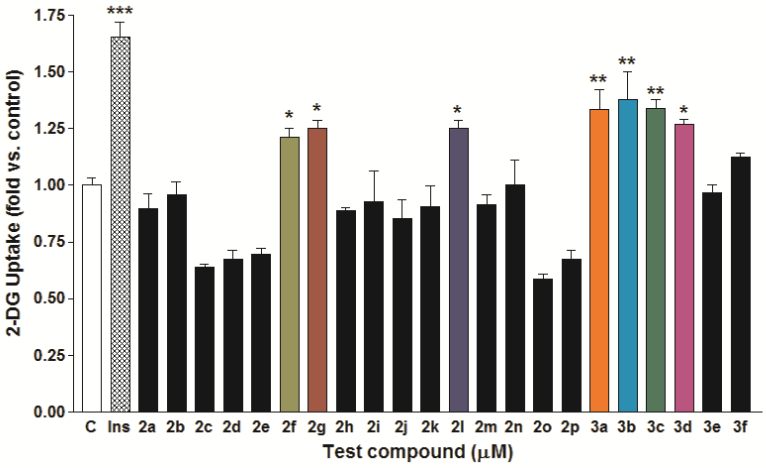

Fig. 4. Glucose uptake stimulatory effect of compounds after overnight treatment in L6-GLUT4*myc* cells. (*P <0.05), (**P <0.001) relative to controls.

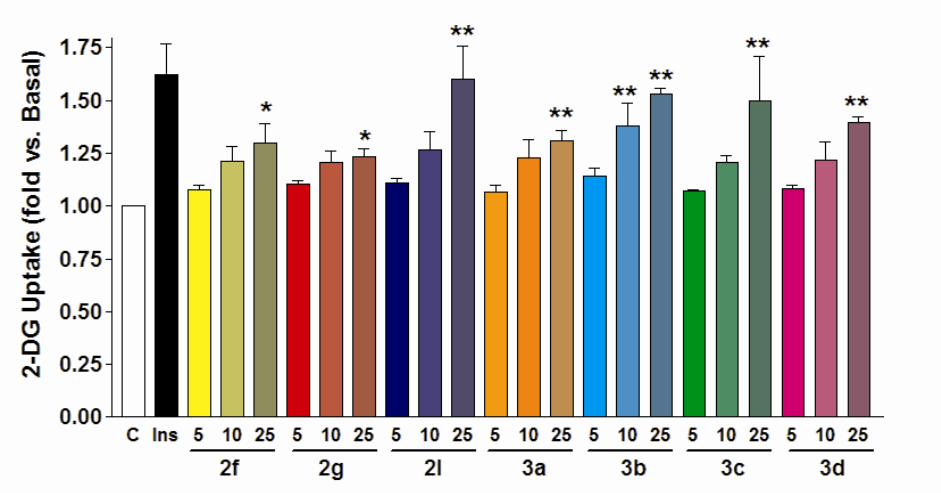

Fig. 5. Concentration-dependent effects of compounds **2f**, **2g**, **2l**, **3a**, **3b, 3c** and **3d** on 2-deoxyglucose uptake in L6-GLUT4*myc* myotubes. Results shown are mean ± S.E.M. of three independent experiments. (*P <0.05), (**P <0.001) relative to controls. Insulin is taken as positive control.

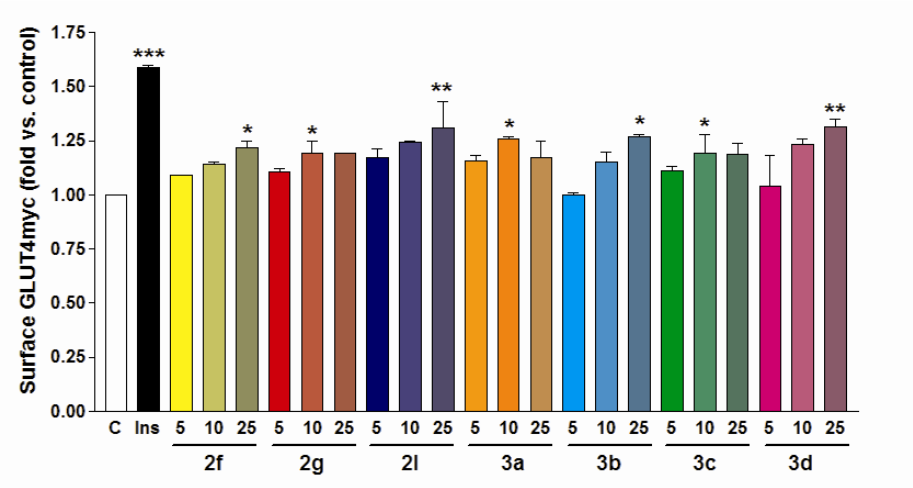

Fig. 6. Effect of test compounds **2f**, **2g**, **2l**, **3a**, **3b**, **3c** and **3d** on GLUT4 translocation in L6 GLUT-4 *myc* myotubes. Cells were incubated with vehicle (DMSO), Insulin (Ins, 100nM) and test compounds at 5μM, 10μM, 25μM for 3 hours and surface density of GLUT4 myc was determined as described. Results are expressed as fold stimulation over control. Results shown are mean±SE of three independent experiments, each performed in triplicate. (*$p<0.05$), (**$p<0.01$) and (***$p<0.001$) relative to controls.

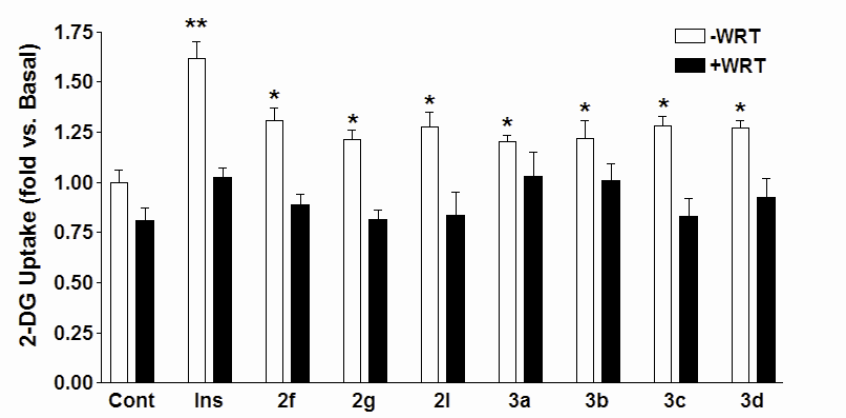

Fig. 7. Effect of wortmannin on insulin and **2f**, **2g**, **2l**, **3a**, **3b**, **3c** and **3d-** induced glucose uptake in L6-GLUT 4*myc* myotubes. Left bars represent the individual effects of **2f**, **2g**, **2l**, **3a**, **3b**, **3c** and **3d** and insulin (Grey bar) and right bar represents the effect of compounds or insulin in presence of wortmannin (Black bar). Results shown are mean ± S.E.M. of three independent experiments, each performed in triplicate. (*P <0.05), (**P <0.01), relative to control basal (-WRT).). (*P<0.05), (**P<0.01) and (***P<0.001) relative to respective compound treated condition in absence of wortmannin.

Highlights

- A library of novel small molecules insulin mimics based on indolylkojic acid scaffold
- The synthetic strategy used is scalable, broad,and flexible enough to create diversity
- Glucose uptake stimulatory effect of the compounds in rat L6 skeletal muscle cells
- Exert biological action by enhancing GLUT4 translocation to cell surface via PI3K-dependent signaling pathway

Supporting Information

Synthesis of heteroaryl/aryl kojic acid conjugates as stimulators of glucose uptake by GLUT4 translocation

Deepak K. Sharma,[a,b] *Jyotsana Pandey,*[c] *Akhilesh K. Tamrakar,* [a,c] *Debaraj Mukherjee*[a,b]*

Spectral data: ^{1}HNMR and ^{13}CNMR

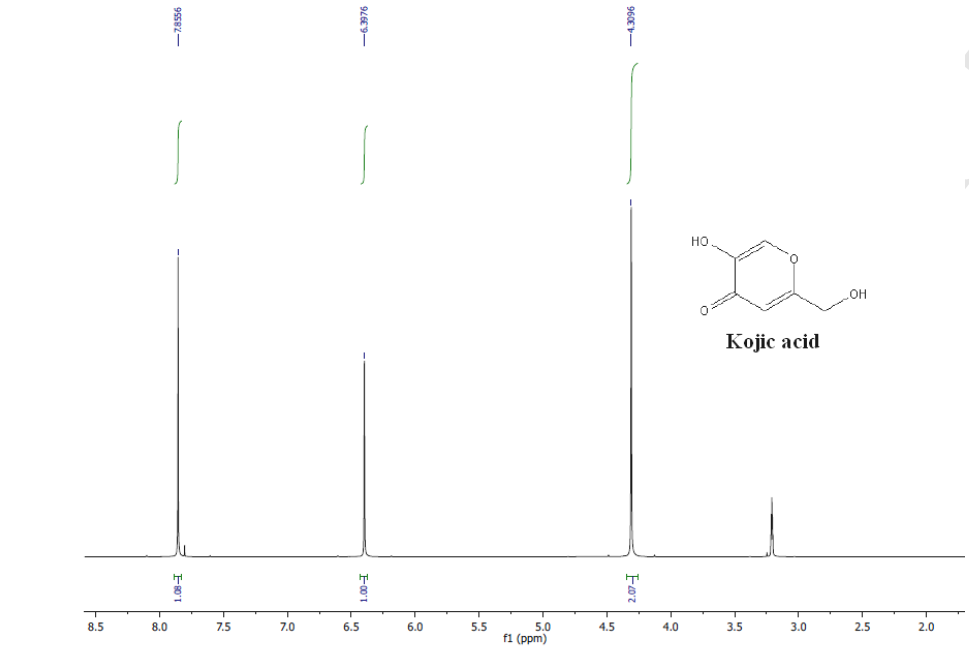

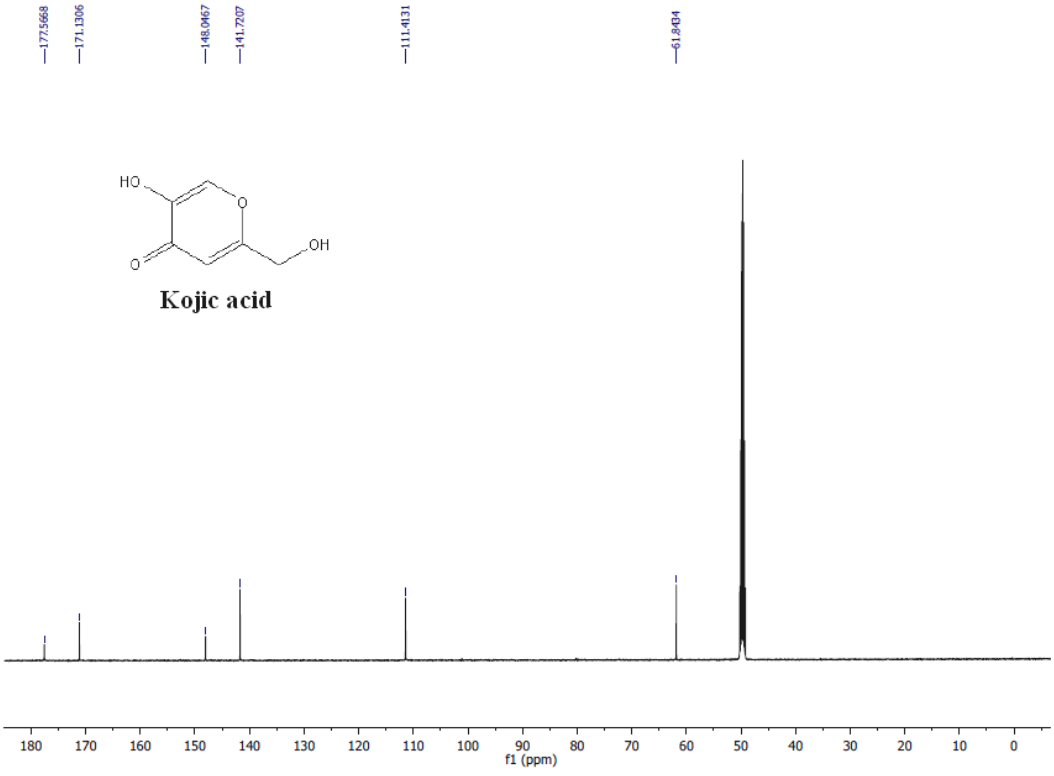

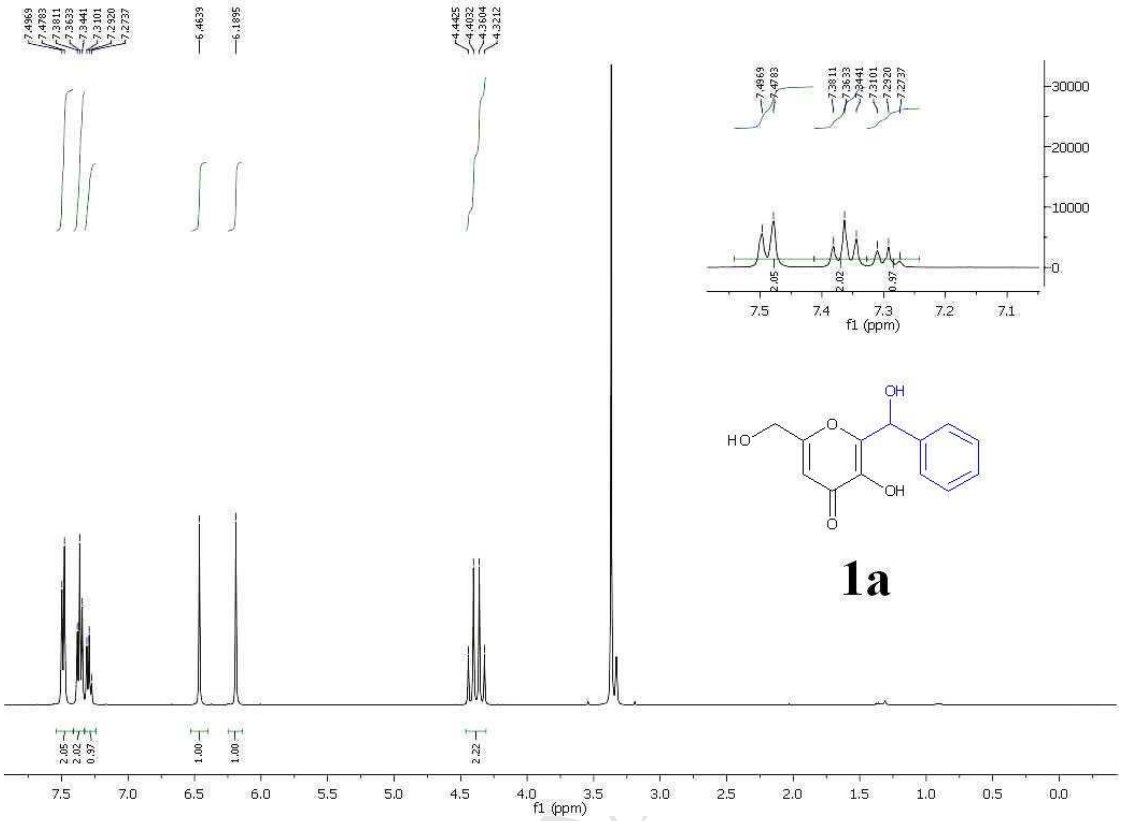
7.4969
7.4783
7.3811
7.3633
7.3441
7.3101
7.2920
7.2737
6.4639
6.1895
4.4425
4.4032
4.3604
4.3212
2.05
2.02
0.97
1.00
1.00
2.22
f1 (ppm)
OH
HO
O
OH
O
1a

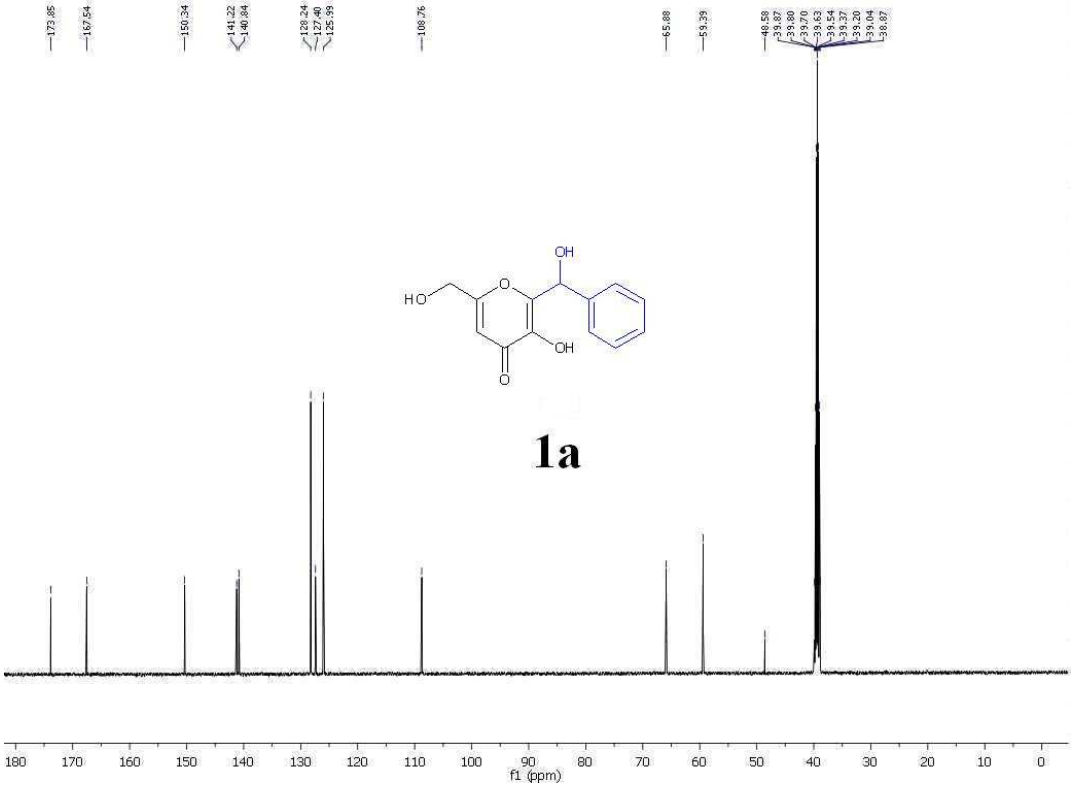
173.85
167.54
150.34
141.22
140.84
128.24
127.48
125.99
108.76
65.88
59.39
40.58
39.87
39.80
39.70
39.63
39.54
39.37
39.20
39.04
38.87
f1 (ppm)
OH
HO
O
OH
O
1a

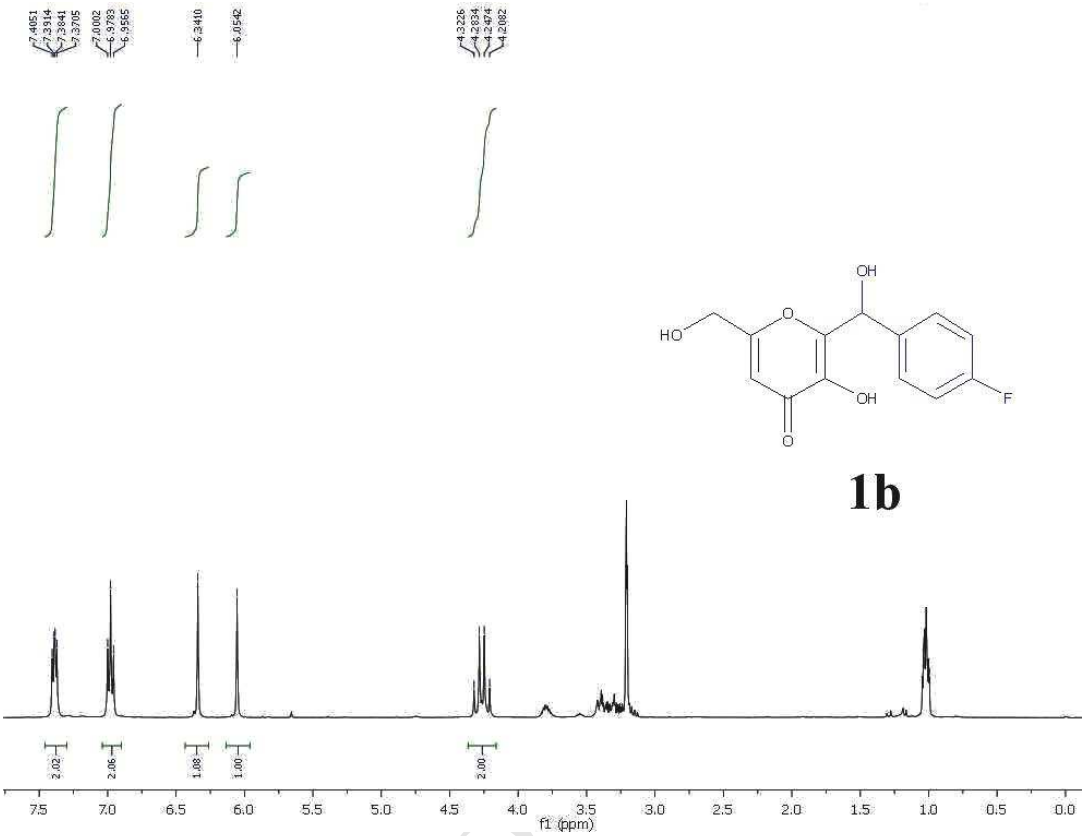
OH
HO
O
OH
F
O
1b
f1 (ppm)

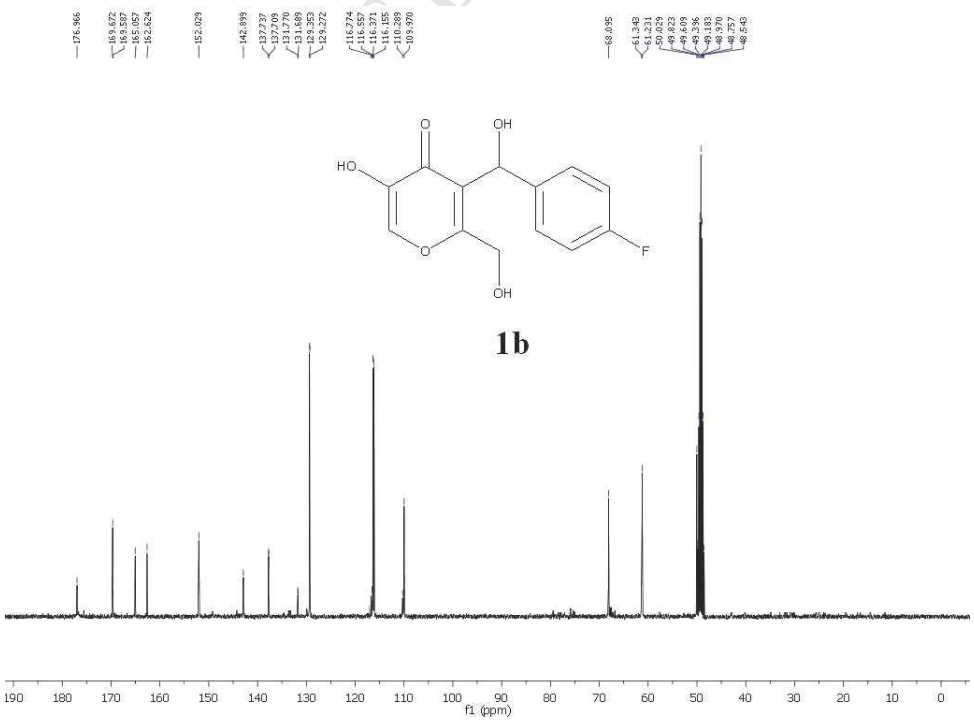
O
OH
HO
F
O
OH
1b
f1 (ppm)

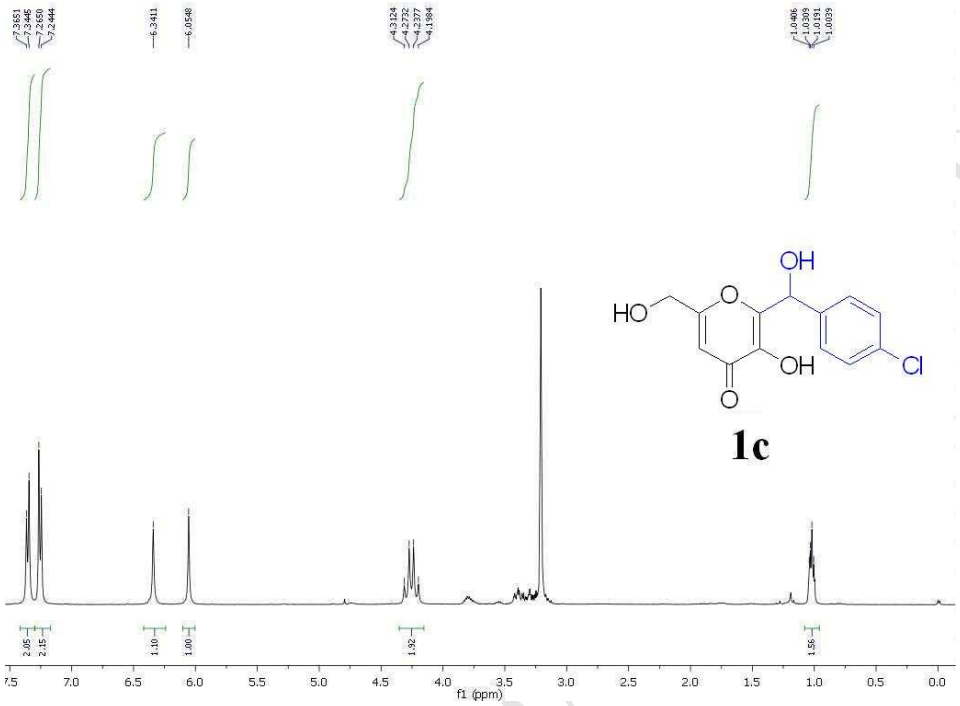
OH
HO
O
OH
Cl
O
1c
f1 (ppm)

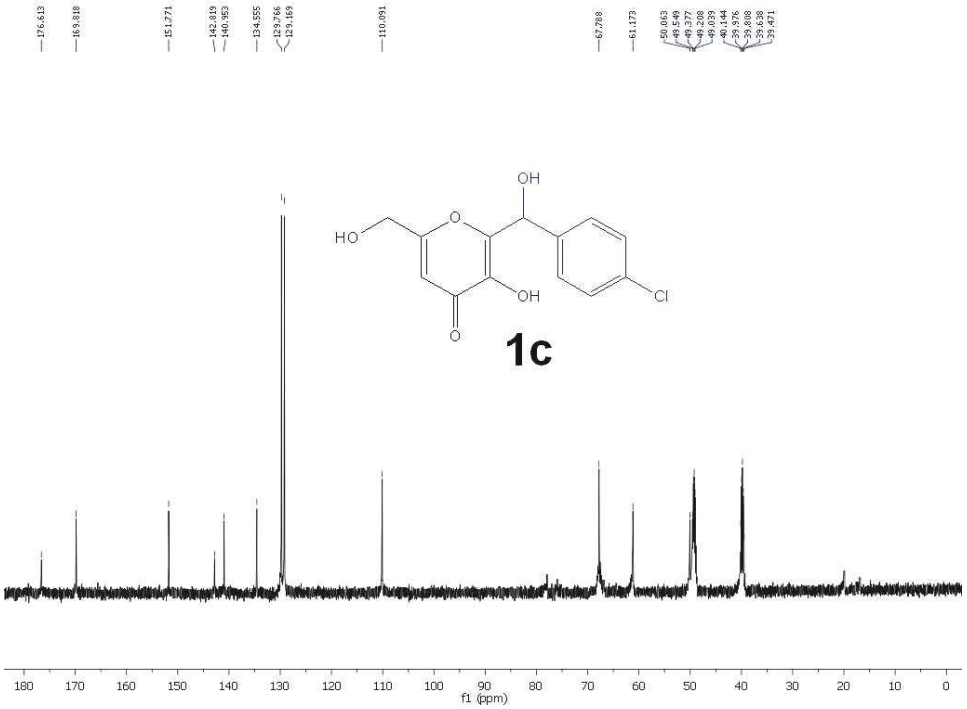
OH
HO
O
OH
Cl
O
1c
f1 (ppm)

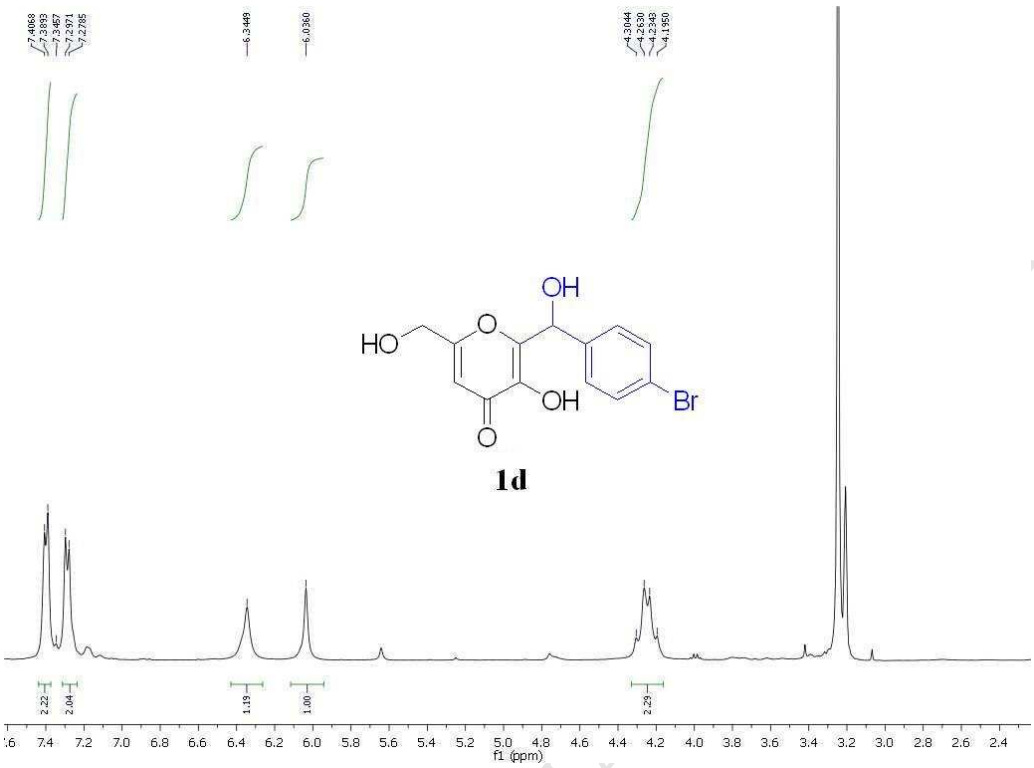
7.4068
7.3893
7.3457
7.2971
7.2785
6.3449
6.0360
4.3044
4.2630
4.2348
4.1950
OH
HO
O
OH
Br
O
1d
2.22
2.04
1.19
1.00
2.29
f1 (ppm)

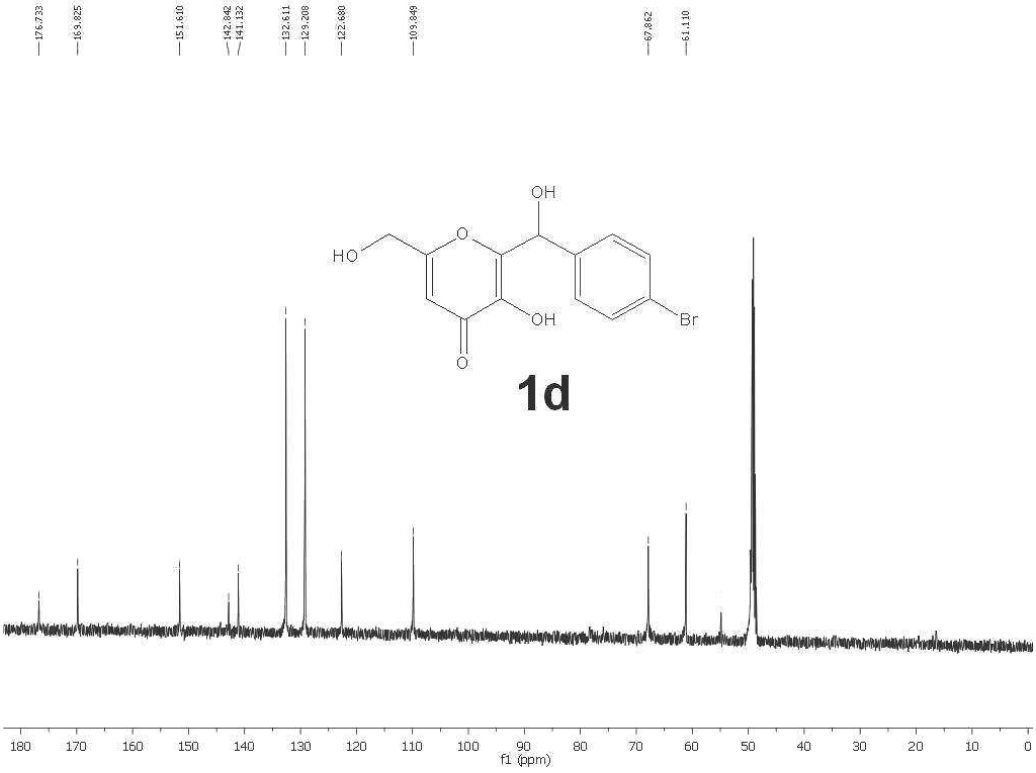
176.733
163.825
151.610
142.842
141.132
132.611
129.208
122.680
109.849
67.862
61.110
OH
HO
O
OH
Br
O
1d
f1 (ppm)

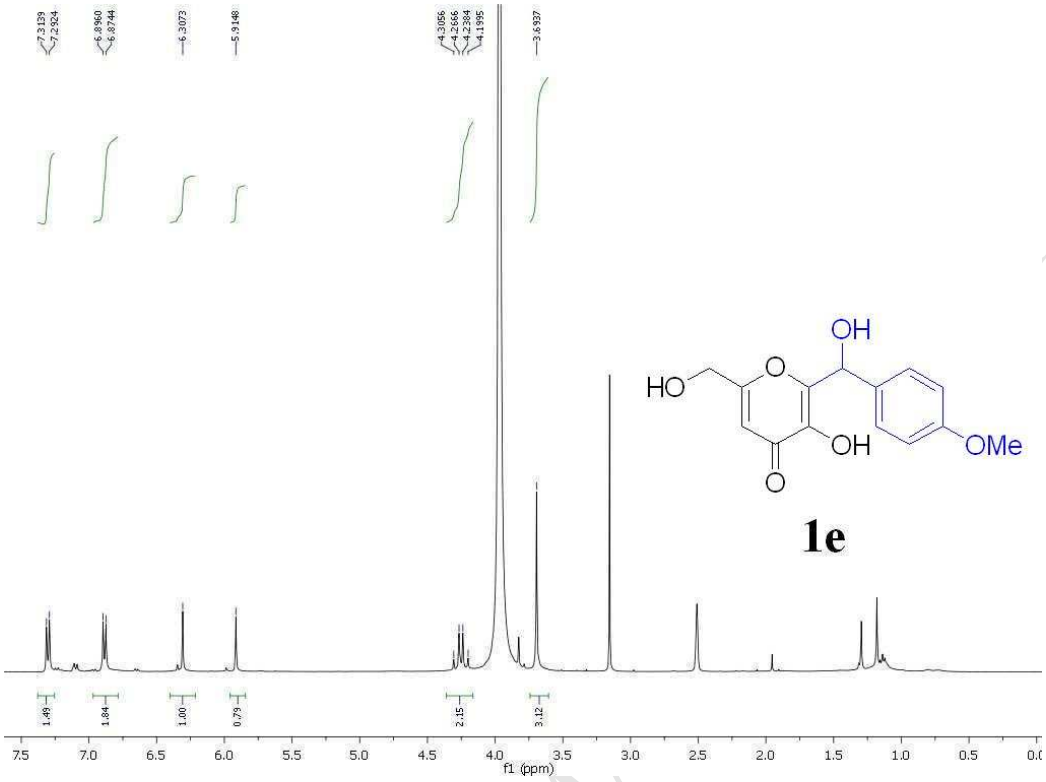
OH
HO
O
OH
OMe
O
1e
f1 (ppm)

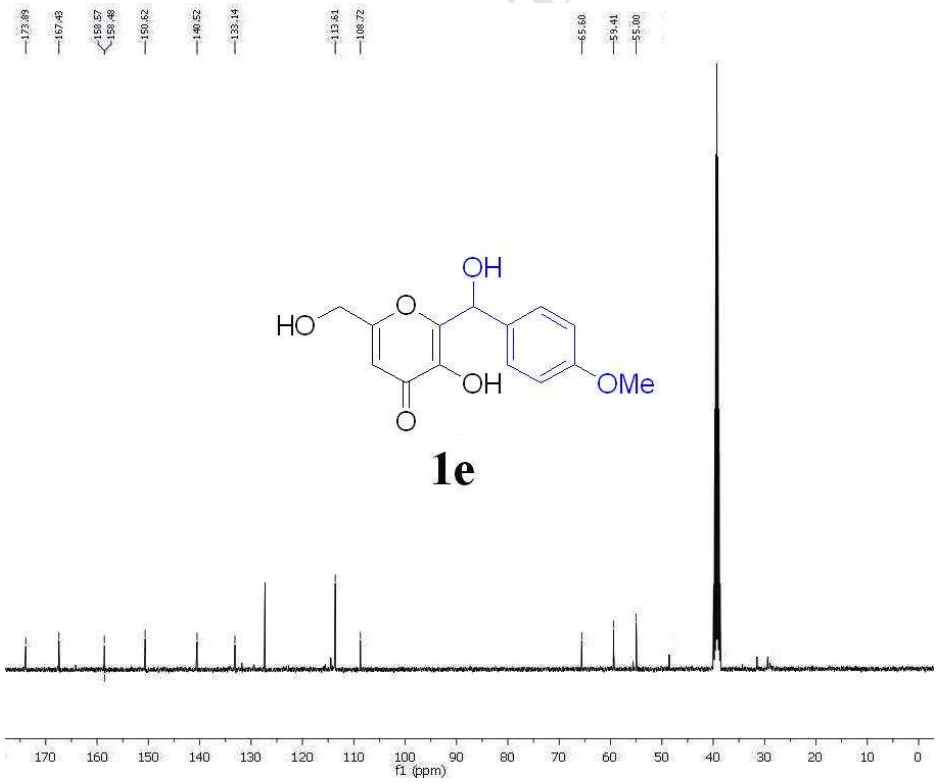
OH
HO
O
OH
OMe
O
1e
f1 (ppm)

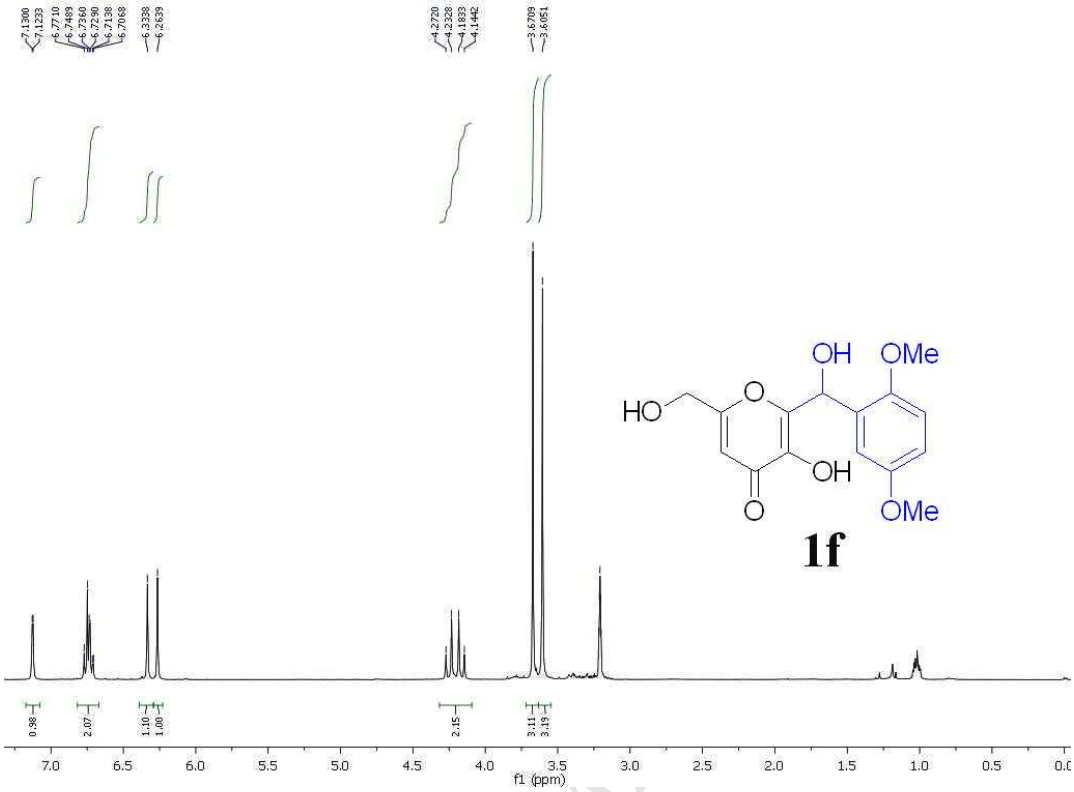
OH
OMe
HO
O
OH
O
OMe
1f
f1 (ppm)

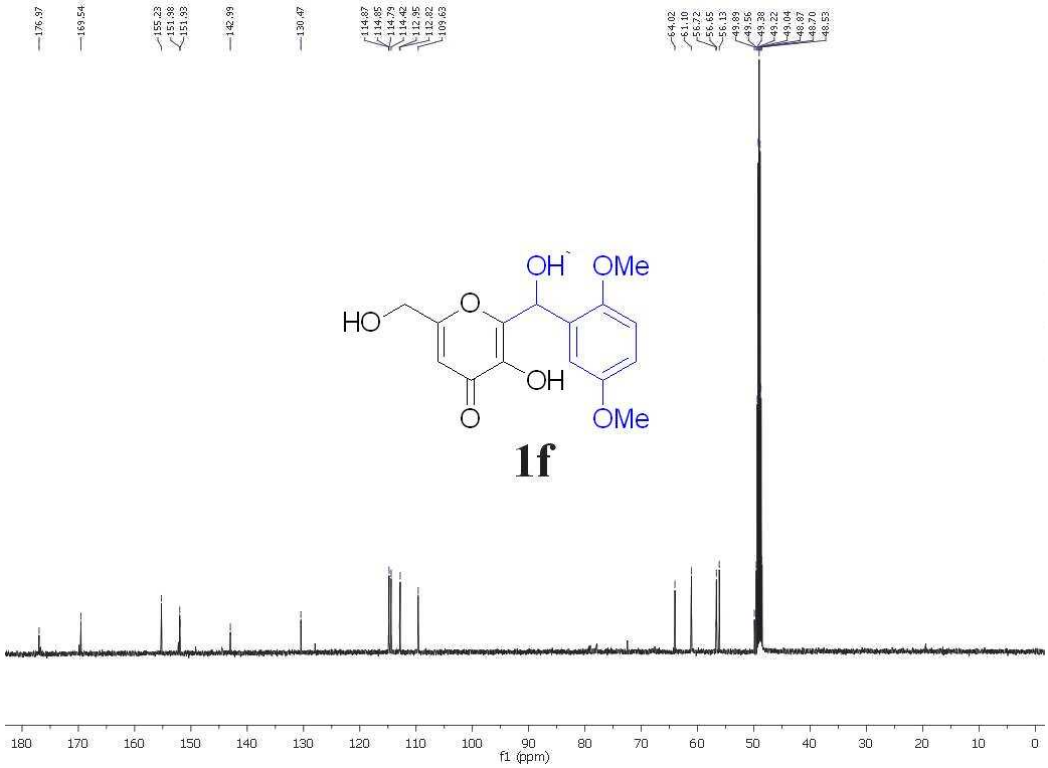
OH
OMe
HO
O
OH
O
OMe
1f
f1 (ppm)

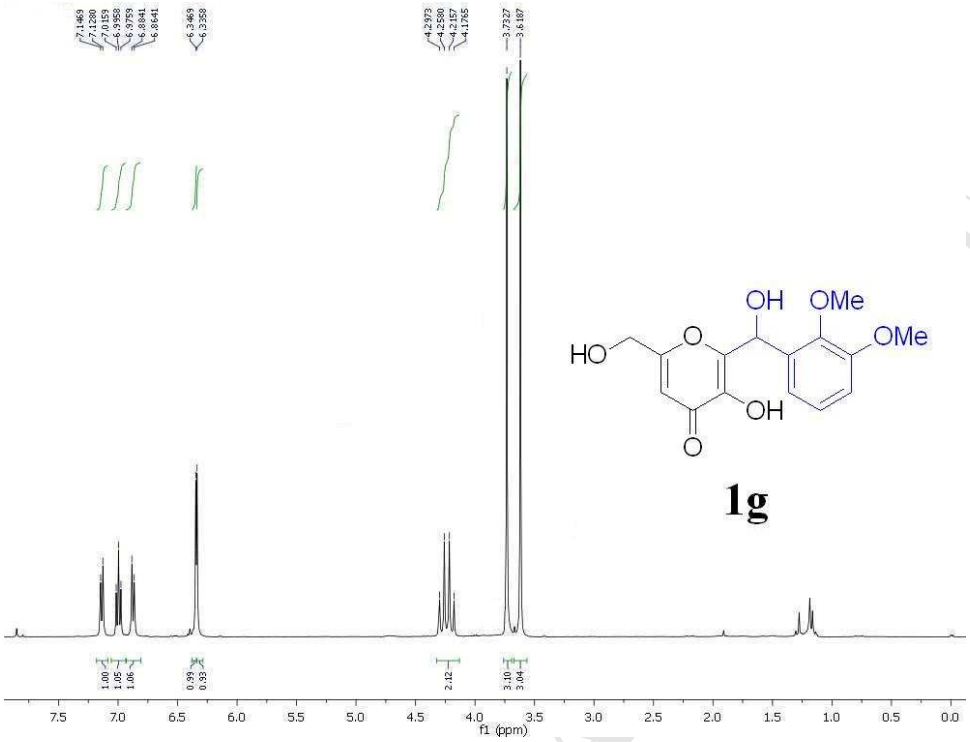
7.1469
7.1280
7.0159
6.9958
6.9759
6.8841
6.8641
6.3469
6.3358
4.2973
4.2580
4.2157
4.1765
3.7327
3.6187
OH
OMe
OMe
HO
O
OH
O
1g
1.00
1.05
1.06
0.99
0.99
2.12
3.10
3.04
7.5
7.0
6.5
6.0
5.5
5.0
4.5
4.0
3.5
3.0
2.5
2.0
1.5
1.0
0.5
0.0
f1 (ppm)

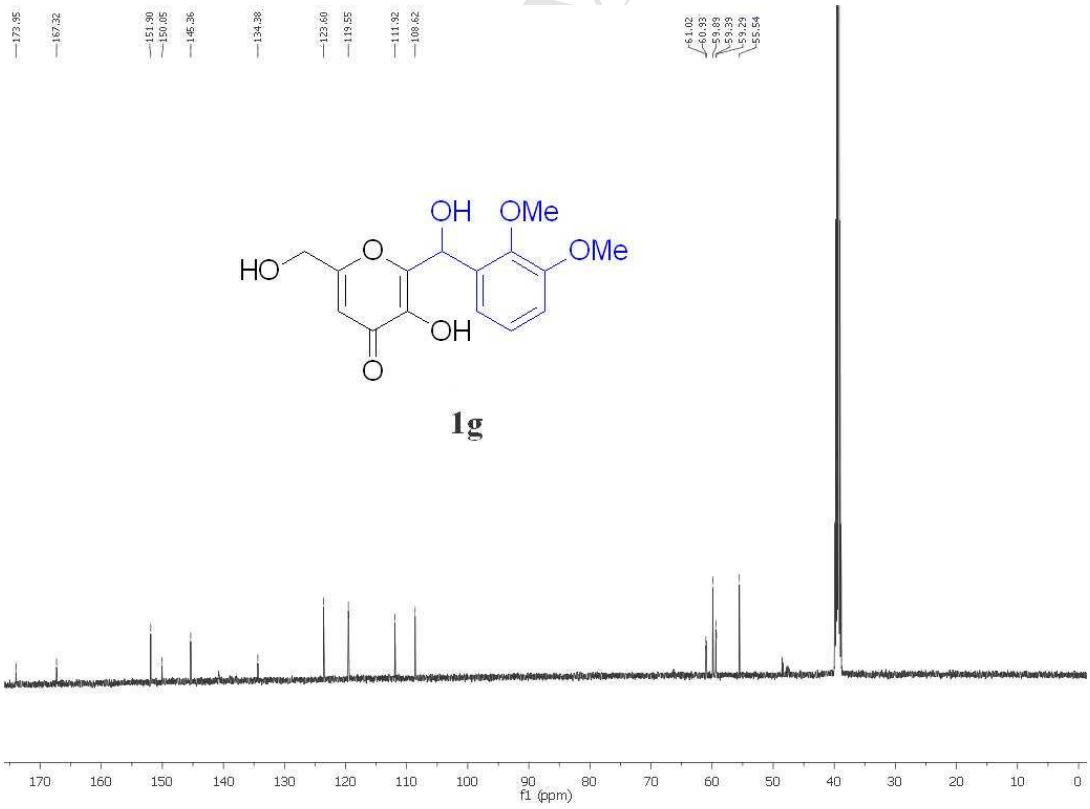
173.95
167.32
151.90
150.05
145.36
134.38
123.60
119.55
111.92
108.62
61.02
60.93
59.09
53.39
53.29
55.54
OH
OMe
OMe
HO
O
OH
O
1g
170
160
150
140
130
120
110
100
90
80
70
60
50
40
30
20
10
0
f1 (ppm)

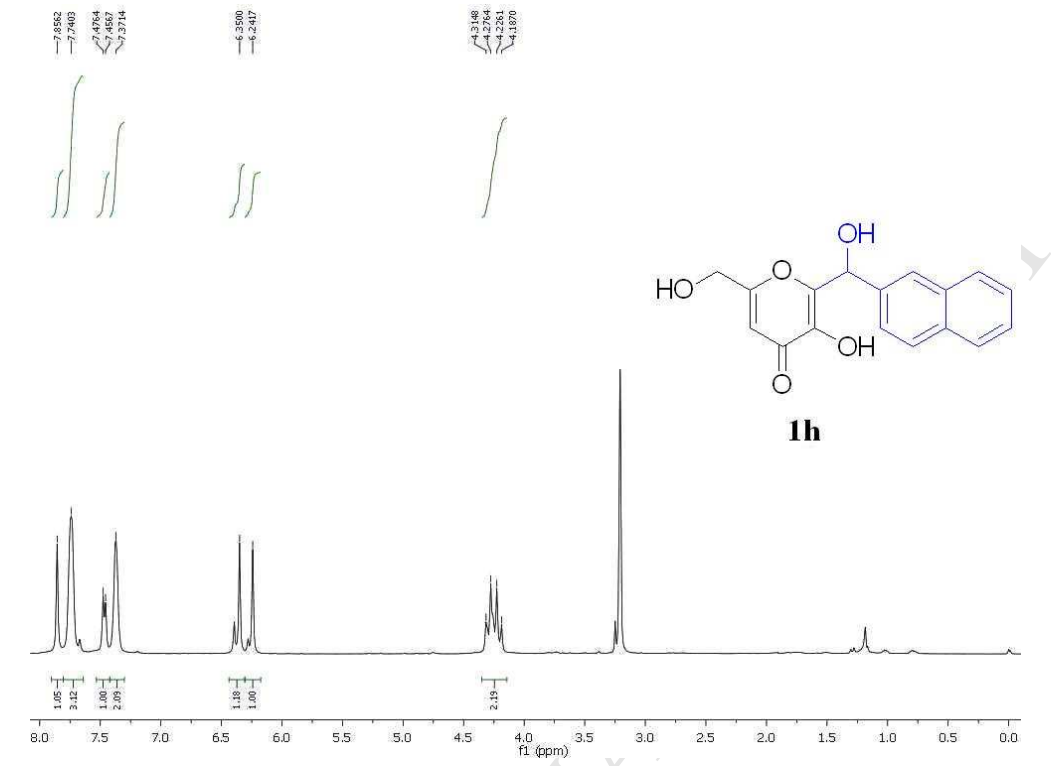
OH
HO
O
OH
O
1h
f1 (ppm)

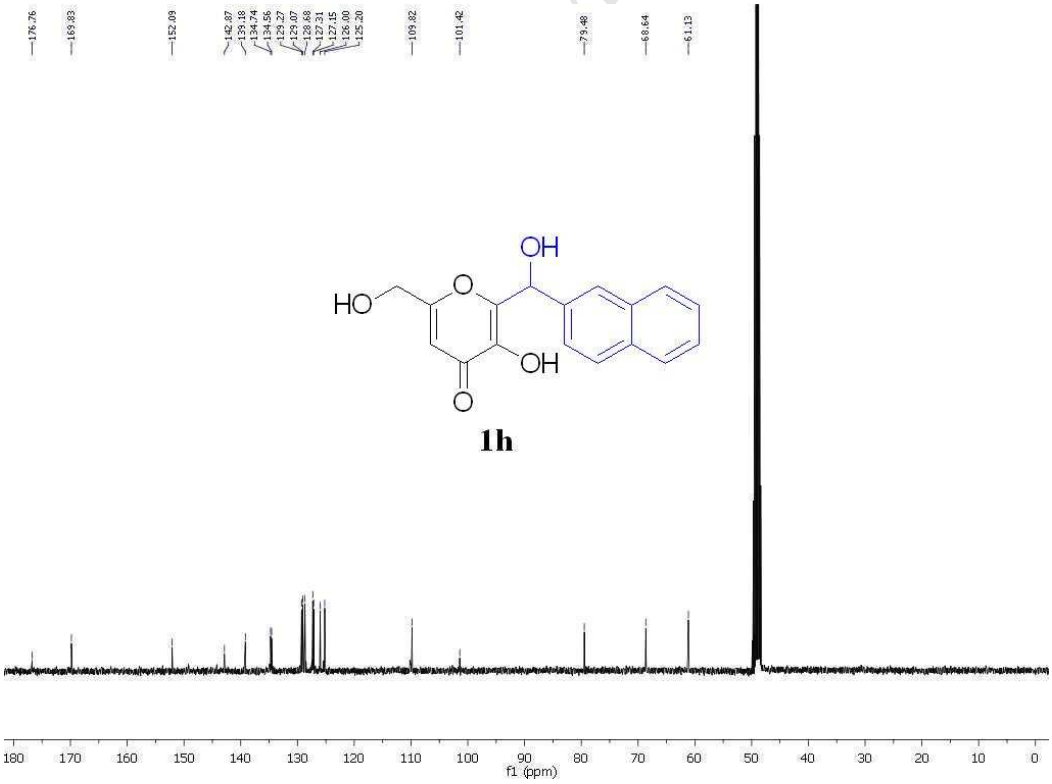
OH
HO
O
OH
O
1h
f1 (ppm)

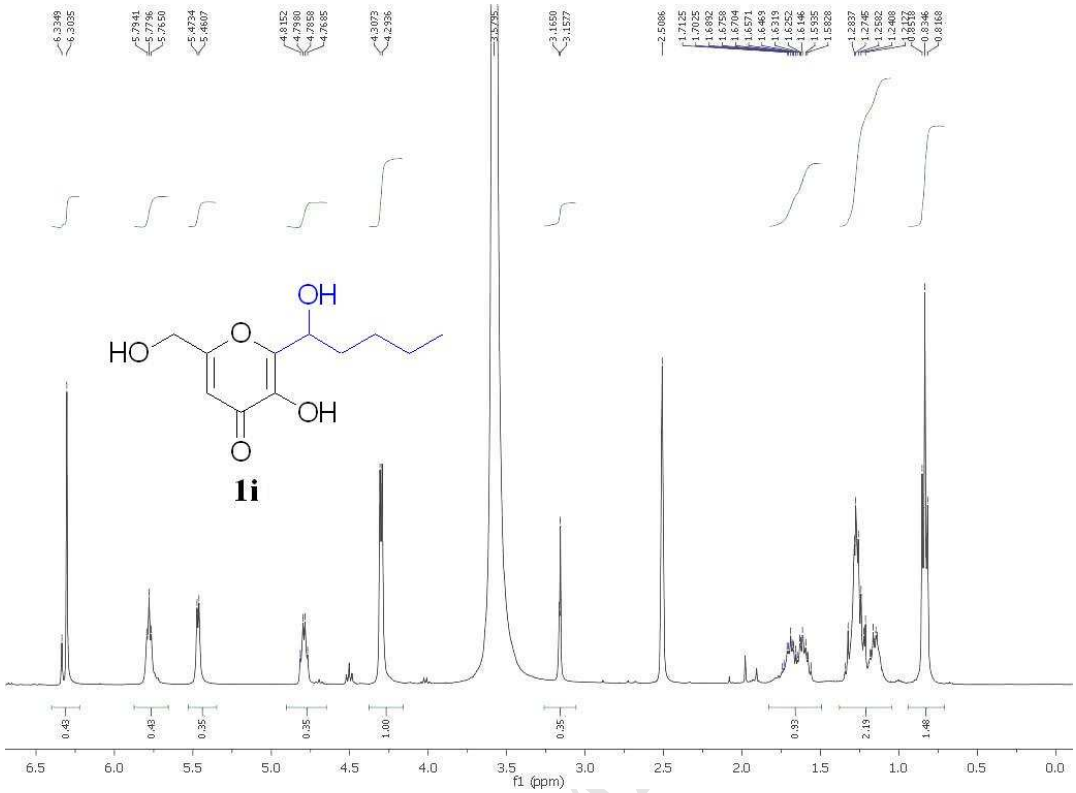
OH
HO
O
OH
O
1i
f1 (ppm)

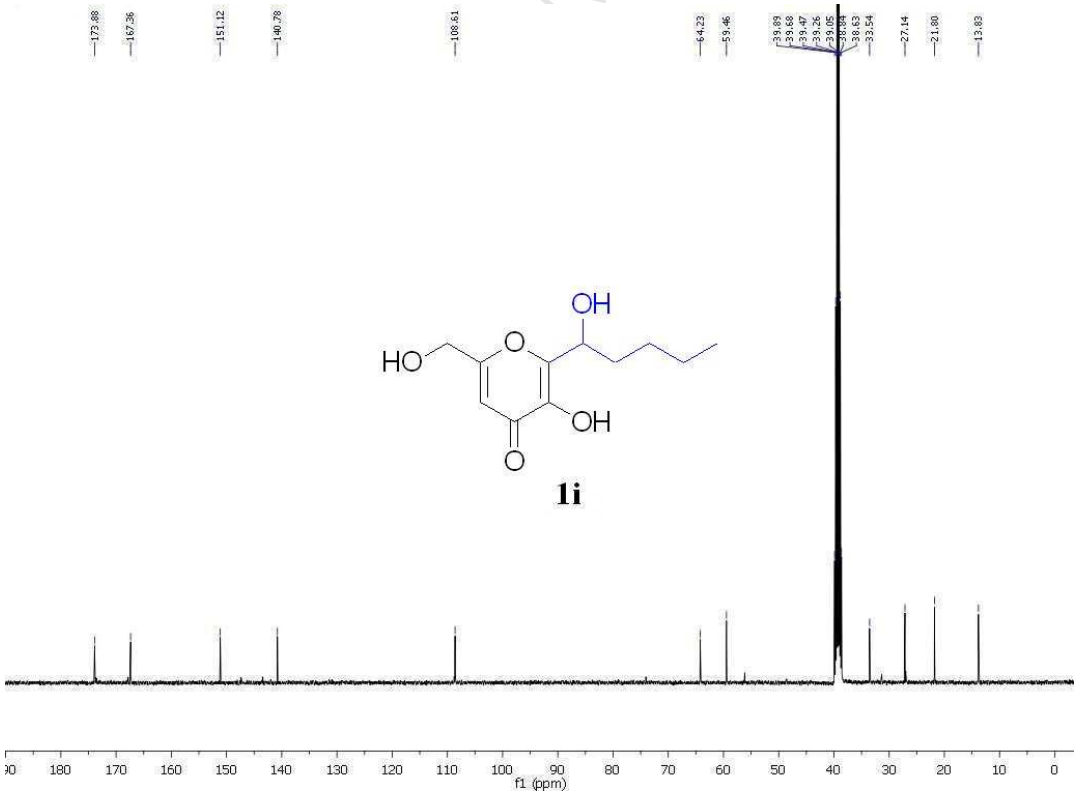
OH
HO
O
OH
O
1i
f1 (ppm)

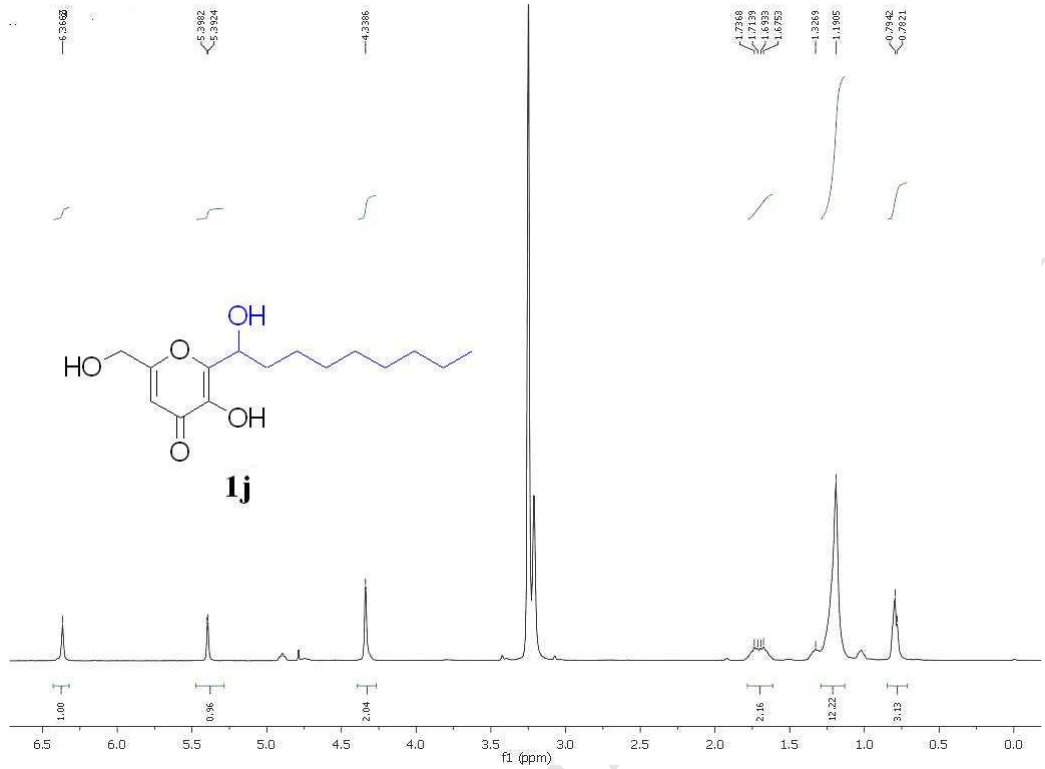
OH
HO
O
OH
O
1j
f1 (ppm)

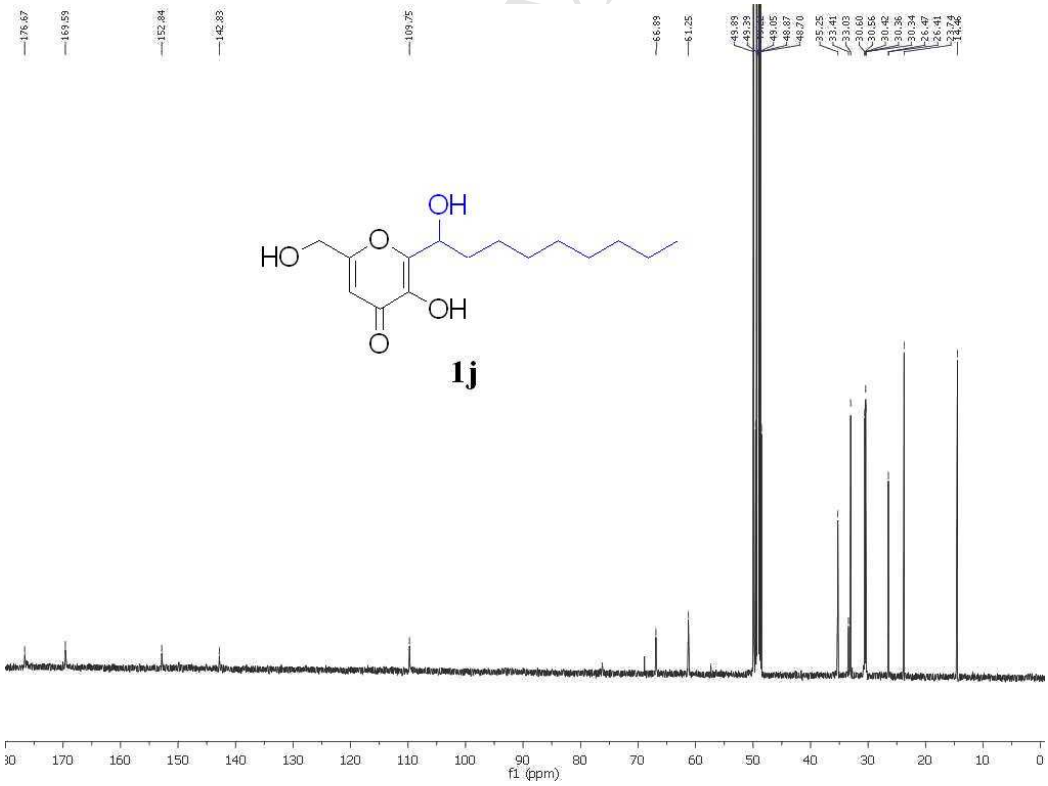
OH
HO
O
OH
O
1j
f1 (ppm)

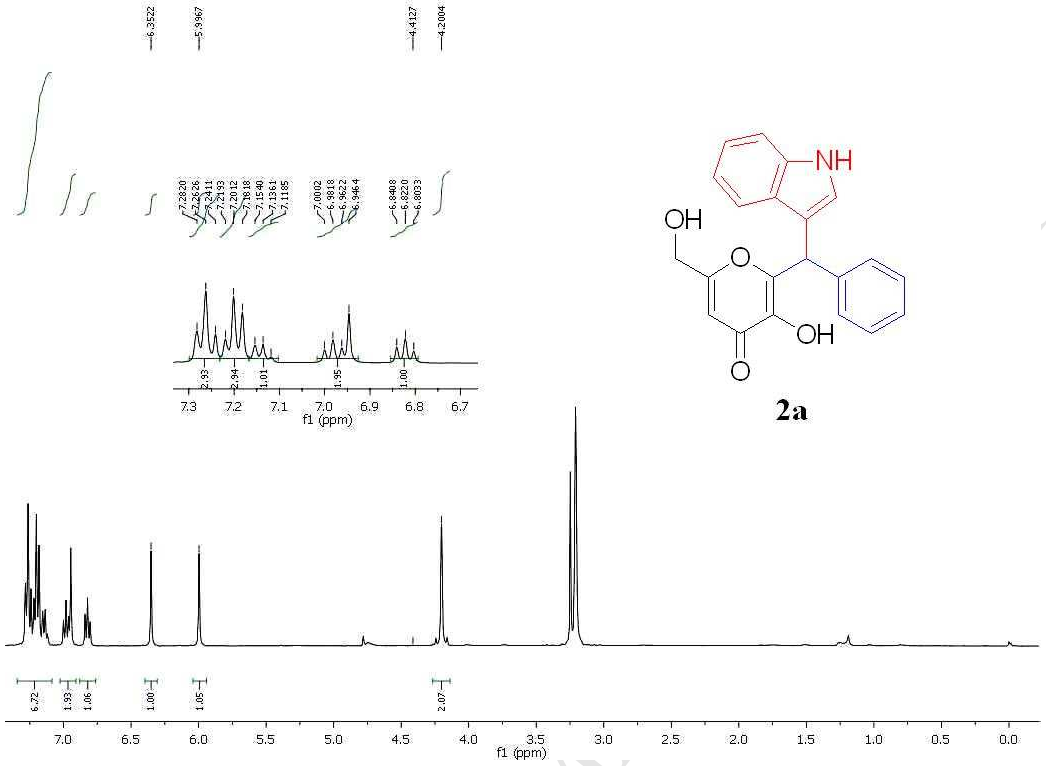
NH
OH
O
OH
O
2a
f1 (ppm)

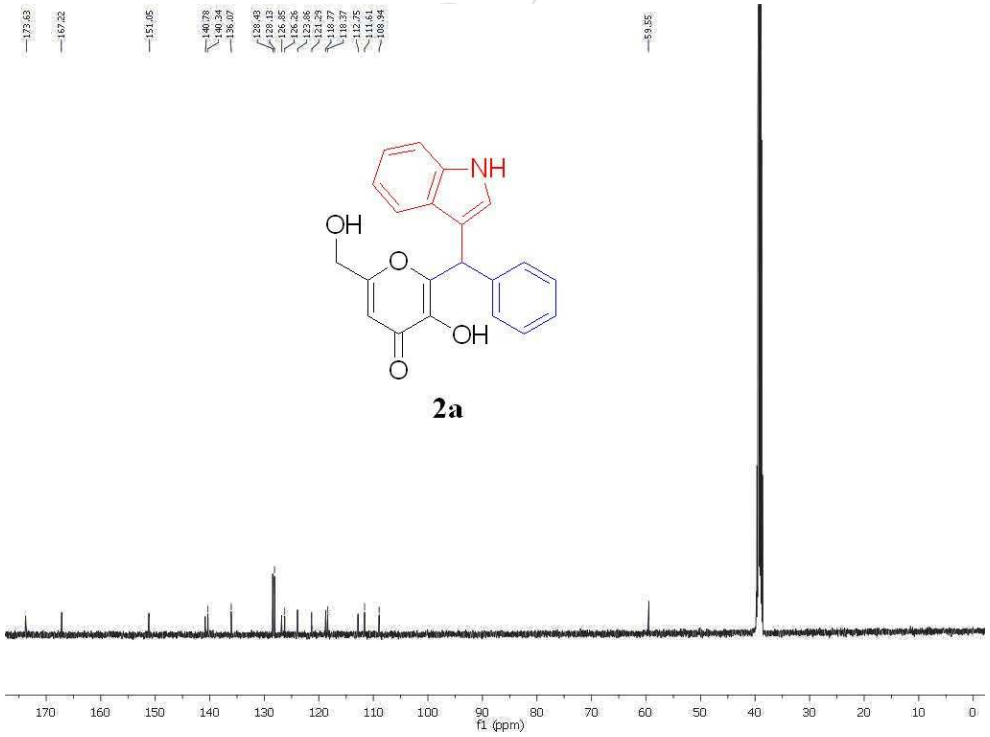
NH
OH
O
OH
O
2a
f1 (ppm)

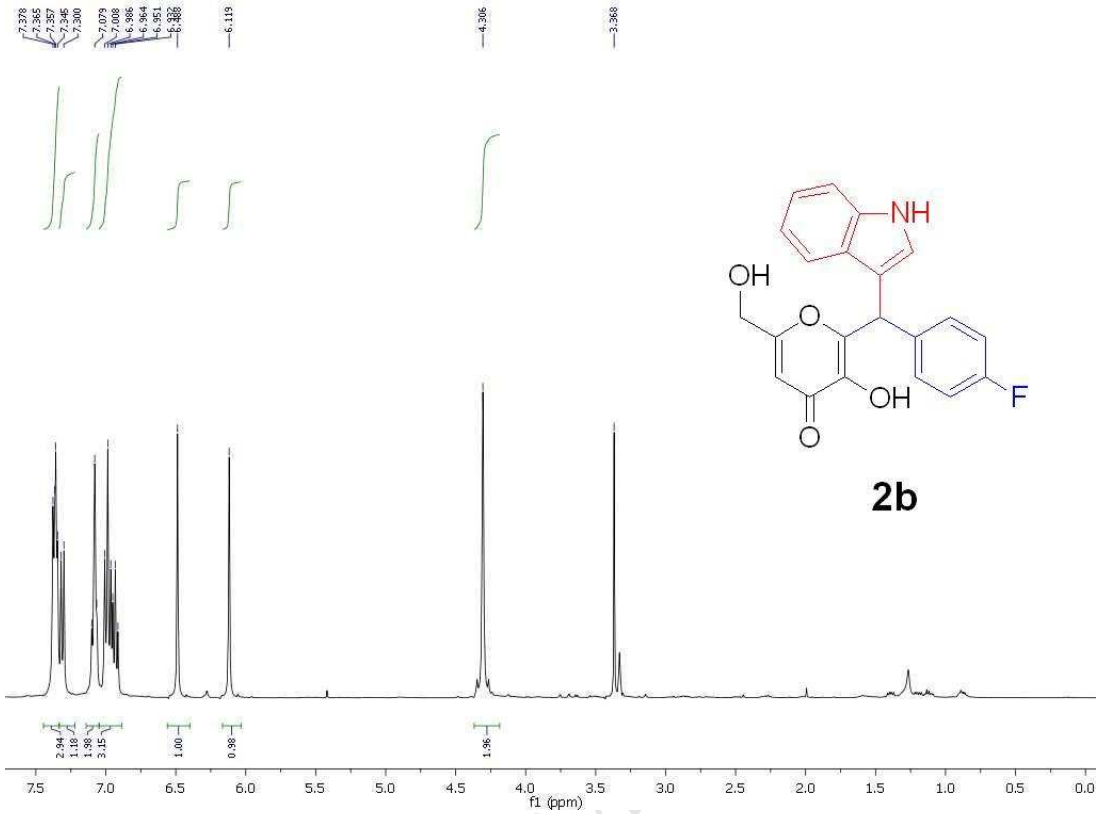
NH
OH
O
OH
F
O
2b
f1 (ppm)

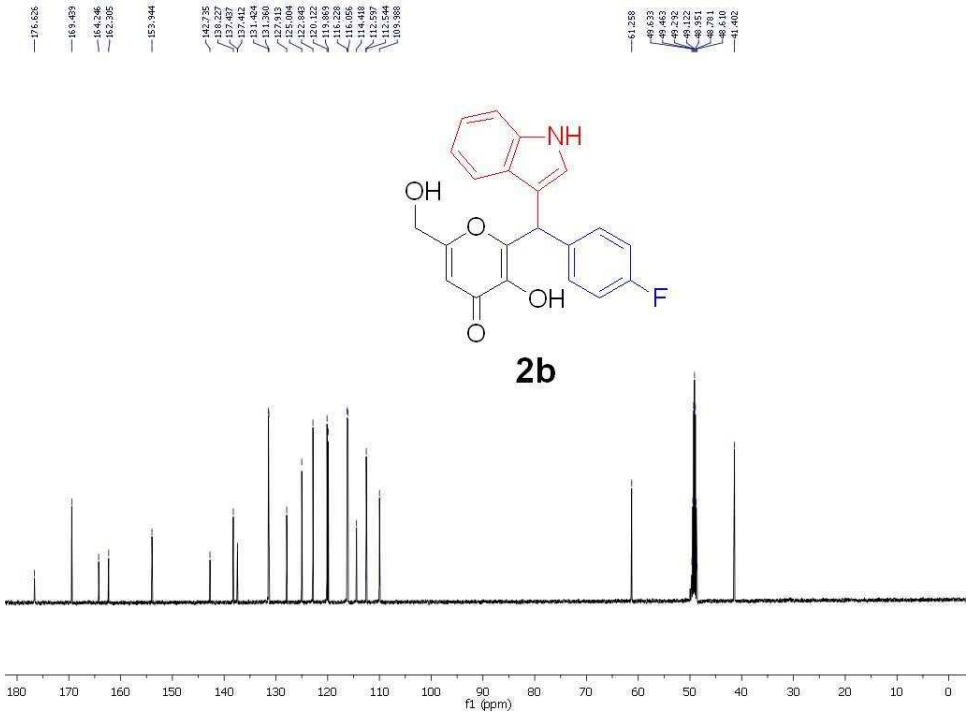
NH
OH
O
OH
F
O
2b
f1 (ppm)

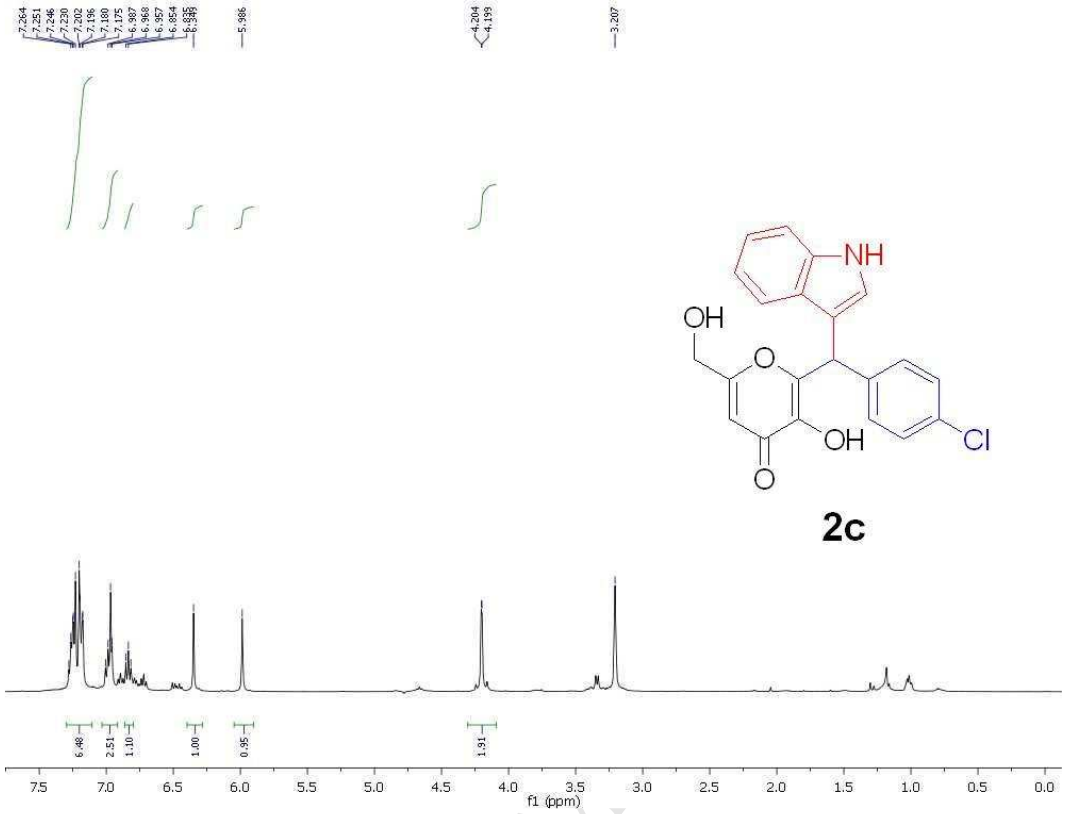
NH
OH
O
OH
Cl
O
2c
f1 (ppm)

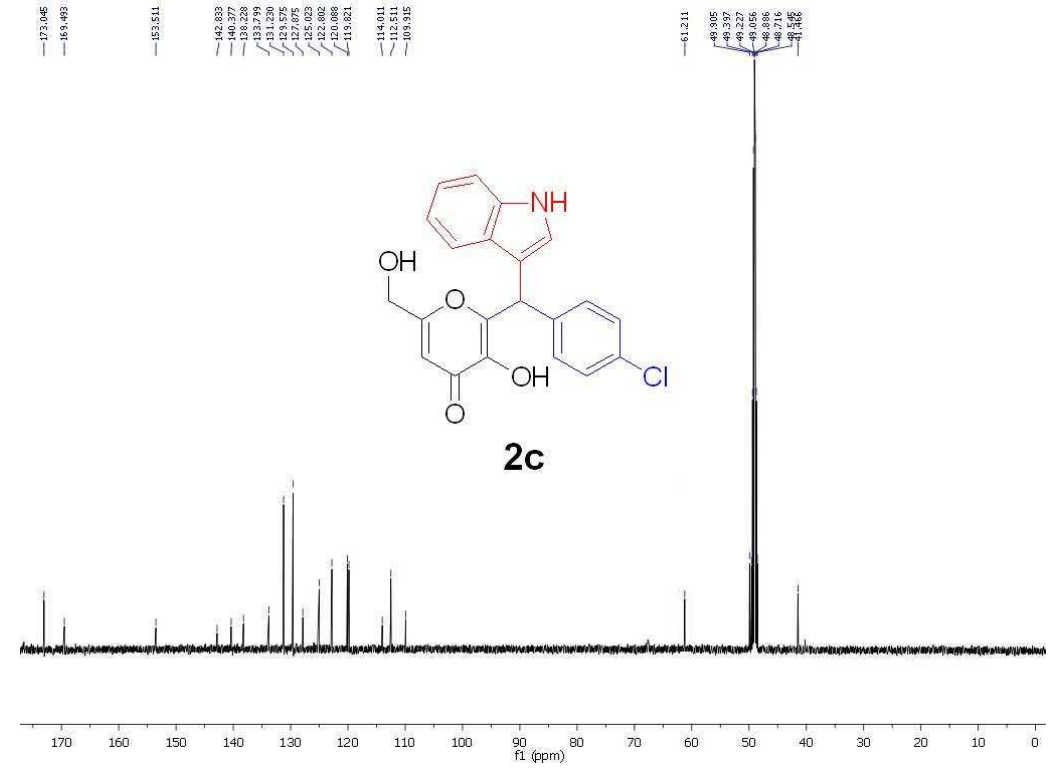
NH
OH
O
OH
Cl
O
2c
f1 (ppm)

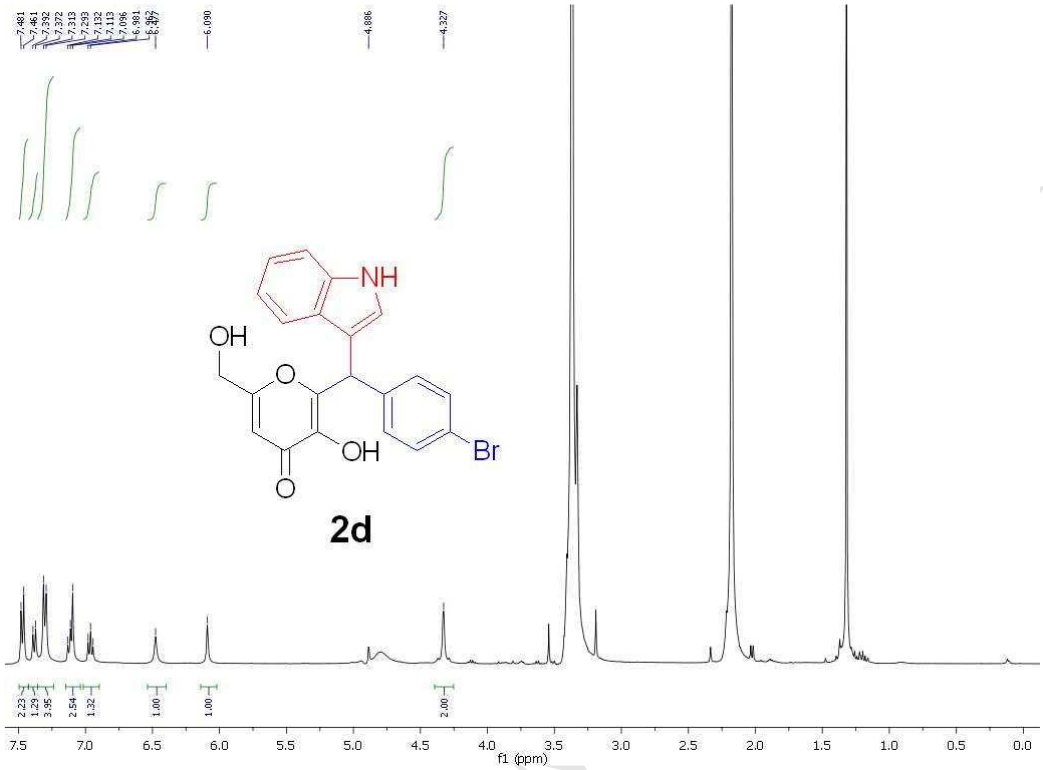
NH
OH
O
OH
Br
O
2d
f1 (ppm)

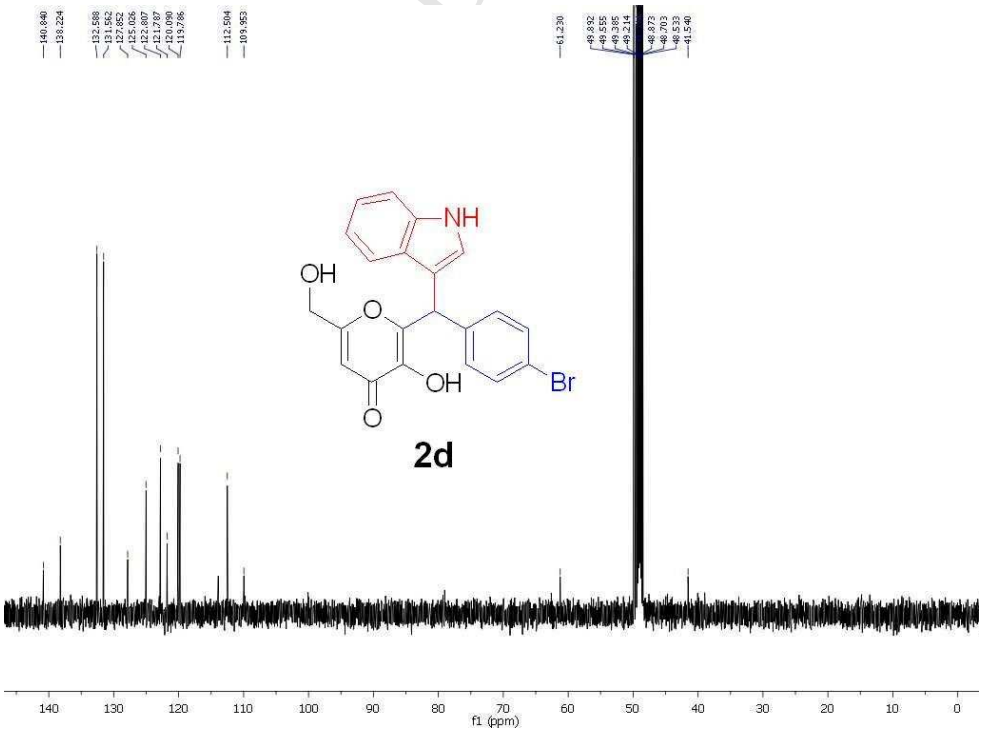
NH
OH
O
OH
Br
O
2d
f1 (ppm)

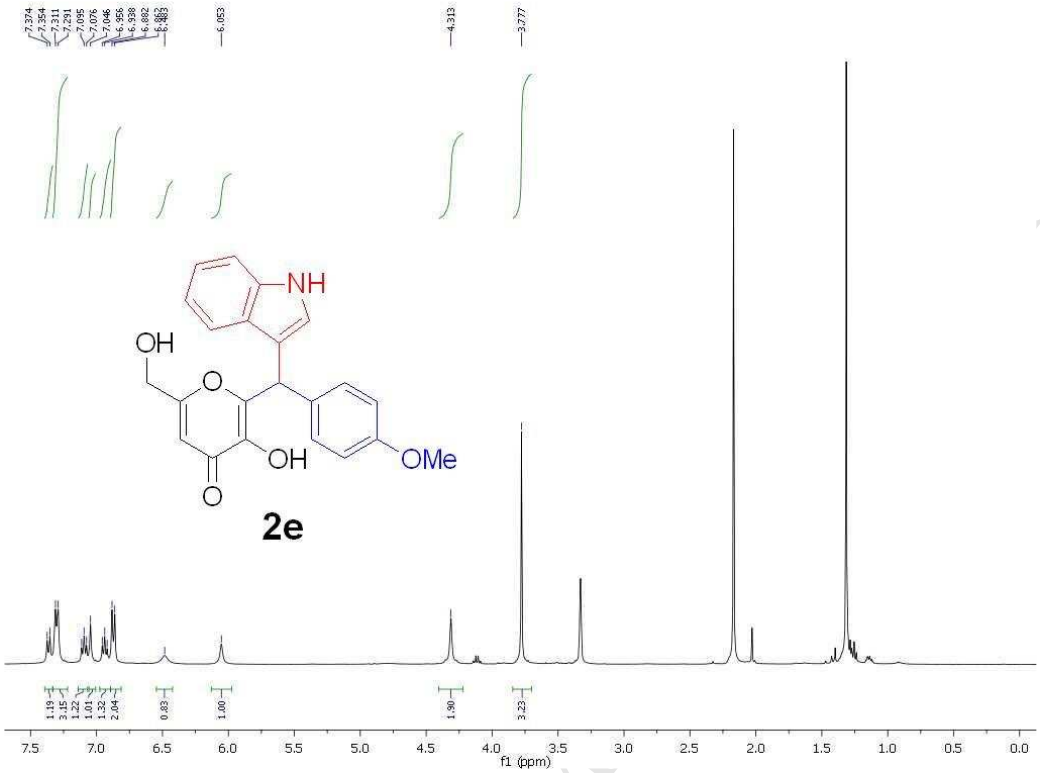
NH
OH
O
OH
OMe
O
2e
f1 (ppm)

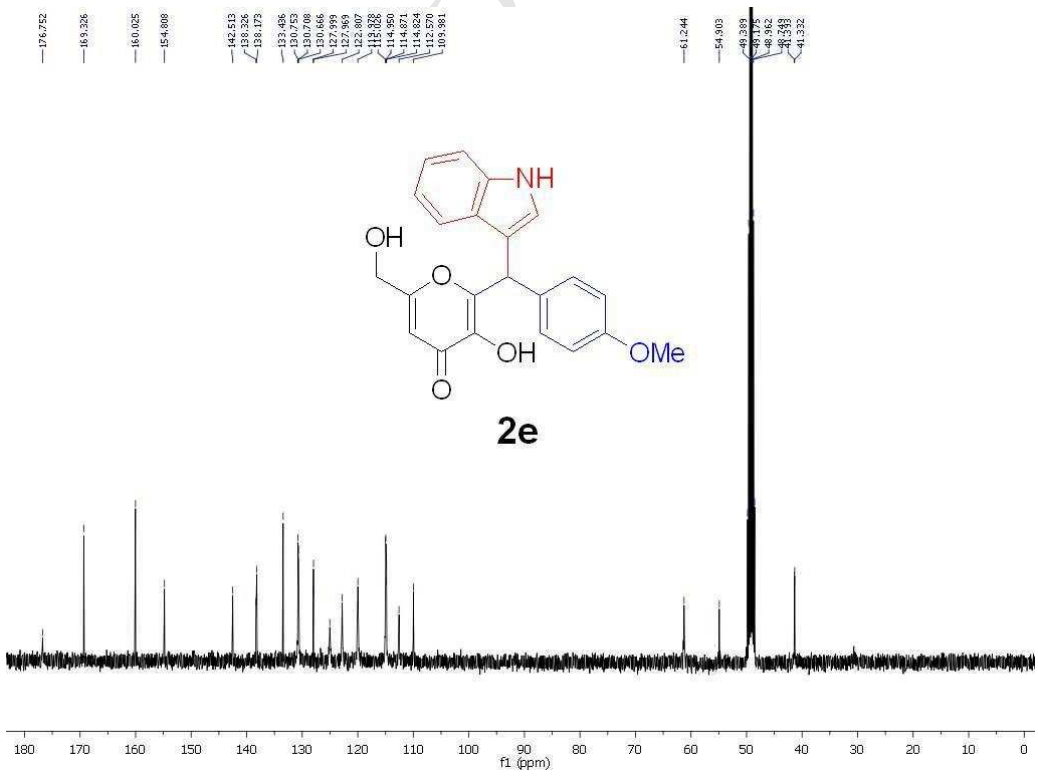
NH
OH
O
OH
OMe
O
2e
f1 (ppm)

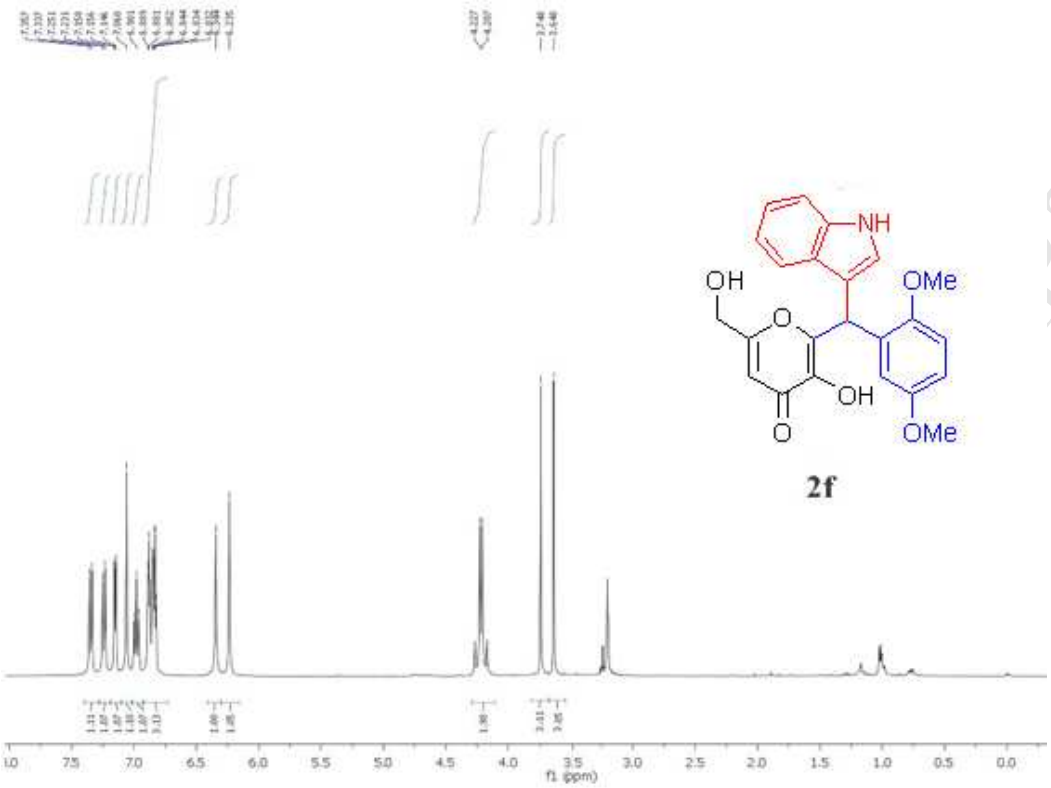
NH
OH
OMe
O
OH
O
OMe
2f
f1 (ppm)

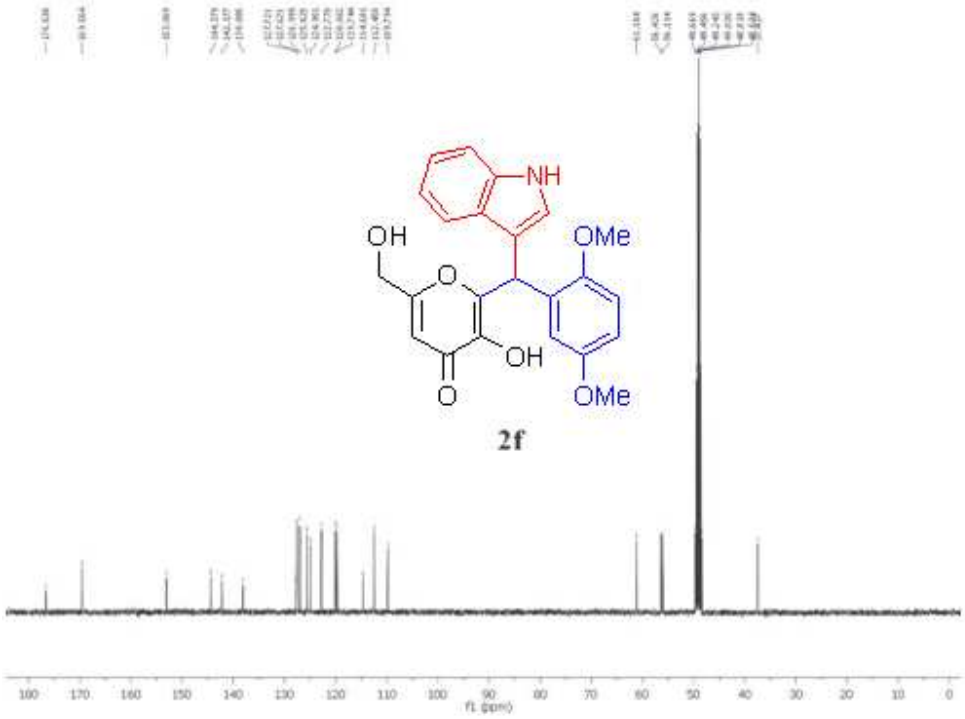
NH
OH
OMe
O
OH
O
OMe
2f
f1 (ppm)

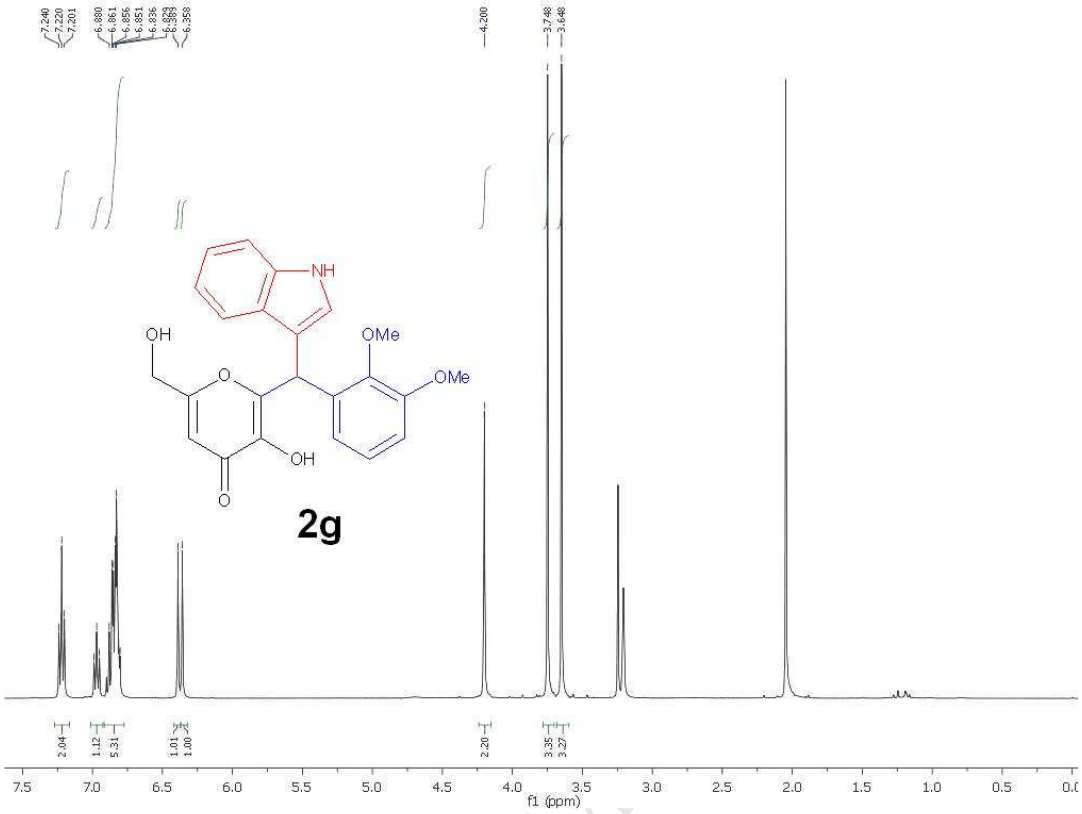
NH
OH
OMe
OMe
O
OH
O
2g
f1 (ppm)

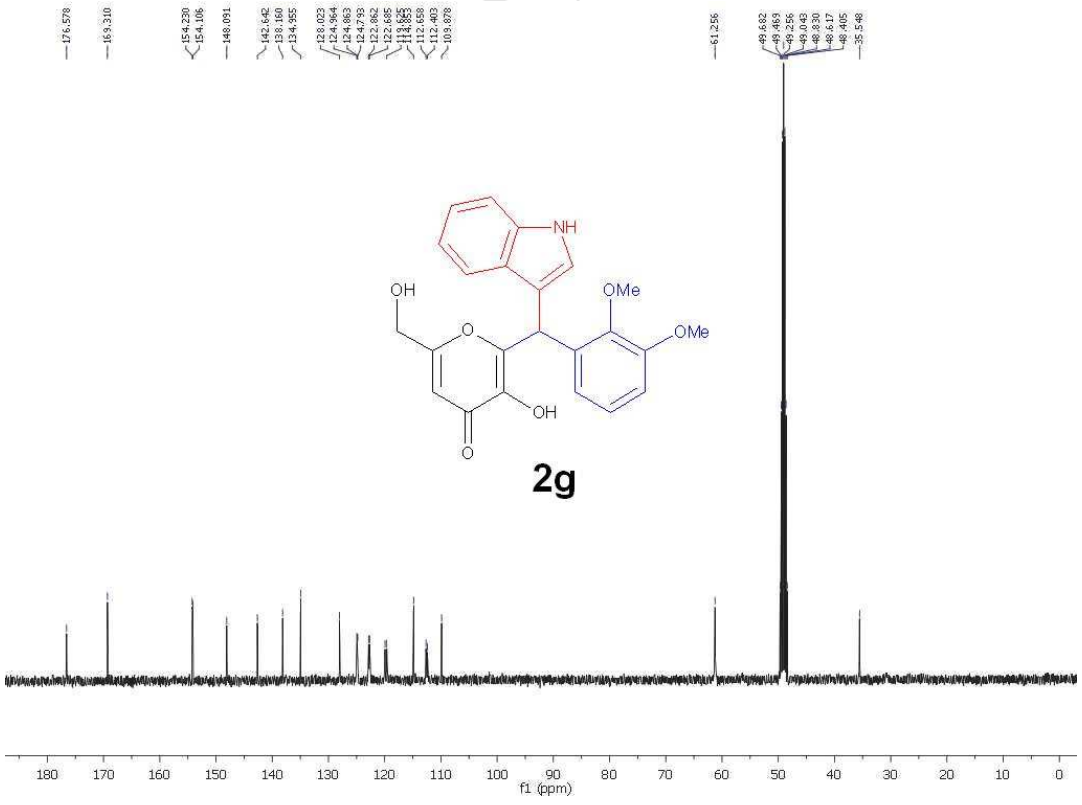
NH
OH
OMe
OMe
O
OH
O
2g
f1 (ppm)

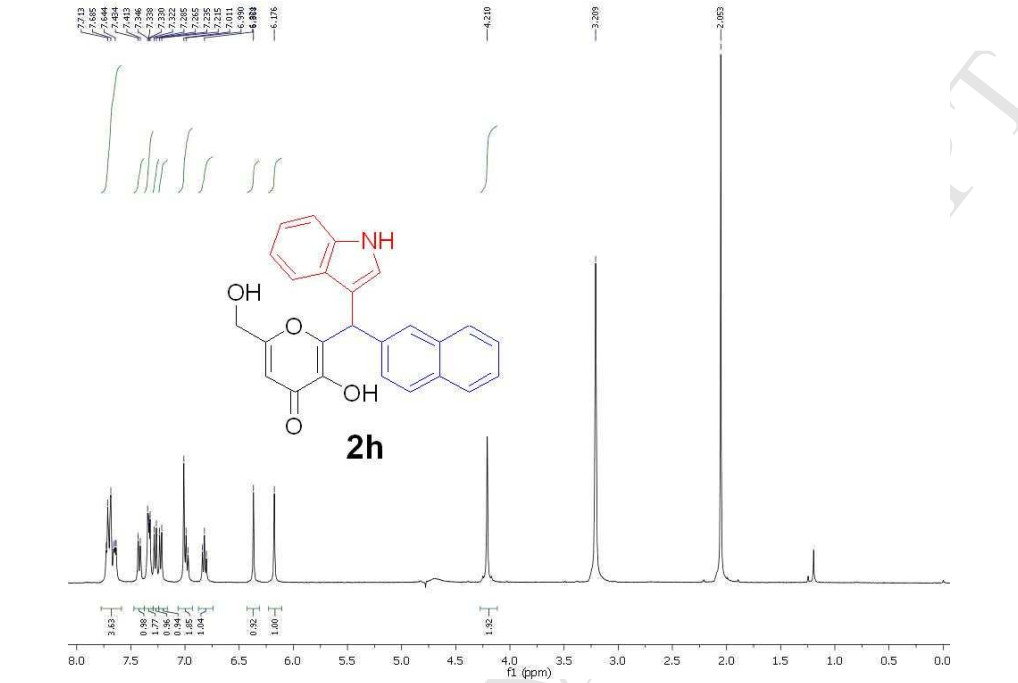
NH
OH
O
OH
O
2h
f1 (ppm)

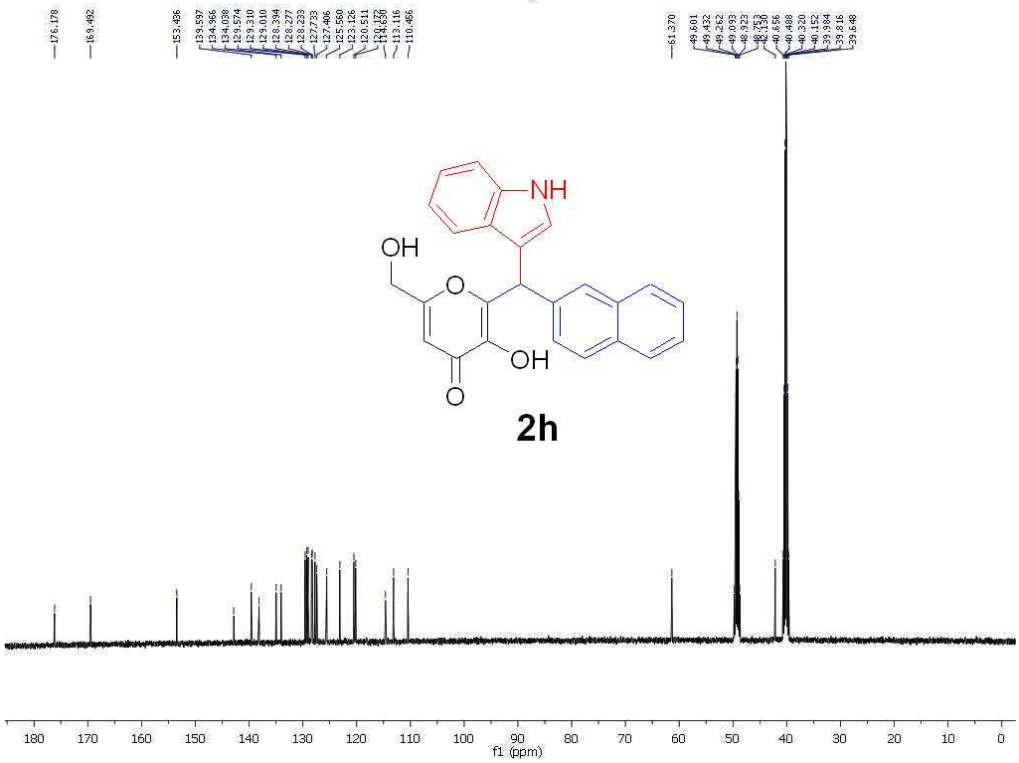
NH
OH
O
OH
O
2h
f1 (ppm)

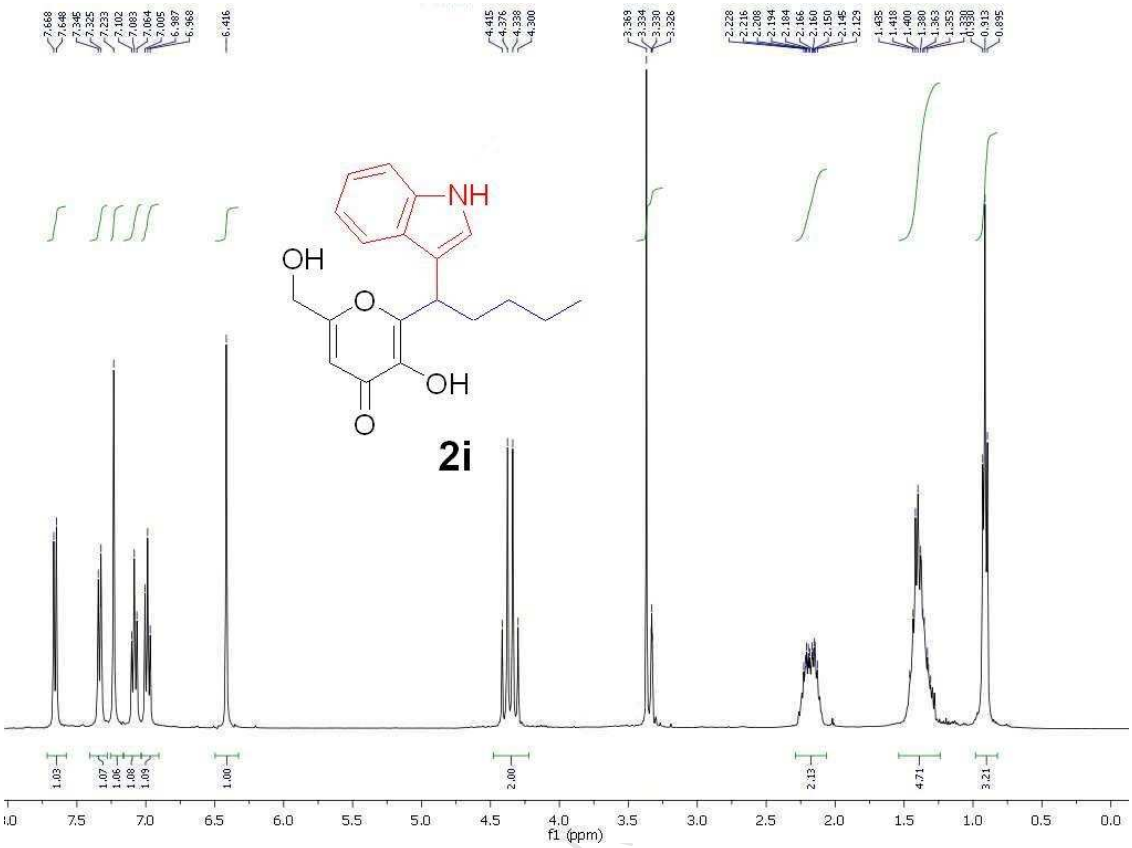
NH
OH
O
OH
O
2i
f1 (ppm)

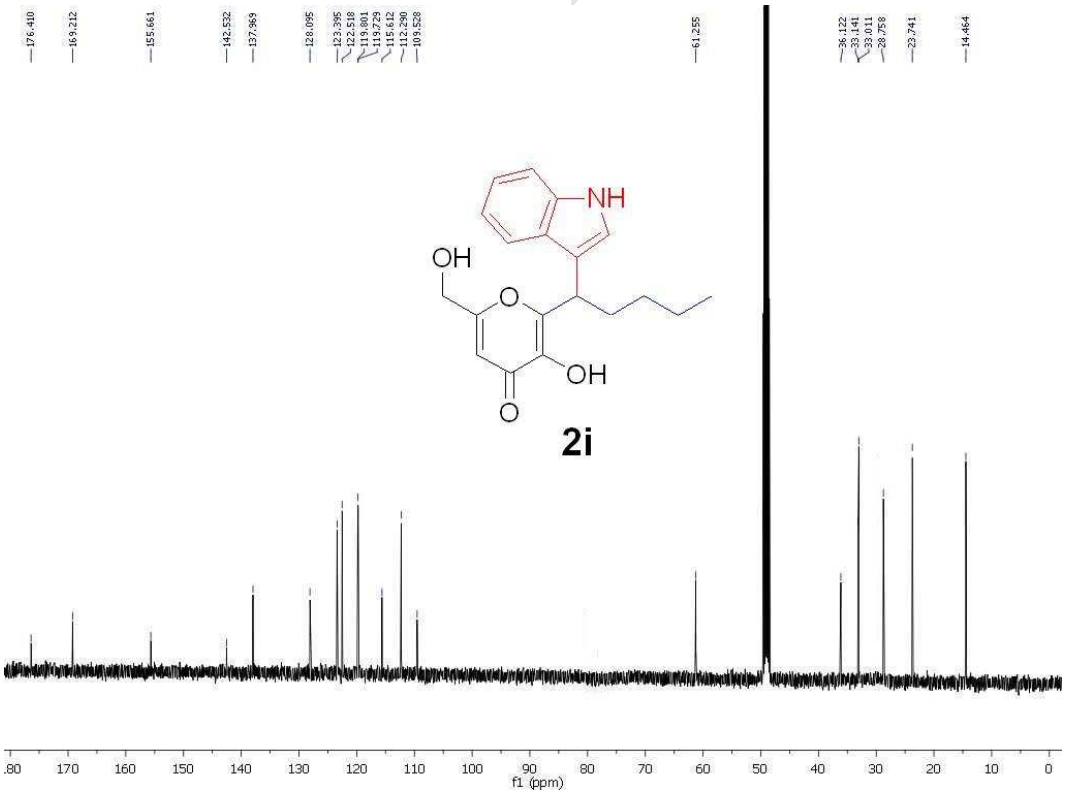
NH
OH
O
OH
O
2i
f1 (ppm)

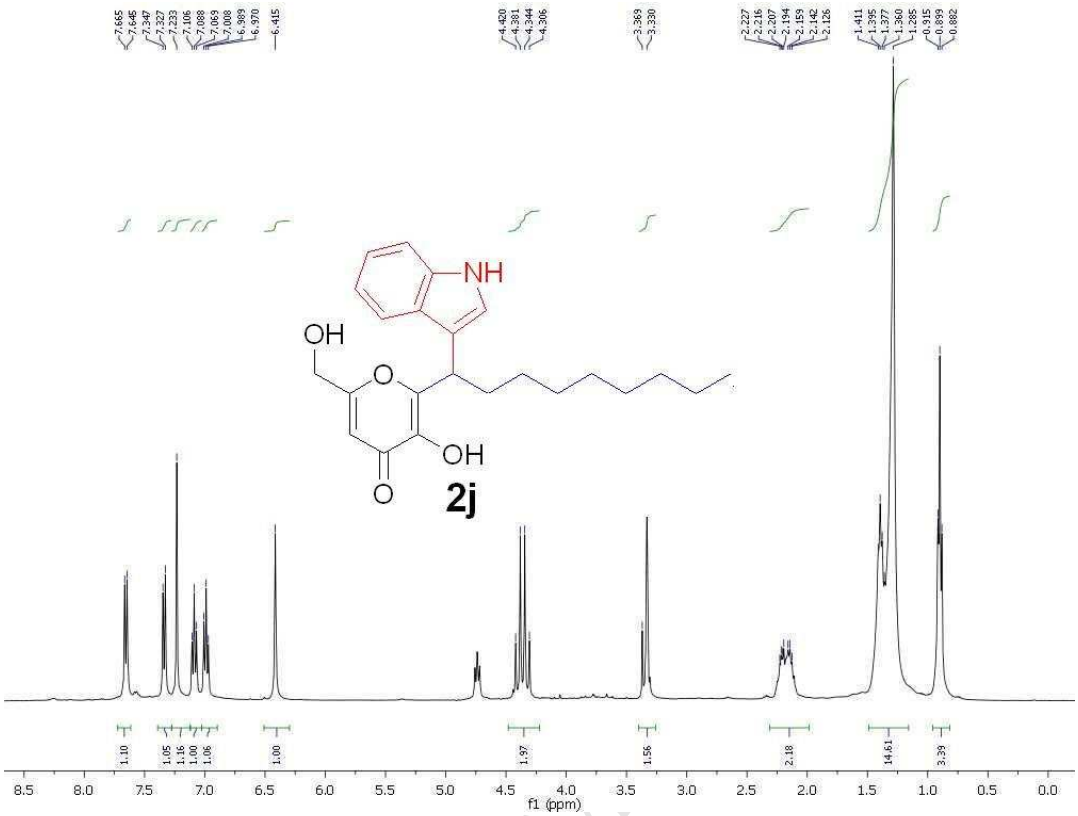
NH
OH
O
OH
O
2j
f1 (ppm)

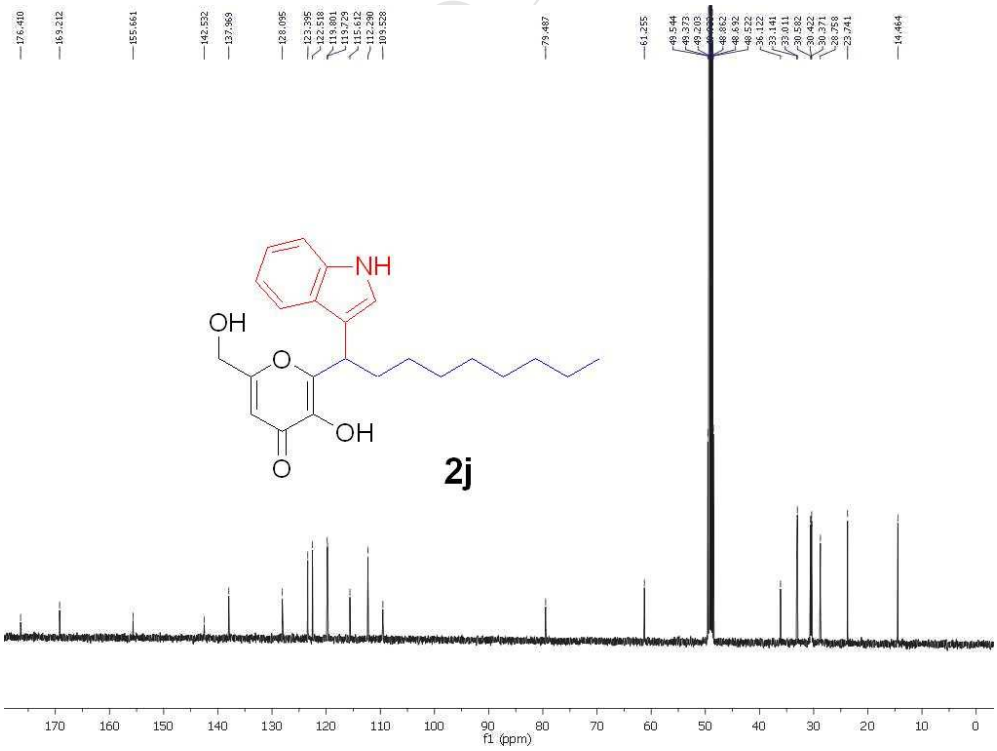
NH
OH
O
OH
O
2j
f1 (ppm)

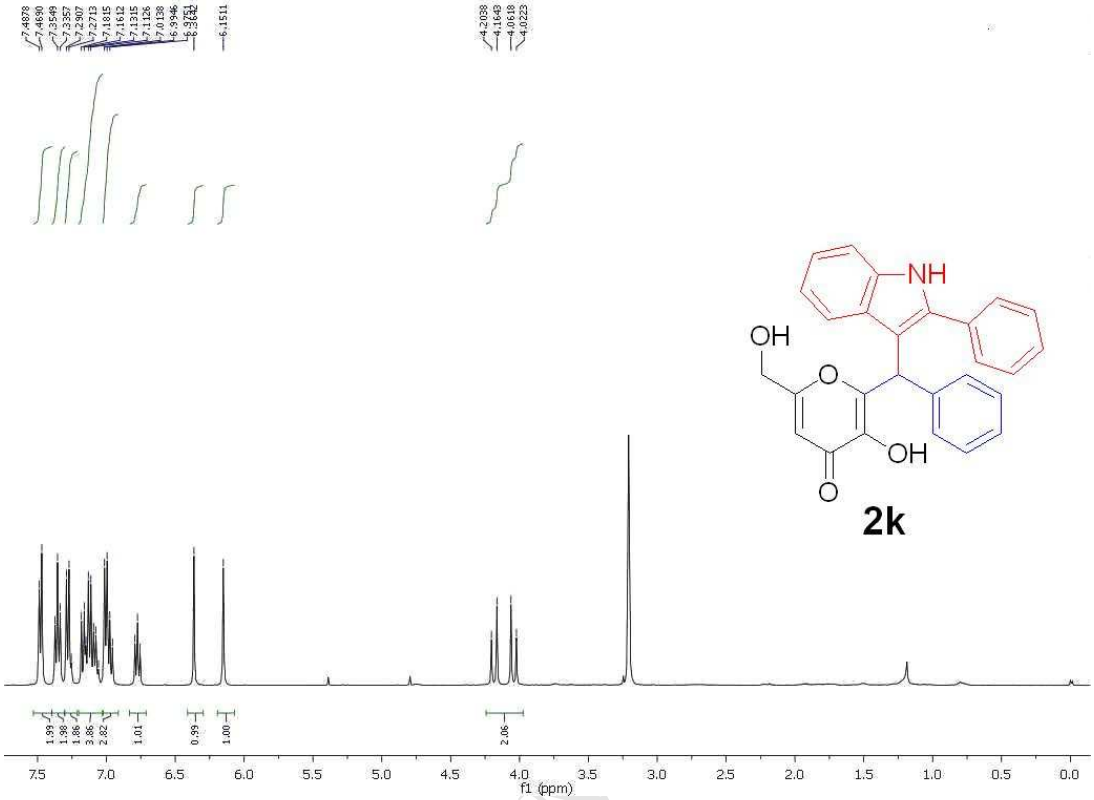
NH
OH
O
OH
O
2k
f1 (ppm)

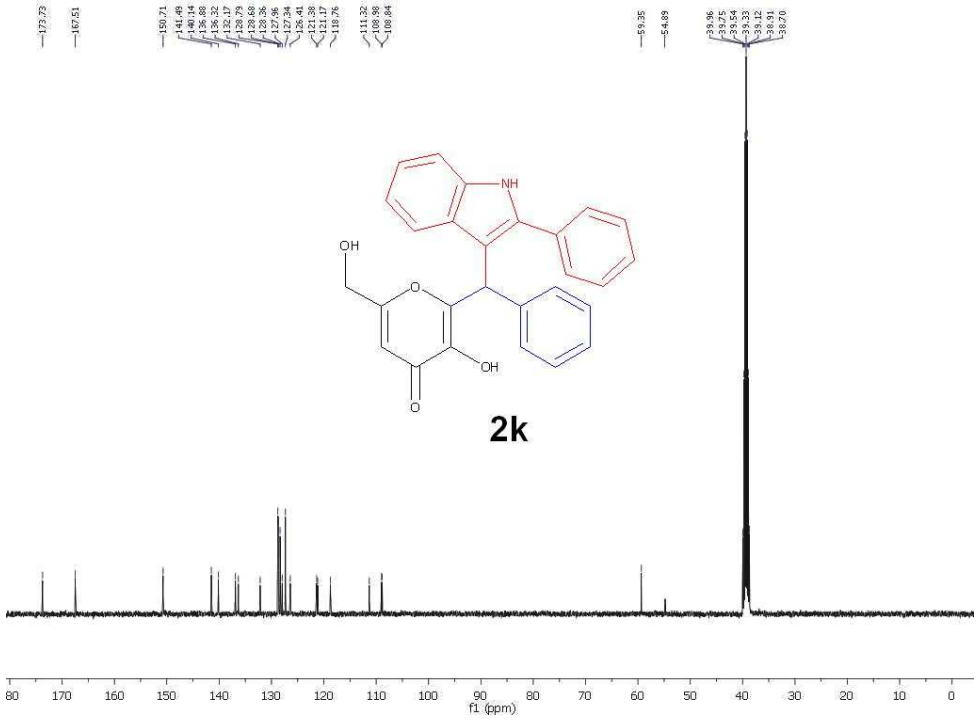
NH
OH
O
OH
O
2k
f1 (ppm)

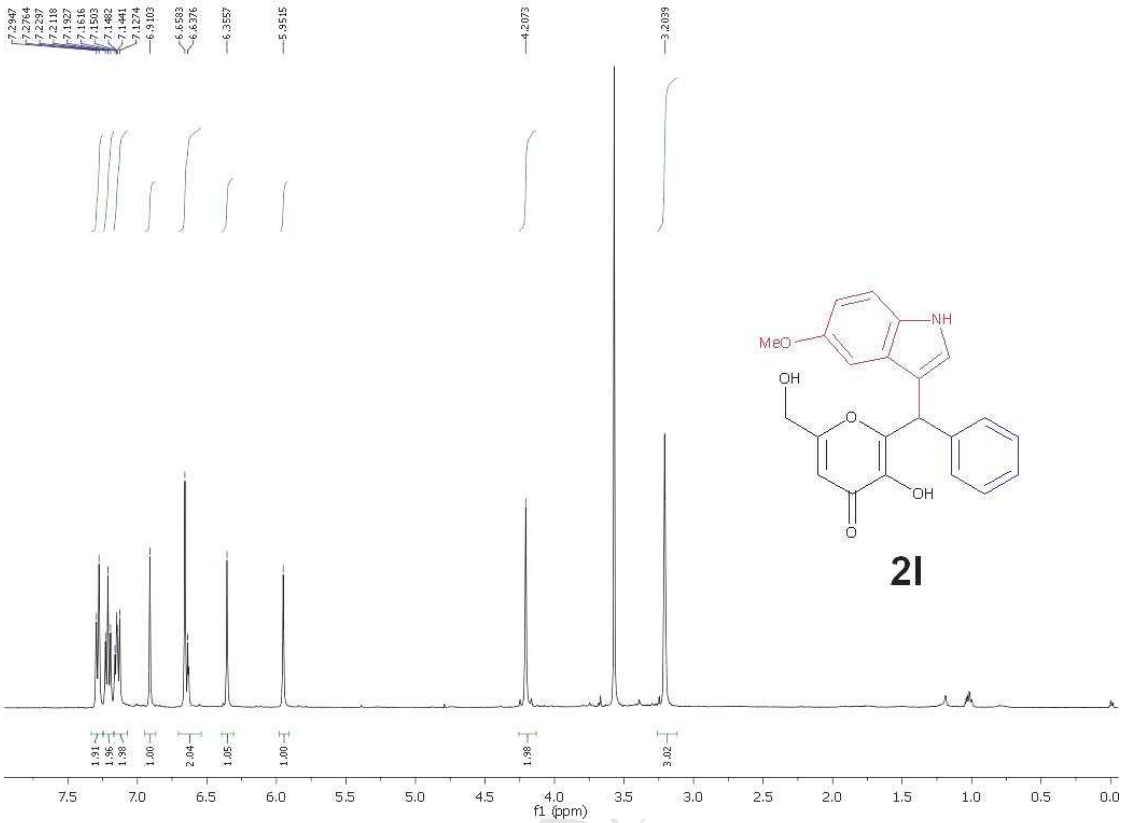
7.2947
7.2764
7.2297
7.2118
7.1927
7.1616
7.1503
7.1482
7.1441
7.1274
6.9103
6.8583
6.8376
6.3557
5.9515
4.2073
3.2039
MeO
NH
OH
O
OH
O
2l
1.91
1.96
1.98
1.00
2.04
1.05
1.00
1.98
3.02
7.5
7.0
6.5
6.0
5.5
5.0
4.5
4.0
3.5
3.0
2.5
2.0
1.5
1.0
0.5
0.0
f1 (ppm)

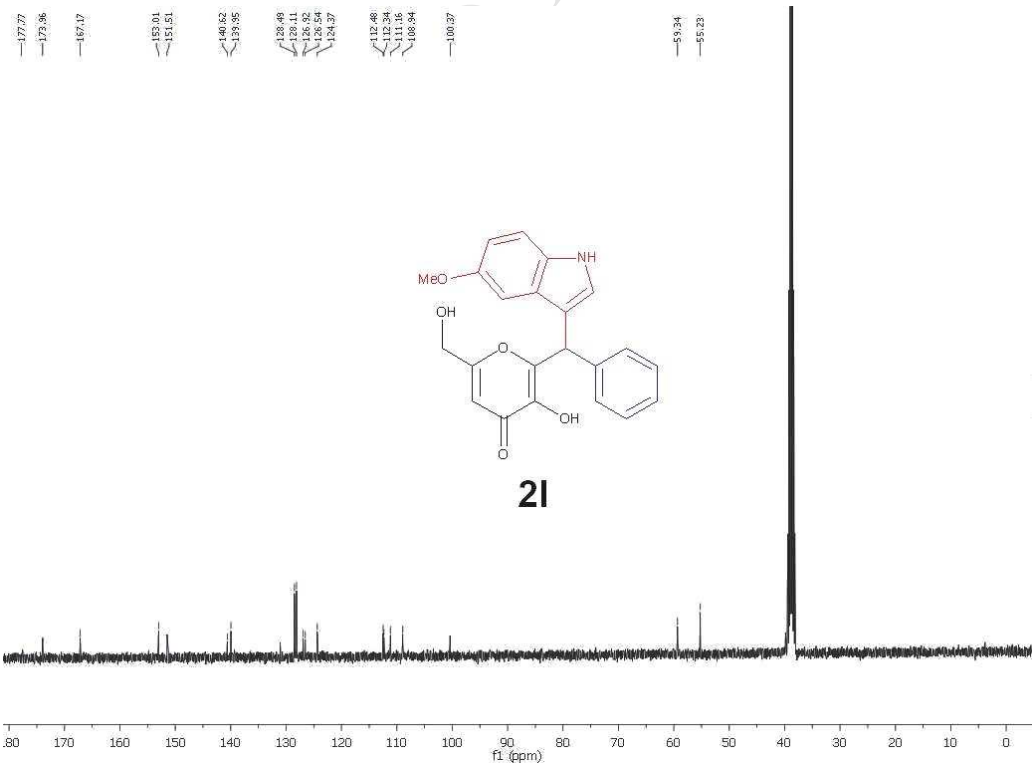
177.77
173.86
167.17
153.01
151.51
140.62
139.95
128.49
128.11
126.92
126.54
124.37
112.48
112.34
111.16
108.94
100.37
59.34
55.23
MeO
NH
OH
O
OH
O
2l
180
170
160
150
140
130
120
110
100
90
80
70
60
50
40
30
20
10
0
f1 (ppm)

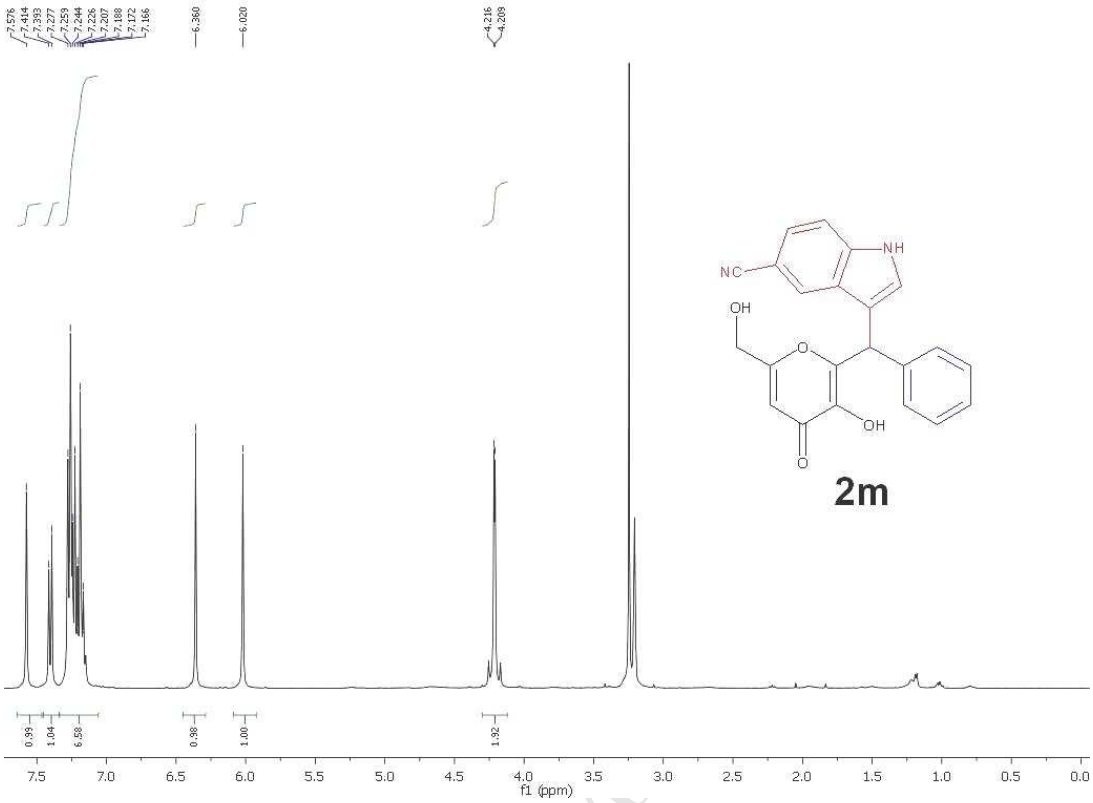
NC
NH
OH
O
OH
O
2m
f1 (ppm)

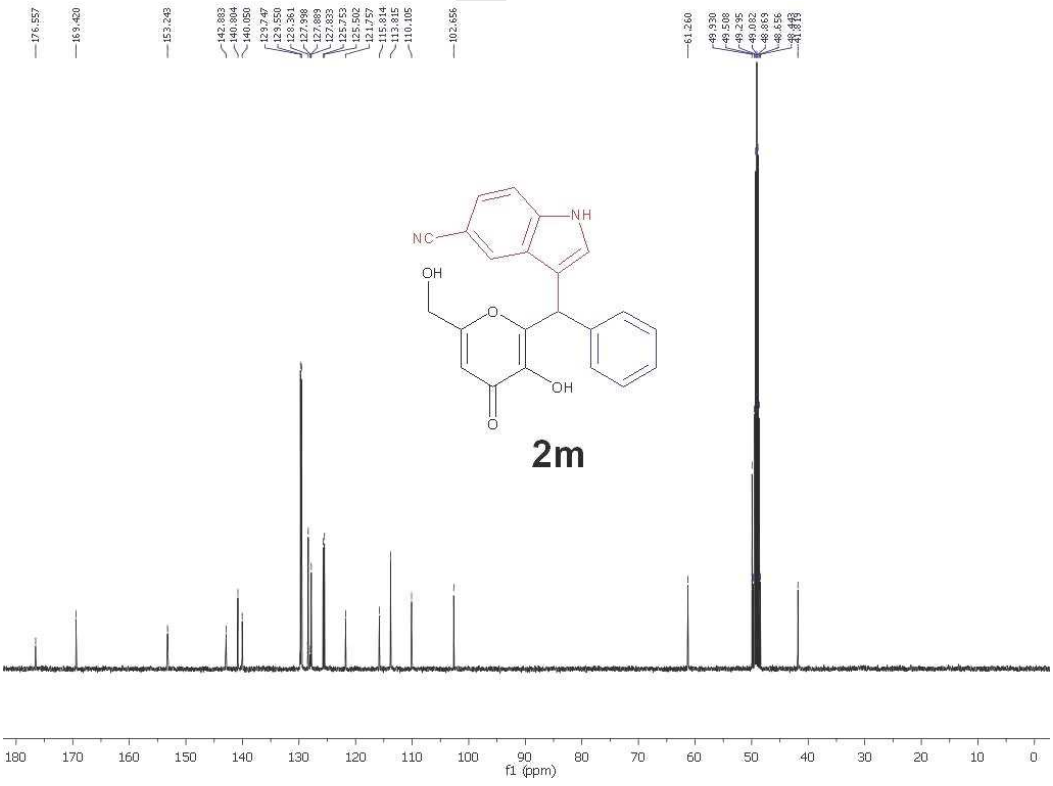
NC
NH
OH
O
OH
O
2m
f1 (ppm)

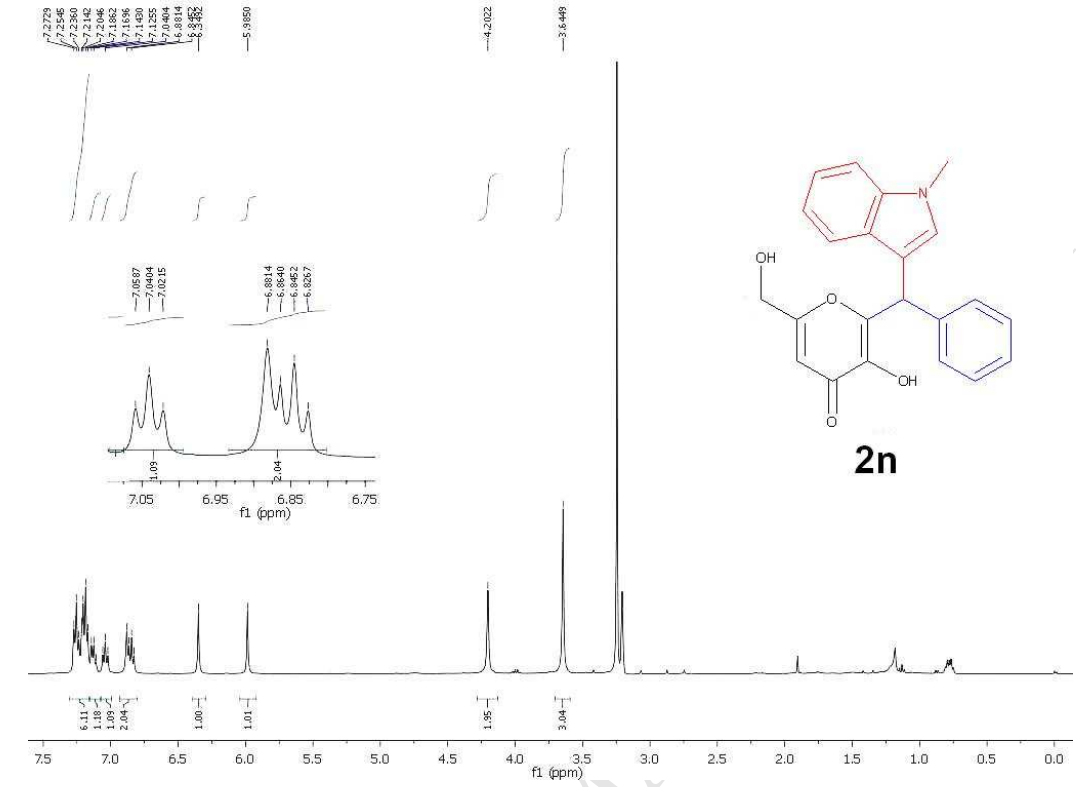
7.2729
7.2546
7.2360
7.2142
7.2046
7.1882
7.1696
7.1430
7.1255
7.0404
6.8814
5.9850
4.2022
3.6449
7.0587
7.0404
7.0215
6.8814
6.8640
6.8462
6.8267
1.09
2.04
7.05
6.95
6.85
6.75
f1 (ppm)
OH
O
OH
O
N
2n
6.11
1.18
1.09
2.04
1.00
1.01
1.95
3.04
7.5
7.0
6.5
6.0
5.5
5.0
4.5
4.0
3.5
3.0
2.5
2.0
1.5
1.0
0.5
0.0
f1 (ppm)

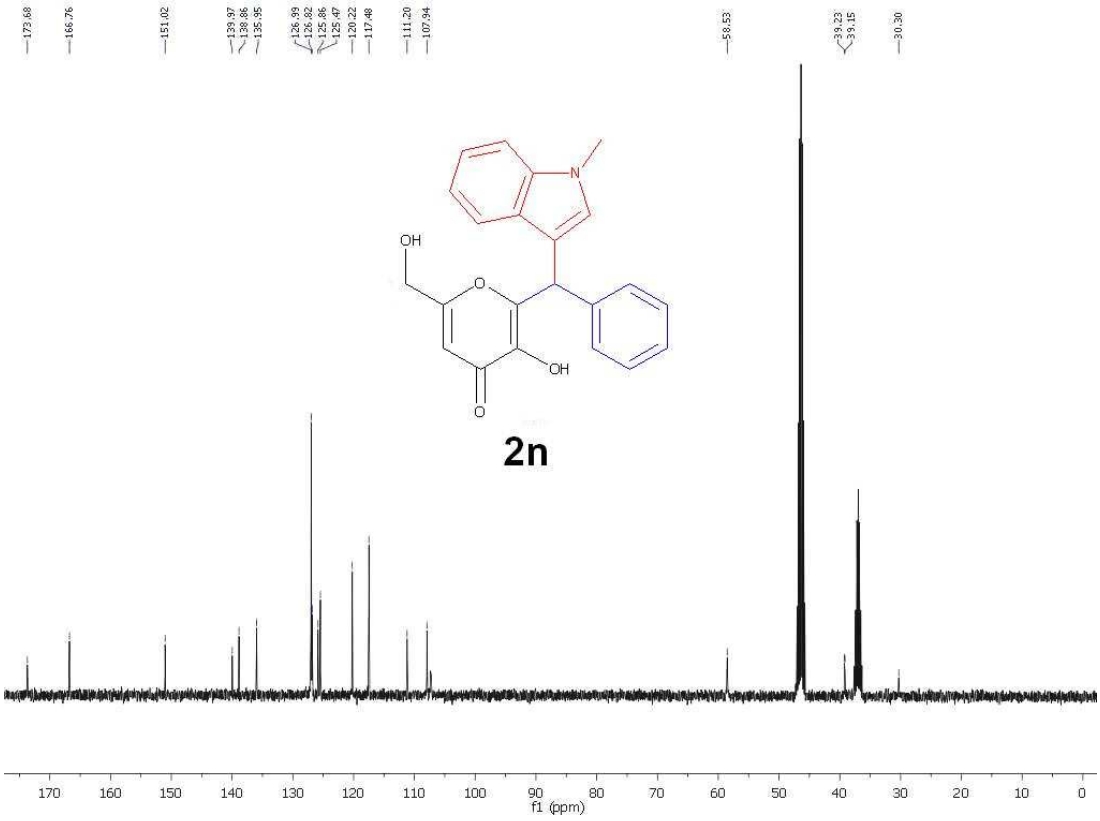
179.68
166.76
151.02
139.97
138.86
135.95
126.99
126.82
125.86
125.47
120.22
117.48
111.20
107.94
58.53
39.23
39.15
30.30
OH
O
OH
O
N
2n
170
160
150
140
130
120
110
100
90
80
70
60
50
40
30
20
10
0
f1 (ppm)

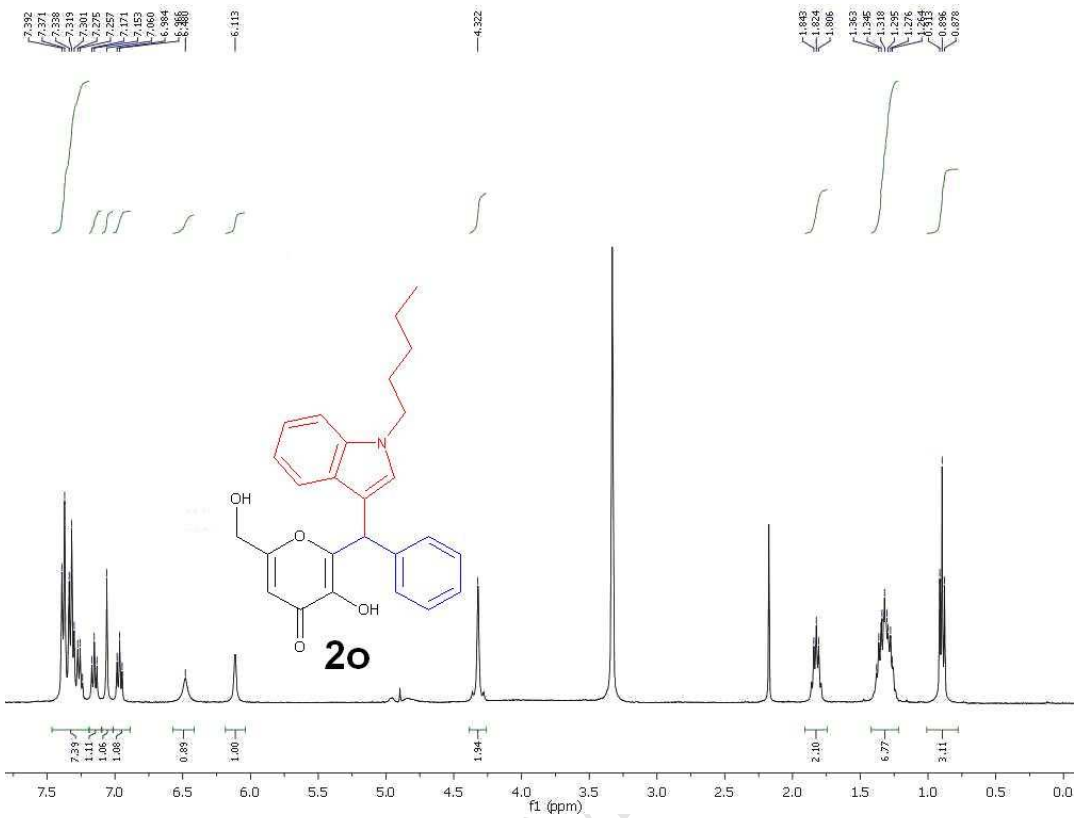
OH
O
OH
O
N
2o
f1 (ppm)

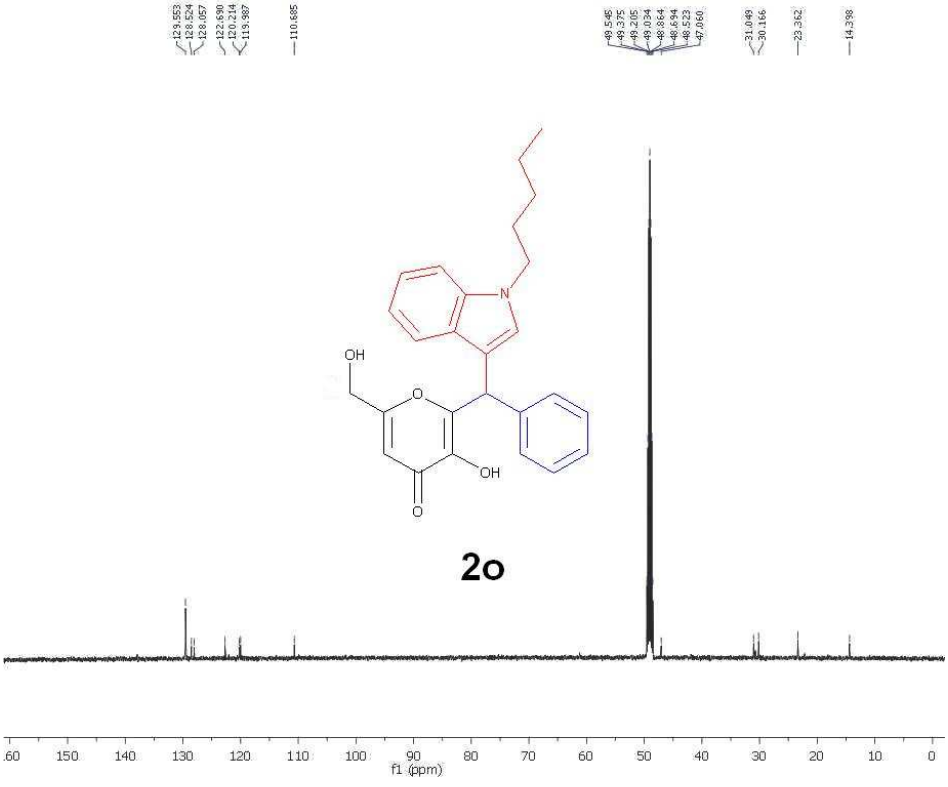
OH
O
OH
O
N
2o
f1 (ppm)

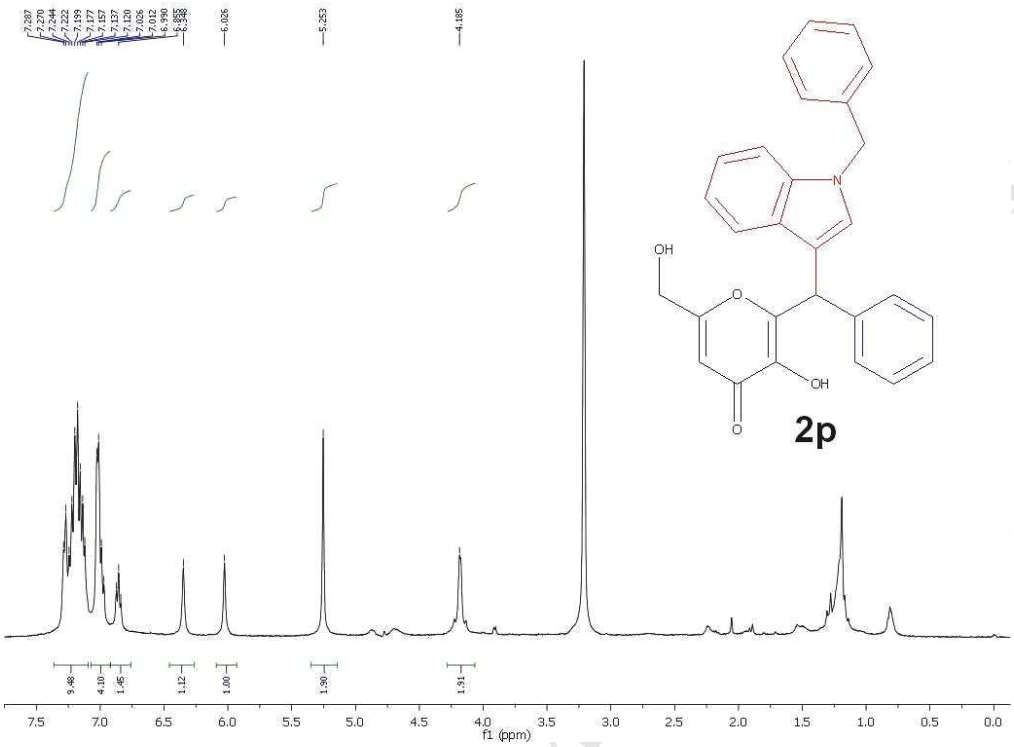
OH
O
OH
O
N
2p
f1 (ppm)

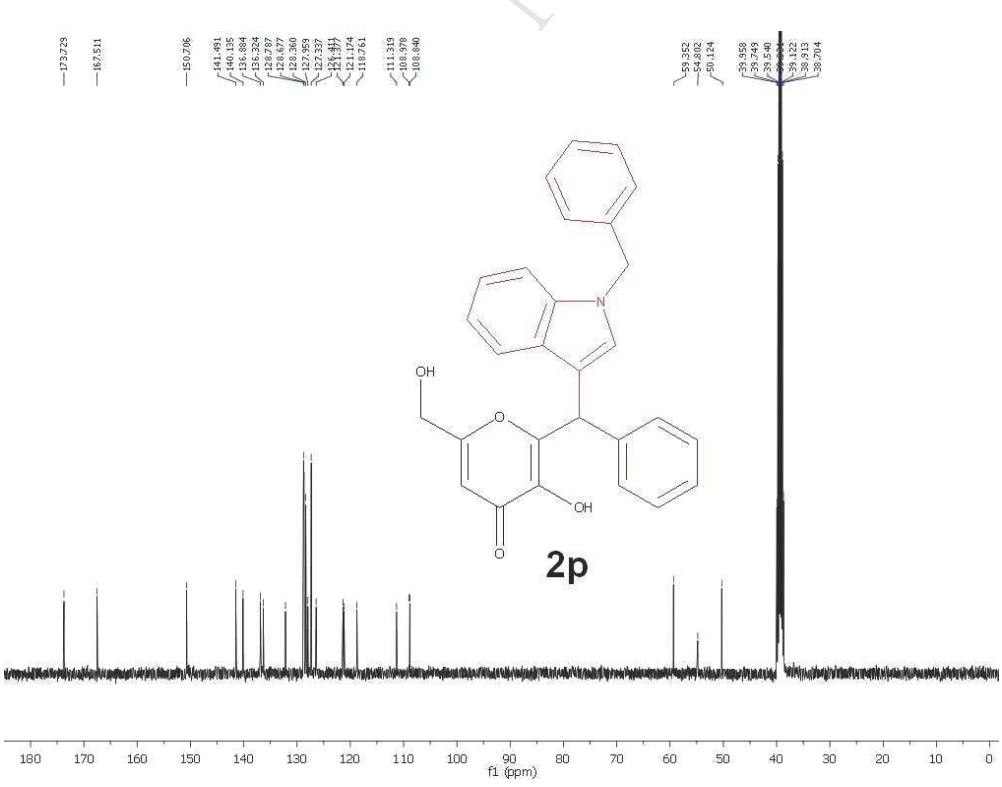
OH
O
OH
O
N
2p
f1 (ppm)

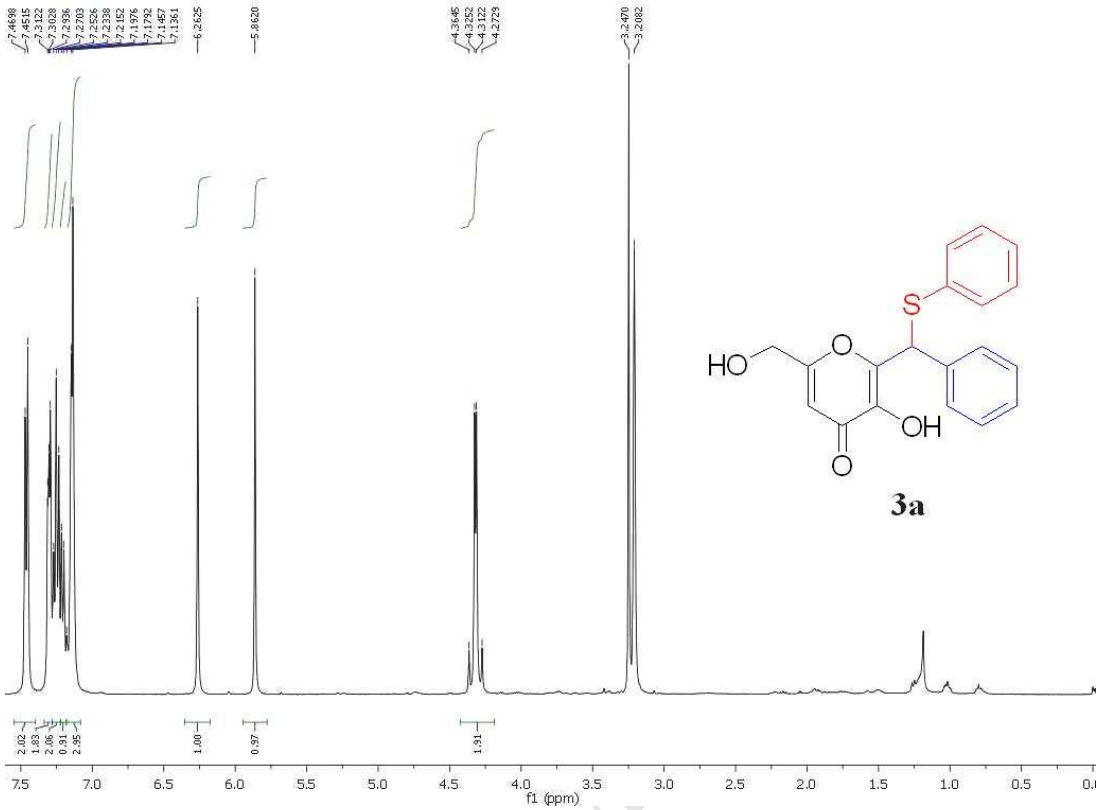
HO
O
S
OH
O
3a
f1 (ppm)

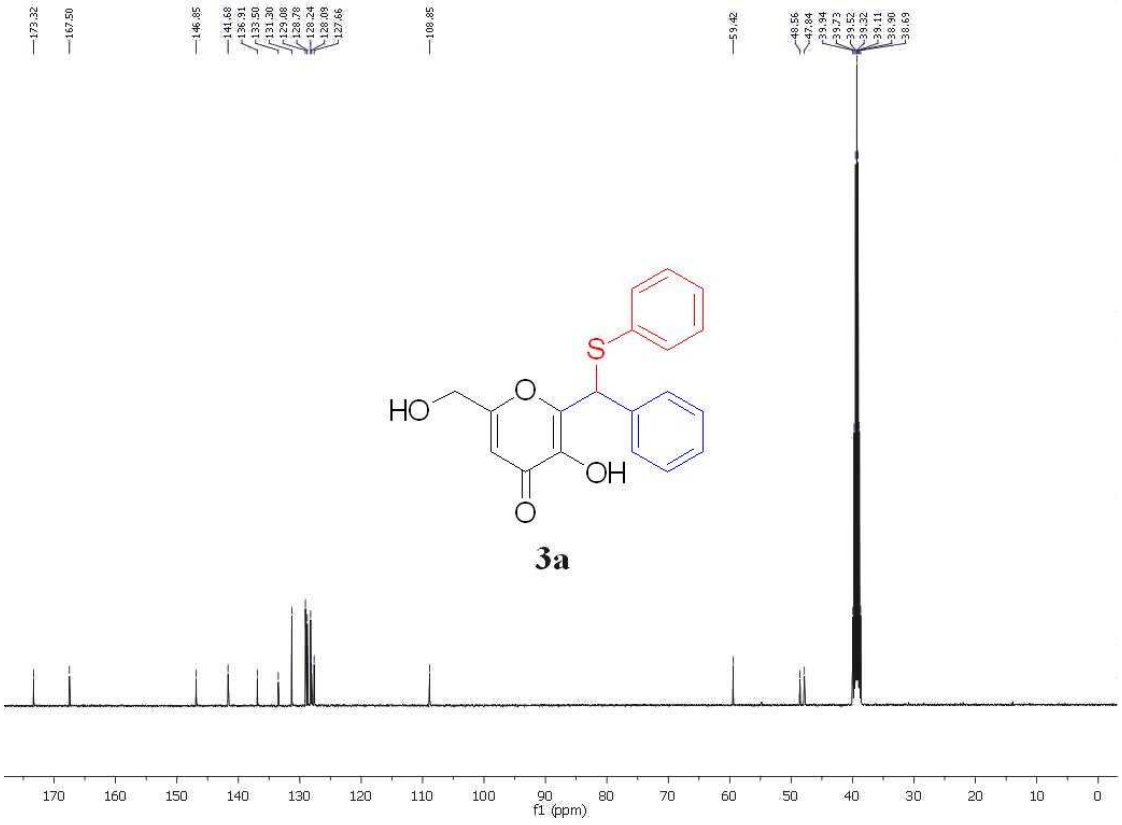
HO
O
S
OH
O
3a
f1 (ppm)

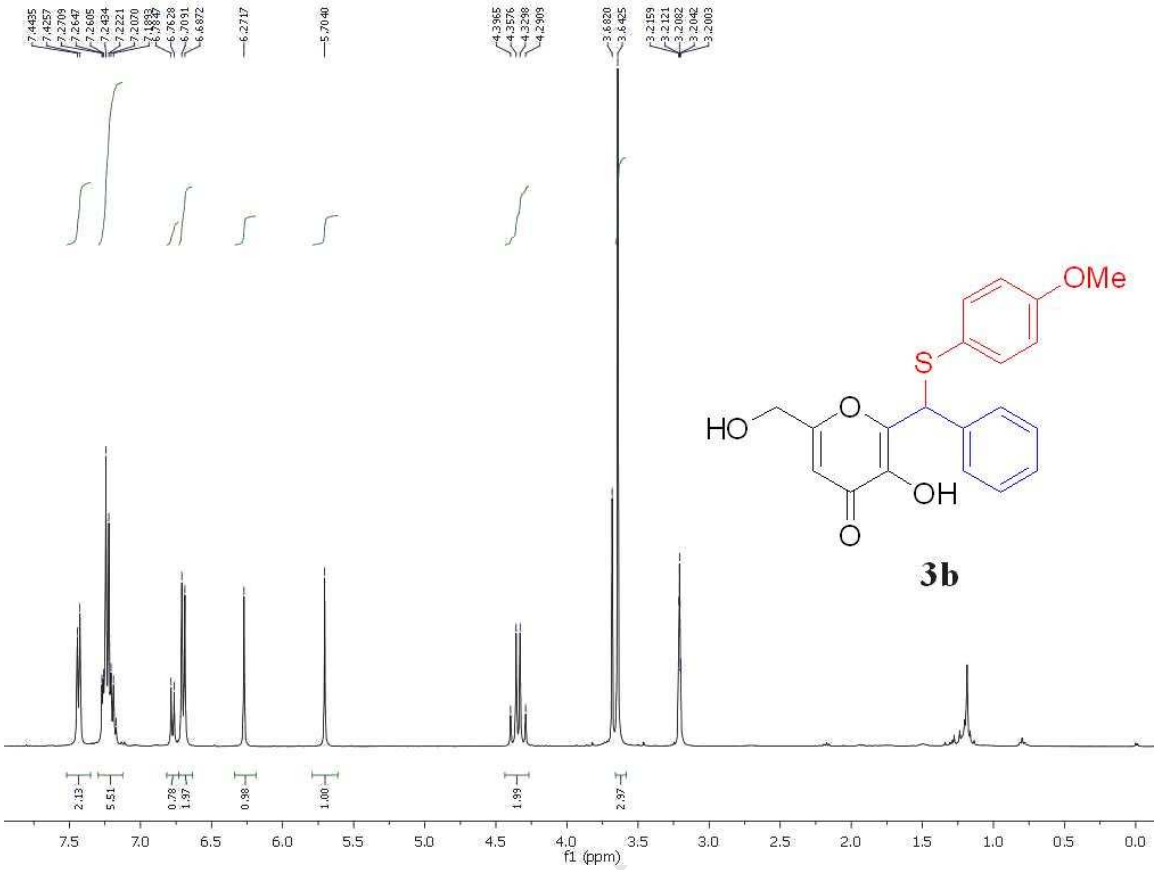
OMe
S
HO
O
OH
O
3b
f1 (ppm)

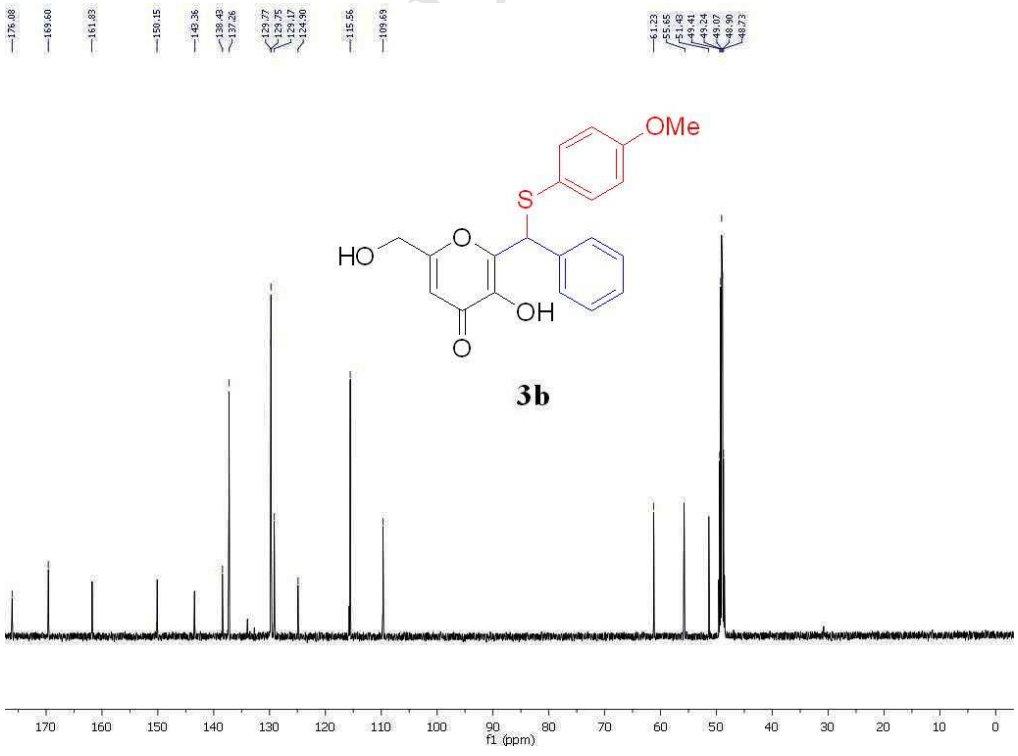
OMe
S
HO
O
OH
O
3b
f1 (ppm)

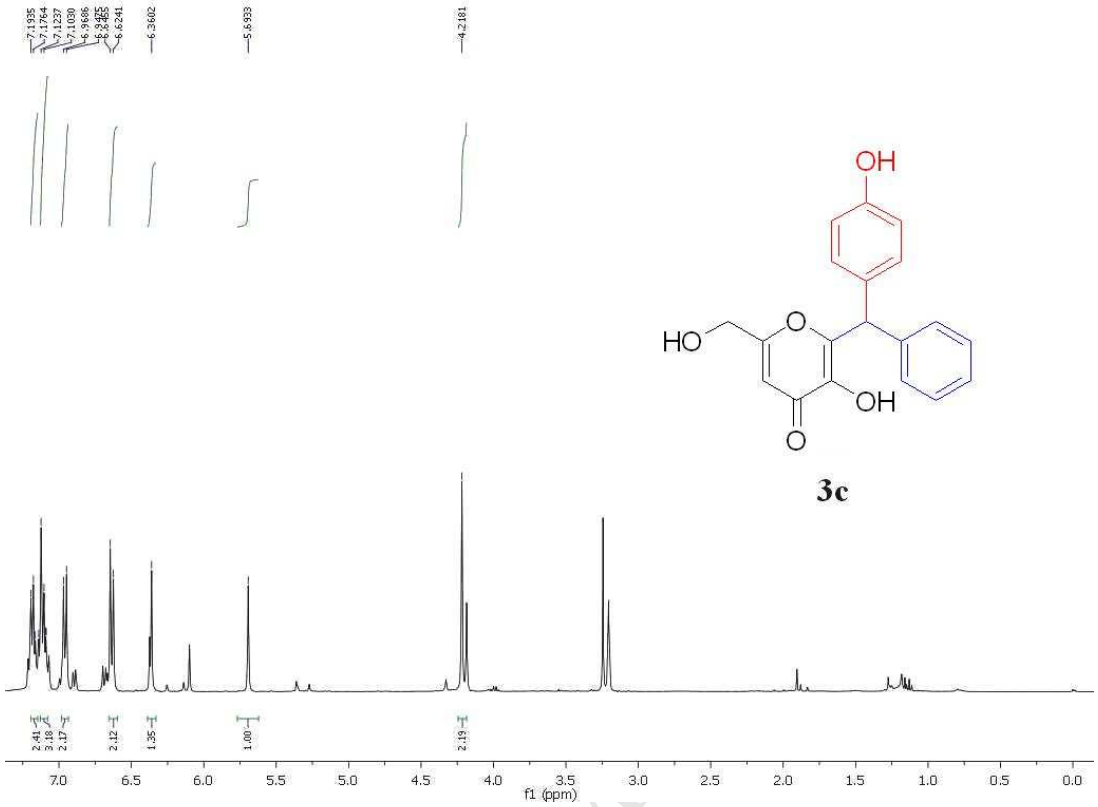
OH
HO
O
OH
O
3c
f1 (ppm)

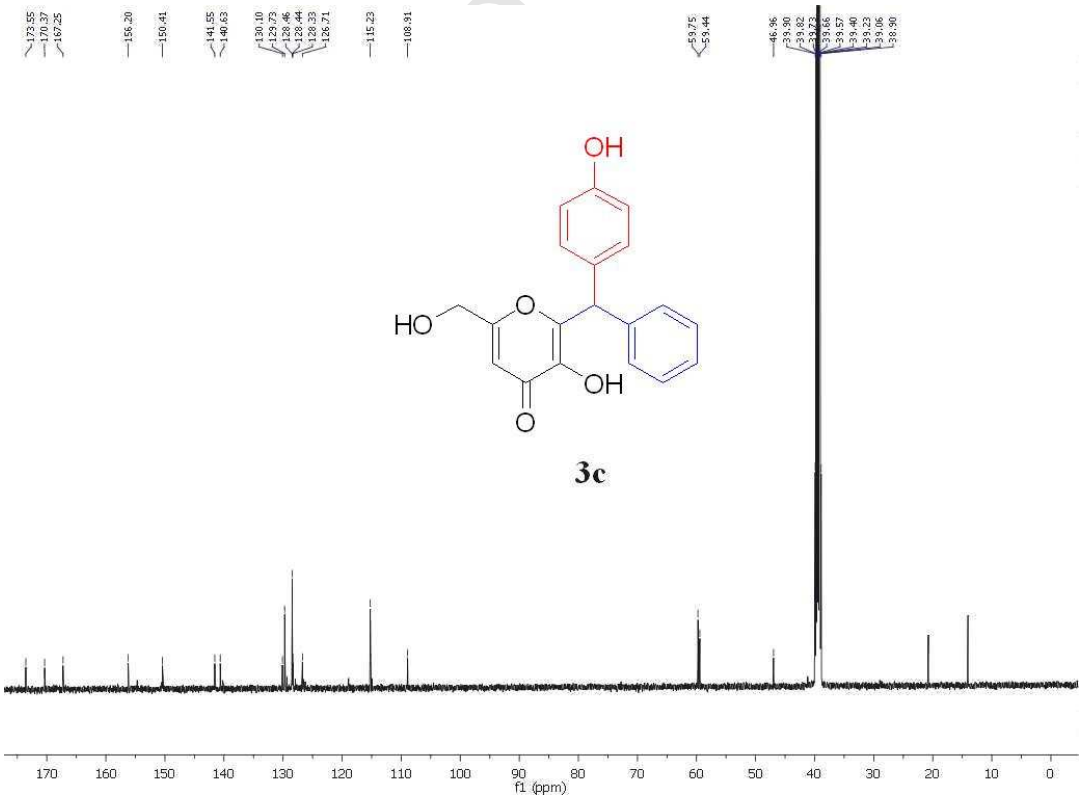
OH
HO
O
OH
O
3c
f1 (ppm)

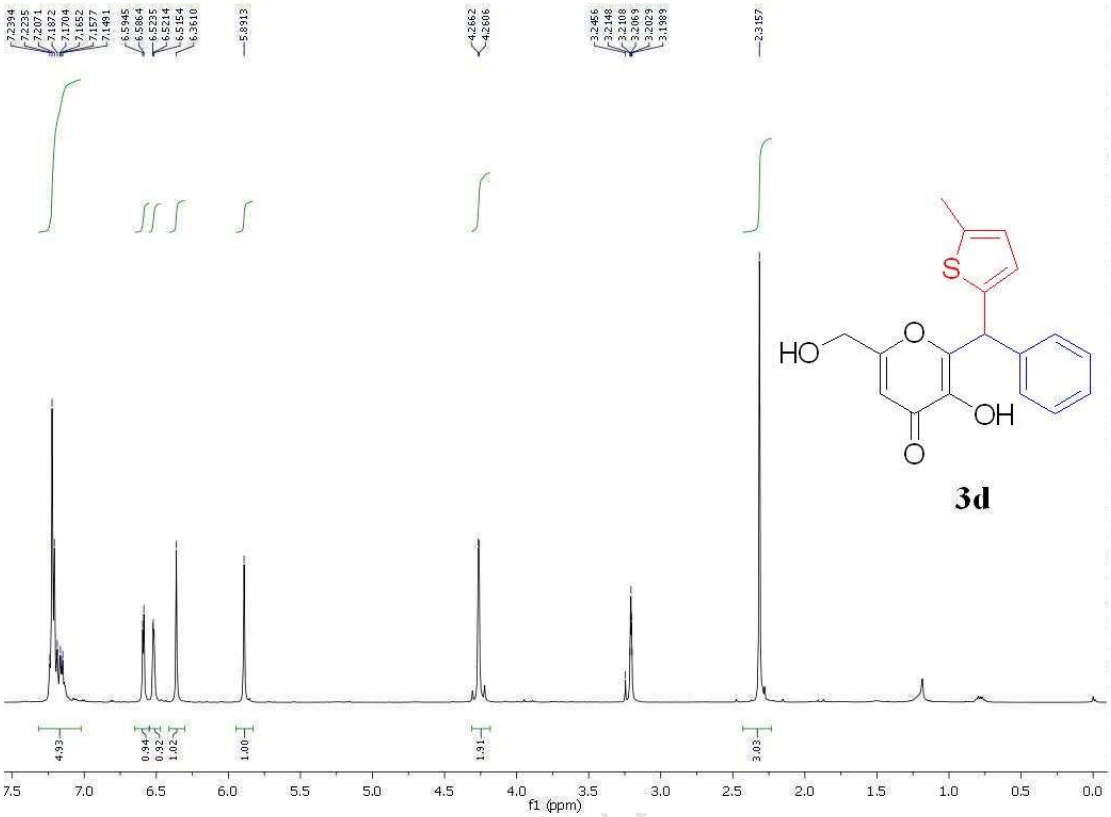
7.2394
7.2235
7.2071
7.1872
7.1704
7.1652
7.1577
7.1491
6.5945
6.5864
6.5235
6.5214
6.5154
6.3610
5.8913
4.2662
4.2606
3.2456
3.2148
3.2108
3.2069
3.2029
3.1989
2.3157
4.93
0.94
0.92
1.02
1.00
1.91
3.03
7.5 7.0 6.5 6.0 5.5 5.0 4.5 4.0 3.5 3.0 2.5 2.0 1.5 1.0 0.5 0.0
f1 (ppm)
S
HO
O
OH
O
3d

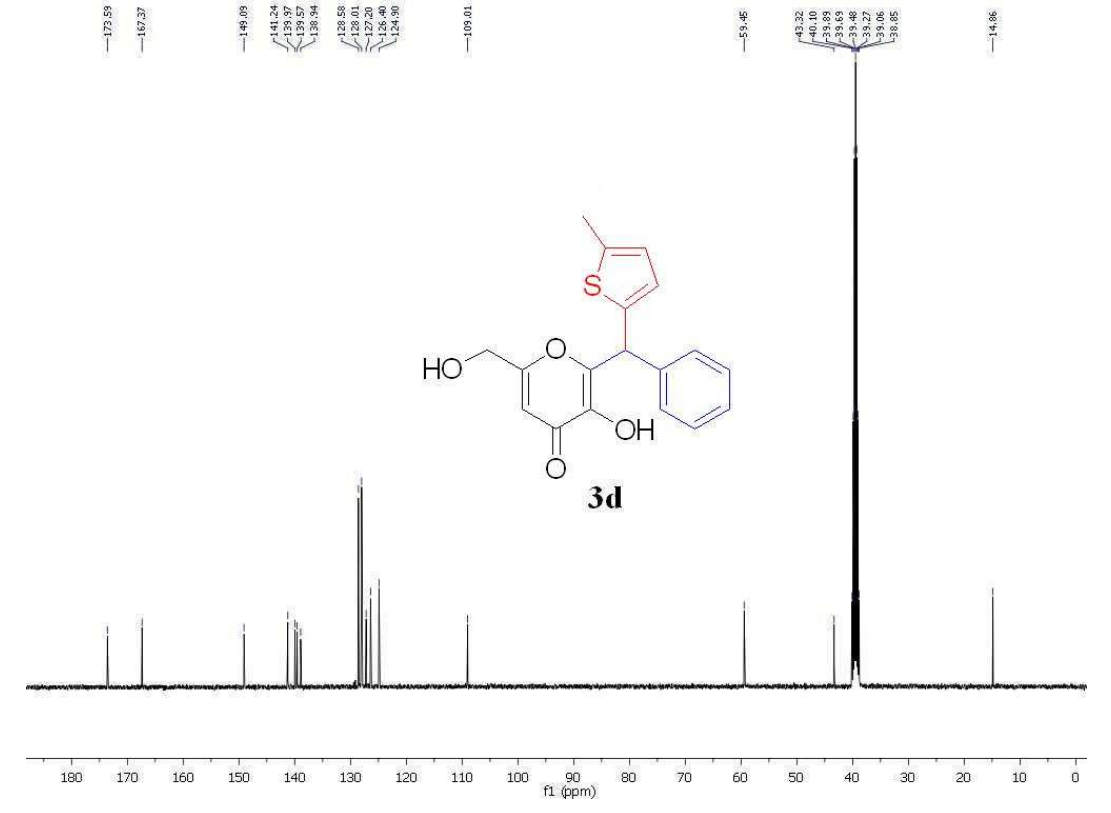
173.59
167.37
149.09
141.24
139.97
139.57
138.94
128.58
128.01
127.20
126.40
124.90
109.01
59.45
43.32
40.10
39.89
39.68
39.48
39.27
39.06
38.85
14.86
180 170 160 150 140 130 120 110 100 90 80 70 60 50 40 30 20 10 0
f1 (ppm)
S
HO
O
OH
O
3d

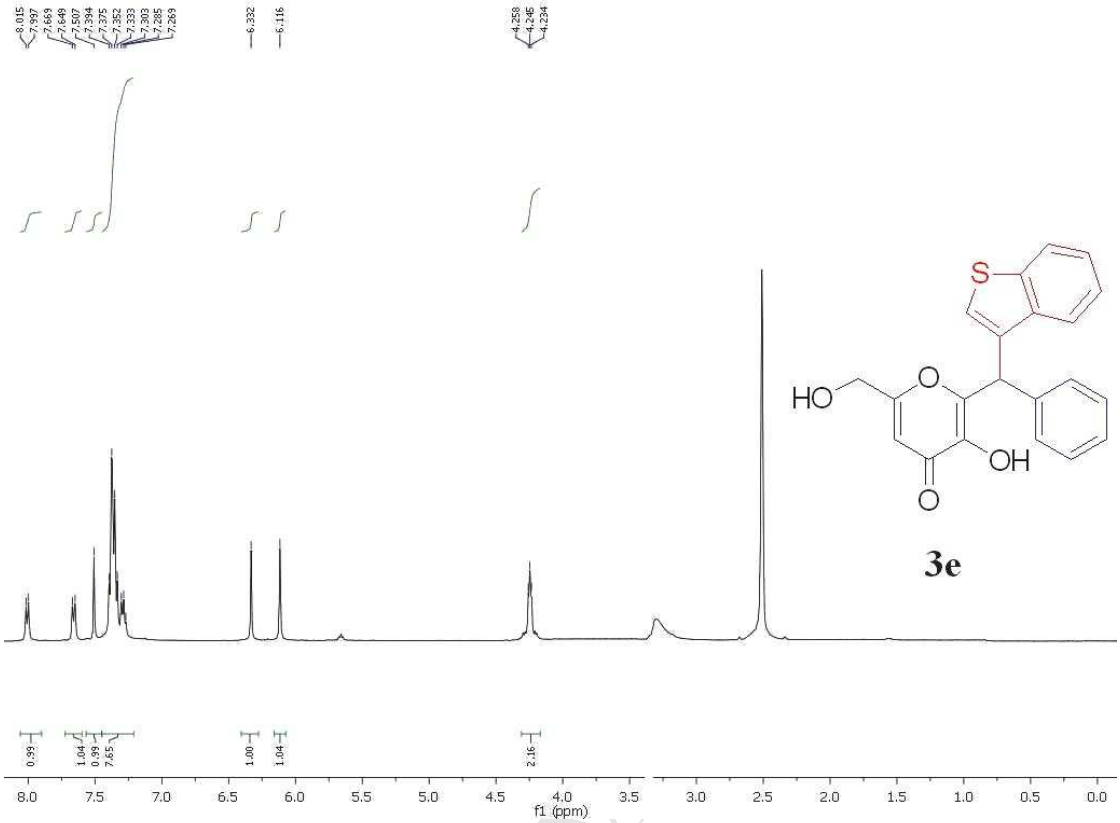
8.015
7.997
7.669
7.649
7.507
7.394
7.375
7.352
7.333
7.303
7.285
7.269
6.332
6.116
4.258
4.245
4.234
S
HO
O
OH
O
3e
0.99
1.04
0.99
7.65
1.00
1.04
2.16
8.0
7.5
7.0
6.5
6.0
5.5
5.0
4.5
4.0
3.5
3.0
2.5
2.0
1.5
1.0
0.5
0.0
f1 (ppm)

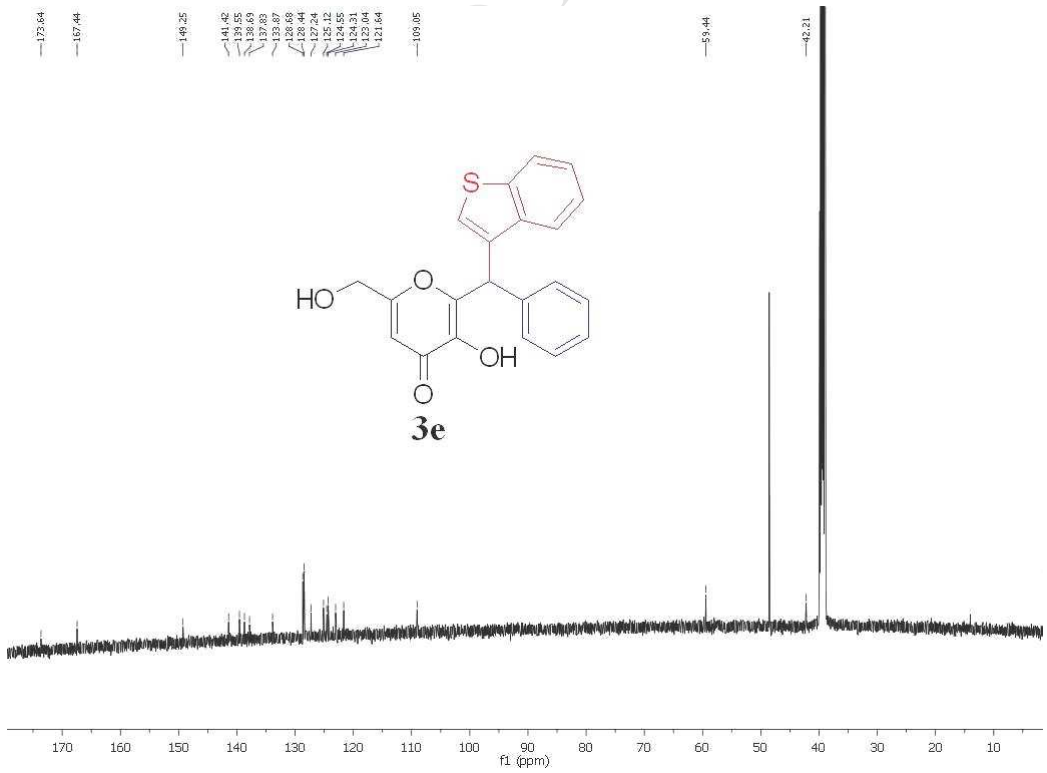
173.64
167.44
149.25
141.42
139.55
138.69
137.89
137.07
128.69
128.44
127.24
125.12
124.55
124.31
123.04
121.64
109.05
59.44
42.21
S
HO
O
OH
O
3e
170
160
150
140
130
120
110
100
90
80
70
60
50
40
30
20
10
f1 (ppm)

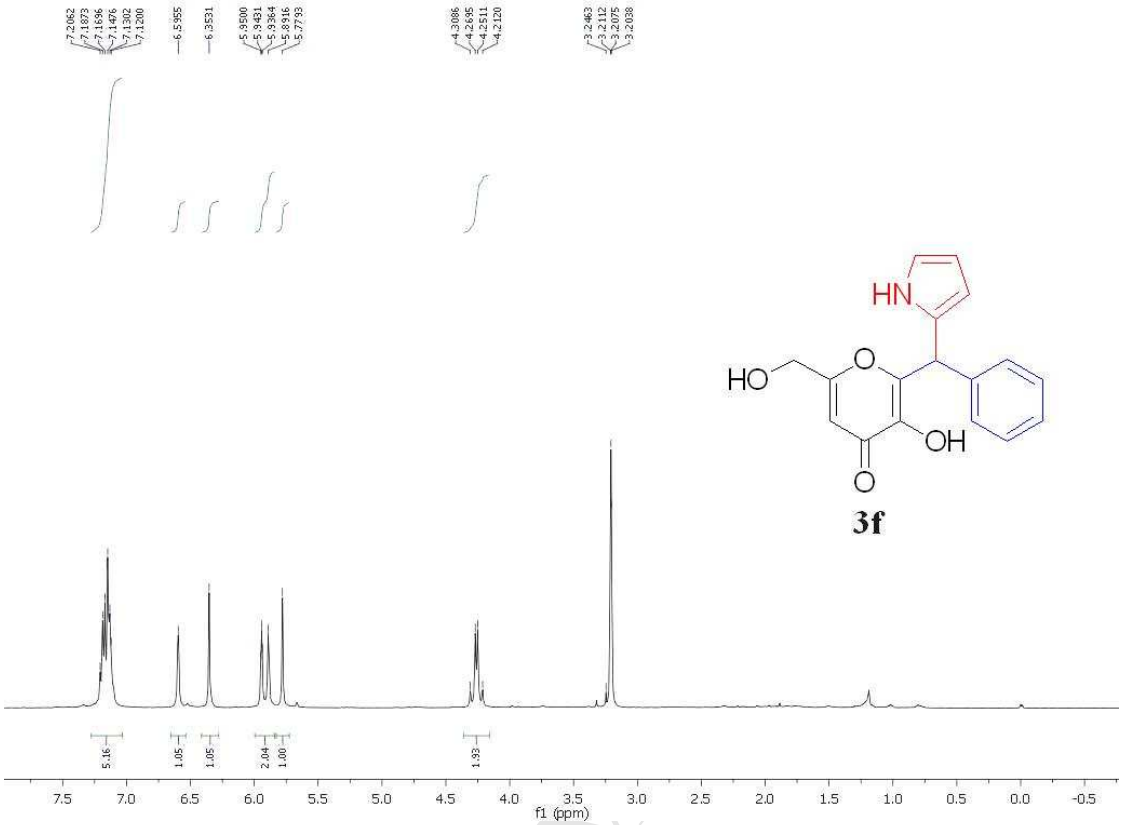
HN
HO
O
OH
O
3f
f1 (ppm)

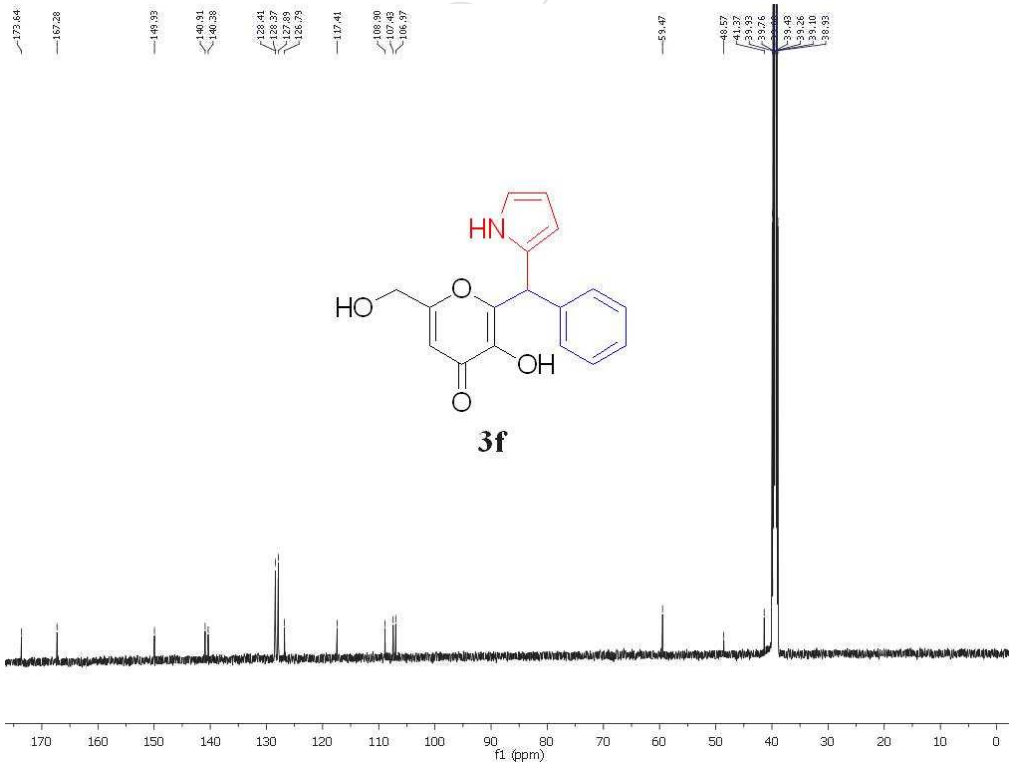
HN
HO
O
OH
O
3f
f1 (ppm)